2017

Supercritical Carbon Dioxide Treatment Of Natural Biomaterials For Tissue Engineering Applications

Dominic M. Casali
University of South Carolina

SUPERCRITICAL CARBON DIOXIDE TREATMENT OF NATURAL BIOMATERIALS FOR TISSUE ENGINEERING APPLICATIONS

by

Dominic M. Casali

Bachelor of Science
Florida Institute of Technology, 2011

Submitted in Partial Fulfillment of the Requirements

For the Degree of Doctor of Philosophy in

Chemical Engineering

College of Engineering and Computing

University of South Carolina

2017

Accepted by:

Michael A. Matthews, Major Professor

Ehsan Jabbarzadeh, Committee Member

Tarek Shazly, Committee Member

Mark J. Uline, Committee Member

John W. Weidner, Committee Member

Cheryl L. Addy, Vice Provost and Dean of the Graduate School

Dedication

To Grandpa Carmine, who could have written a great dissertation about gardening and making wine.

Acknowledgements

First and foremost, thanks be to God above, whose assistance has been needed regularly throughout the past few years. Thanks as well to my parents, Al and Ann, and my brother, Joe, for their constant and unconditional love and support, as well as Grandma Terry and my extended family in New York.

On a professional level, I'd like to first thank my advisor, Dr. Mike Matthews, whose continual input and patience have been invaluable throughout my journey. Thanks also to Drs. Ehsan Jabbarzadeh, Tarek Shazly, and Mark Uline for serving on my committee and for their helpful feedback. I would also like to acknowledge two chemical engineering faculty that have become great friends and mentors throughout my time at USC: Dr. J.R. Regulbuto and Dr. Ed Gatzke. Thanks as well to Dr. Silke Henrich and Ms. Carol Stork for their technical assistance with some of my experiments. I would also like to acknowledge our great chemical engineering staff members, especially Ms. Loretta Hardcastle; their constant friendliness and dedication to our department are too often overlooked or taken for granted.

Many other graduate students and other lab groups also assisted me at various times and deserve recognition. First, thanks to the undergraduate students who worked with me over the past few years, especially Rachel Handleton, Leland Hartzog, and Jerry Mota, along with the other graduate students in our group, Odell Glenn and Lin Yu. Thanks also to Jason Hsieh, Michael Kempner, Michael Collins, and the IRF and EMC

staff for their expert assistance with various equipment and experiments outside of my lab.

I would also like to thank the many friends who made these past five years a lot more fun and fulfilling. I had a great time being a part of various student organizations: namely the USC Graduate Student Association, Gamecock Toastmasters, and ChEGSO, as well as St. Thomas More Catholic Parish and Columbia YACs. I'd also like to thank my friends from trivia and Magic, and my softball and bowling teammates. All of these experiences have contributed in some small way to completing this once-daunting project.

Abstract

The number of people requiring an organ transplant in the United States has increased considerably over the past 25 years, but the number of organ donations has stagnated; over 8,000 people now die annually while awaiting a transplant or become too sick to receive one. Tissue engineering (TE), the design and production of artificial tissues and organs *in vitro*, has been proposed to alleviate this problem. Though synthetic polymers offer tunable mechanical and biochemical properties, natural biomaterials have recently garnered attention in TE for their high degree of biocompatibility and ability to direct cell proliferation and constructive tissue remodeling. Yet scaffold processing remains challenging and a need for novel treatment and fabrication methods still exists.

One underexplored method for creating TE scaffolds is treatment with supercritical fluids (SCFs). SCFs are appealing for treating biomaterials because of their desirable solvent properties; liquid-like densities and gas-like viscosities allow supercritical fluids to wet and penetrate matrices easily without damaging surface tension effects. Supercritical carbon dioxide ($scCO_2$) is of particular interest. $scCO_2$ is a non-toxic, non-flammable substance that is relatively inert and can be used to process biomaterials at physiologic temperatures and mild pressures. $scCO_2$ treatment avoids organic solvents, does not leave cytotoxic residue, and has already been utilized in similar biomedical applications, including sterilization, pasteurization, biomolecule extraction, and removal of endotoxins, bioburden, and allergenic proteins.

Supercritical CO_2 has been used in foaming of synthetic polymer scaffolds, but it is almost completely unexplored in treatment of natural biomaterials for TE. In this dissertation, the potential of $scCO_2$ in natural biomaterial TE is extensively explored. Two commonly-studied natural TE scaffold biomaterials were examined: a single-component biomaterial, type I collagen, and a multi-component biomaterial, extracellular matrix (ECM) obtained by decellularization of porcine aorta. Both biomaterials were studied at the fundamental and applied level.

First, the chemical compatibility of collagen and liquid and $scCO_2$ was assessed. Compatibility was determined based on changes in four biochemical properties: thermal stability, molecular weight, secondary structure, and overall appearance. For $scCO_2$, no significant differences were observed, indicating chemical compatibility. Liquid CO_2 treatment caused significant denaturing, though it was hypothesized that the apparent incompatibility may be a result of treatment conditions rather than total incompatibility.

After chemical compatibility between collagen and $scCO_2$ was established, $scCO_2$ was applied to crosslinked collagen films to extract residual glutaraldehyde after crosslinking. After 1 hr of $scCO_2$/ethanol treatment, over 95% of residual glutaraldehyde was removed, reducing the concentration below 1 ppm. Differential scanning calorimetry analysis showed a high degree of crosslinking and a denaturation temperature of about 63°C both before and after $scCO_2$ treatment. Tensile testing did reveal a significant increase in both stiffness and tensile strength caused by $scCO_2$ treatment, likely resulting from dehydration caused by the ethanol additive. However, this dehydration is preventable and less disruptive than heat-based removal of residual glutaraldehyde.

Decellularized ECM is also commonly used as a TE scaffolds. Current decellularization methods often utilize chemical detergents, which are residually cytotoxic and can damage ECM composition and ultrastructure. $scCO_2$ has been proposed as a decellularizing agent, but added ethanol severely dehydrates the matrix. The second half of this dissertation explores how $scCO_2$ can decellularize a tissue without dehydrating it. To prevent dehydration, a novel presaturation method was developed where $scCO_2$ and water are thoroughly mixed before treatment. Presaturation with water led to mass retention of over 99% in a model hydrogel and over 97% in porcine aorta during $scCO_2$ treatment, compared to only 46% and 78%, respectively, when dry (pure) $scCO_2$ was used, proving that dehydration during $scCO_2$ treatment is easily prevented.

Finally, $scCO_2$ was used to decellularize porcine aorta. Contrary to a previous report, $scCO_2$ alone was unable to achieve complete cell removal, even with a polar additive. However, when an SDS pretreatment step was used, the same $scCO_2$ treatment completely decellularized porcine aorta as indicated by histology and DNA quantitation. Presaturation of $scCO_2$ with water maintained the hydration state of the matrix, better maintaining the mechanical properties of the native tissue.

This dissertation confirms the potential of supercritical CO_2 as a processing method for naturally-derived biomaterial scaffolds. Further work can be performed to determine the efficacy of CO_2 on different scaffold compositions and morphologies as well as decellularization of other tissue types. More complex treatments may also be possible, such as simultaneous sterilization and decellularization. These studies provide insight into the mechanisms and applications of $scCO_2$ in TE and offer a springboard for impactful discoveries in the future.

Table of Contents

List of Tables

List of Figures

List of Symbols

n	n-value for statistical tests indicating sample size
p	p-value for statistical tests indicating statistical significance
P	Pressure
P_c	Critical Pressure
ρ	Density
T	Temperature
T_c	Critical Temperature
y	Mole fraction

List of Abbreviations

BCA ..... Bicinchonic Acid

βME ..... Beta-Mercaptoethanol

BSA ..... Bovine Serum Albumin

CD ..... Circular Dichroism

CO_2 ..... Carbon Dioxide

CPD ..... Critical Point Drying

DNA ..... Deoxyribonucleic Acid

DSC ..... Differential Scanning Calorimetry

ECM ..... Extracellular Matrix

EDTA ..... Ethylenediaminetetraacetic Acid

EtOH ..... Ethanol

FDA ..... Food and Drug Administration

GAG ..... Glycosaminoglycan

H&E ..... Hematoxylin and Eosin

HHP ..... High Hydrostatic Pressure

MOE ..... Modulus of Elasticity

N_2O ..... Dinitrogen Monoxide (a.k.a. Nitrous Oxide)

PBS ..... Phosphate Buffered Saline

ppm ..... Parts per Million

$scCO_2$ ..... Supercritical Carbon Dioxide

SCF .....Supercritical Fluid

SDS ..... Sodium Dodecyl Sulfate

SDS-PAGE ..... Sodium Dodecyl Sulfate Polyacrylamide Gel Electrophoresis

TE.....Tissue Engineering

UTS ..... Ultimate Tensile Strength

UV..... Ultraviolet

Chapter 1 Introduction

At the end of 2013, over 120,000 individuals in the United States were registered on the national organ transplant waiting list. The size of the waiting list has continually increased over the past 25 years, while the number of donations plateaued in the 2000s and has slightly declined in the 2010s (see Figure 1.1), with the gap between the waiting list and the number of annual donations now exceeding 100,000 people [1]. It follows that the number of deaths for those awaiting transplantation, currently about 8,000 per year, will continue to increase over time. These statistics clearly indicate that merely relying on human organ donation will be insufficient for meeting the medical needs of those requiring organ transplantation, both now and in the future.

One way to address the organ deficit is the production and use of artificial organs. An artificial organ is a manmade construct that can perform the tasks and functions of a native organ which has been damaged or excised. Though the concept of artificial organs has existed for over a century [2], widespread clinical use of artificial organs still does not exist. One exciting and relatively novel method for creating artificial organs is the field of tissue engineering (TE). TE involves culturing healthy cells from a patient (or from a stem cell line if autologous cells are unavailable) to create a new tissue *in vitro*, which can then be used as a graft to treat a tissue or organ defect [3]. The TE process is shown in pictorial form in Figure 1.2.

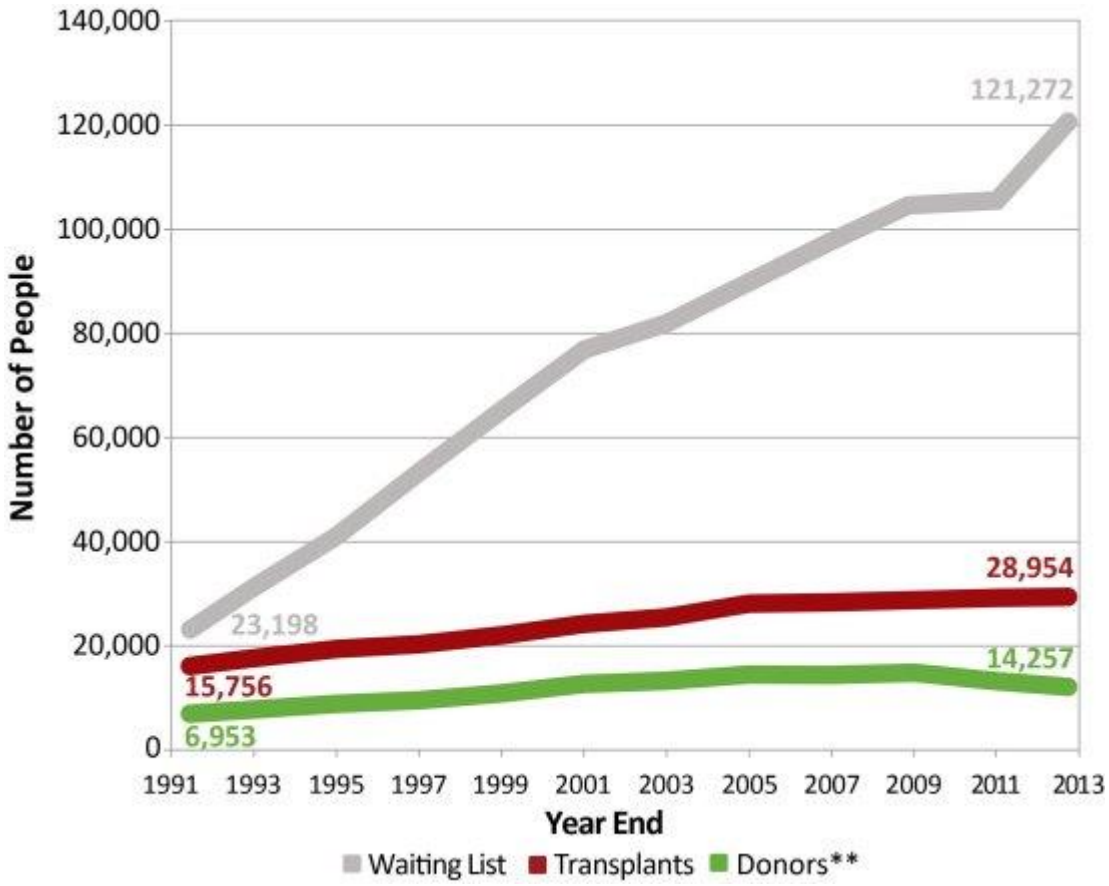

Figure 1.1 – Trends in organ donation in the United States, 1991-2013 (Approved for reuse by the United States Department of Health & Human Services; URL: https://optn.transplant.hrsa.gov/the-need-is-real-data/)

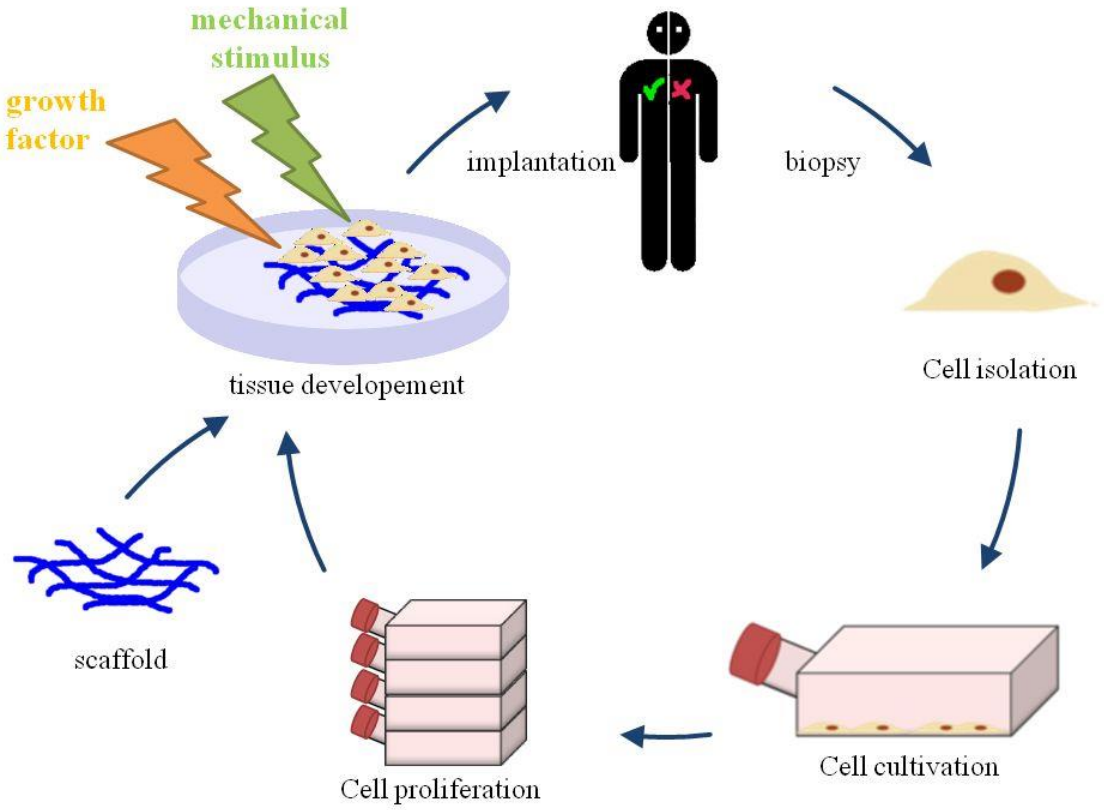

Figure 1.2 – Tissue Engineering Flowchart – (By HIA (Own work) [CC BY 3.0 (http://creativecommons.org/licenses/by/3.0)], via Wikimedia Commons)

For example, one can consider how the TE process would be utilized for a patient with a bone defect. First, a biopsy is taken from the patient's healthy bone tissue. Healthy cells are isolated from the biopsy and then cultured *in vitro* until reaching an appropriate cell density. Next, the cultured cells are seeded onto a biocompatible three-dimensional construct called a TE scaffold along with appropriate growth factors and mechanical stimuli to create a tissue-engineered graft. Finally, the graft is implanted into the damaged bone. Once inside the body, the cells continue to proliferate and differentiate, populating around the scaffold and eventually forming a new tissue or organ to replace the damaged one. The scaffold is designed to naturally degrade over a set timeframe and be replaced by newly-deposited extracellular matrix (ECM).

TE works well in theory, but a number of challenges have prevented its success and widespread clinical use. The biggest challenge is determining the source and design of the scaffold. An effective scaffold biomaterial must satisfy numerous biological, chemical, structural, and mechanical criteria, including [4].

- High biocompatibility/low immunogenicity to prevent host immune response
- Interconnected pore structure that allows cell penetration
- Appropriate morphology for the specific tissue or application
- Suitable elastic modulus (stiffness) and flexural rigidity
- Structural integrity to withstand pressure and mechanical forces
- Surface chemistry that is not too hydrophilic or hydrophobic
- Absence of any residual cytotoxic agents
- Sterility to prevent infection after implantation
- Bioactive and able to promote constructive remodeling

Two main approaches to creating TE scaffolds are possible: (1) producing scaffolds from synthetic biomaterials, and (2) using scaffolds derived from natural and/or xenogeneic sources. Though both approaches have merit, natural biomaterials offer two primary advantages. First, using naturally-derived scaffolds can reduce the possibility of bodily rejection and adverse immune response sometimes observed with synthetic biomaterials [5]. Second, recent research has uncovered the importance of ECM proteins in directing the tissue towards vascularization, innervation, and proper function; these outcomes are collectively called "constructive remodeling" [6]. During constructive remodeling, ECM proteins and their degradation products, including cytokines and chemokines, signal cells on when to migrate, proliferate, and differentiate [7]. In fact, the constructive remodeling effect of ECM proteins is so great that for some biomaterial and tissue combinations, such as collagen for bone tissue and elastin for blood vessels, the primary ECM component alone can be enough to promote constructive remodeling [8, 9].

1.1 Decellularization

Xenogeneic organs or tissues contain non-autologous (foreign) cells, which must be removed prior to seeding the matrix to prevent undesired post-implant immune response [10, 11]. The process of removing foreign cellular material from a tissue or organ is called decellularization. The objective of any decellularization method is twofold: (1) to remove all foreign cellular material, and (2) to preserve the physical, mechanical, and biochemical properties of the ECM [12].

Tissues differ in numerous ways, including variations in cell type, cell density, physical density, ECM composition, morphology, and thickness. Because of these

differences, there are numerous, highly-varied decellularization protocols that exist for different tissues; sometimes there are even very different approaches for decellularizing the same type of tissue [13]. Decellularization is most commonly accomplished by contacting xenogeneic tissue with chemical detergents, sometimes in conjunction with enzymes [14]. Physical methods, such as sonication and agitation, can be used instead of or in tandem with chemical methods to decellularize a tissue [15]. Common decellularization methods are discussed in greater detail in Chapter 2.

There is no universal or perfect decellularization protocol. If treatment is too harsh, the ECM will be damaged, compromising mechanical integrity and bioactive properties. If the treatment is too gentle, not all foreign cells will be removed, stimulating unwanted immune response [10]. In fact, it is accepted in the field that no decellularization treatment will be able to remove all cellular material from a tissue, and no treatment will be able to completely avoid damaging the ECM [13]. Therefore, the goal and challenge of creating a decellularization protocol is finding a balance between preserving enough of the matrix for it to promote constructive remodeling and removing enough foreign cellular matter to prevent an inflammatory immune response. Both of these outcomes are required for the recellularized tissue to develop and function properly; therefore, the efficacy of a given decellularization technique must be determined by evaluating both criteria. Currently, there are no universally-accepted standards for determining the extent of decellularization. However, Badylak's group has recently proposed standards based on the mass and length of residual DNA fragments and the absence of cellular material in stained micrographs [12]. There are no universal criteria at all for successful ECM preservation, but mechanical properties, pore size and structure,

and ECM protein composition are often evaluated after treatment and compared to the properties of the native tissue.

1.2 Supercritical Carbon Dioxide

An optimal decellularization technique has not yet been discovered, and conventional decellularization techniques have several weaknesses that need to be addressed. Most protocols, especially ones that use chemical detergents, are fairly time-consuming. Many treatments last on the order of days [16], while treating denser tissues like blood vessels can take multiple weeks [17], and this time does not include post-decellularization processing steps such as sterilization. Residual detergents can be cytotoxic [10], as can residual crosslinking agents [18]. Detergents also can have additional deleterious effects in tissues containing basement membranes, such as bladder and skin [19, 20]. Because of these issues, novel decellularizing agents and methods for applying them are still being pursued.

One method of processing biomaterials that has gained interest in recent years is supercritical fluids (SCFs). A substance enters the one-phase SCF state upon exceeding both its critical temperature (T_c) and critical pressure (P_c), collectively known as the critical point (T_c, P_c). Supercritical fluids are effective solvents because they have desirable transport properties, including minimal surface tension, low viscosity, and high diffusivity like gases, but they also have liquid-like density and solvation power that are much greater than those of most gases [21]. This combination of properties allows SCFs to penetrate through surfaces easily without damaging them because of their lack of surface tension. Upon depressurization, the supercritical fluid outgases and exits the

system, avoiding problems with residual cytotoxic components often encountered in other methods.

Supercritical carbon dioxide ($scCO_2$), shown in Figure 1.3 (b), is especially promising for biomedical applications. The primary reason is thermodynamic: $scCO_2$ has unusually low critical conditions. Its T_c of 31.1°C allows treatment of biological materials at or near physiologic temperature (37°C), and its P_c of 7.4 MPa is mild enough to treat biomaterials safely. Additionally, CO_2 is readily available and safe – it is relatively inert, non-flammable, non-toxic, and non-mutagenic [21]. Equipment and processes utilizing supercritical CO_2 have already been demonstrated in pasteurization [22-24], extraction of biological compounds [25, 26], production of TE scaffolds from synthetic polymers [27-29], and sterilization, the latter being a research thrust in our group [30-37].

Sterilization is of particular importance in TE to prevent nosocomial (hospital-acquired) infection during surgery. Traditional sterilization methods like steam autoclaving, ethylene oxide, and gamma irradiation are often unsuitable for biomaterials [30, 33]. Supercritical CO_2 has been proven effective in the sterilization of decellularized porcine dermis and lung ECM [38, 39] and has been identified as an important subject of future research in scaffold sterilization [12]. Though not directly investigated in this dissertation, the possibility of simultaneous decellularization and sterilization or high-level disinfection using a single CO_2 treatment would be a potential boon for the field. Additionally, $scCO_2$ has recently been used to aid in other TE processes, including for hydrogel foaming [40] and crosslinking of chitosan aerogels [41]. Furthermore, recent improvements in $scCO_2$ processing techniques have eliminated the pore interconnectivity

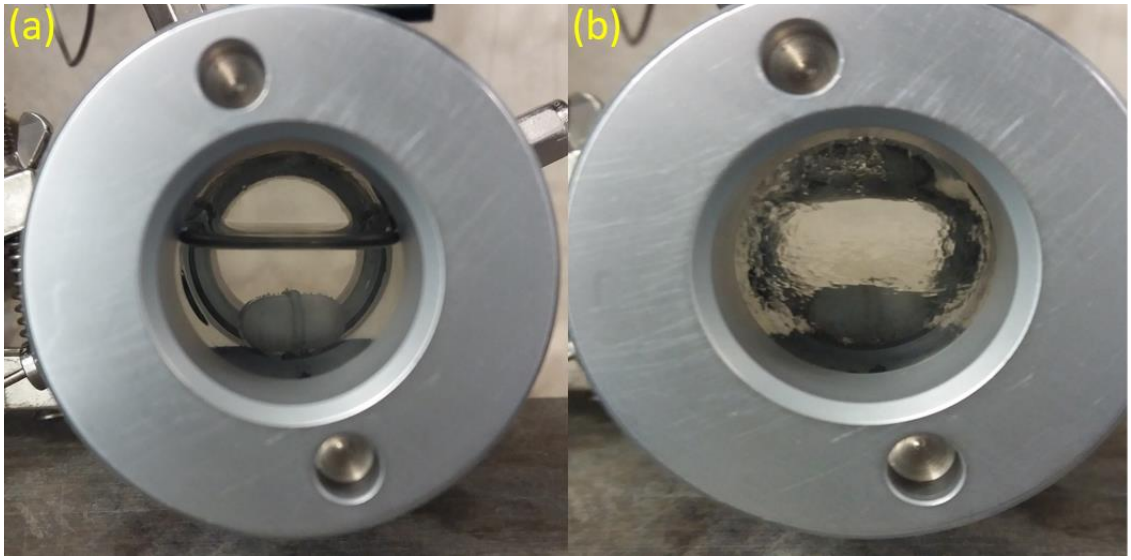

Figure 1.3 – Visual Appearance of Dense-Phase CO_2: Photographs of (a) CO_2 in vapor-liquid equilibrium and (b) CO_2 in the supercritical state.

issues that were once a major hindrance to $scCO_2$ polymer foaming techniques [42]. However, despite the efficacy of $scCO_2$ in the aforementioned applications, its use in treatment of natural TE scaffold biomaterials is very limited. To the best of our knowledge, there has been no fundamental research on the chemical compatibility of $scCO_2$ with natural biomaterials, such as collagen, and applied work in the literature is very limited. Decellularization with $scCO_2$ is completely unexplored aside from a single publication by Sawada's group in 2008, where significant matrix dehydration was reported and no further reports were published [43].

1.3 Dissertation Objectives

The overarching objective of this dissertation is to evaluate the potential of $scCO_2$ for use in the processing and fabrication of naturally-derived TE scaffolds. This objective was accomplished by using $scCO_2$ to treat a simple natural biomaterial, type I collagen, and a more complex natural biomaterial, porcine aorta tissue. As shown in Figure 1.4, a fundamental study and an applied study were performed for each biomaterial. The specific aims of this work are: (1) to determine the fundamental compatibility of type I collagen with liquid and supercritical CO_2, (2) to extract residual glutaraldehyde from crosslinked type I collagen films using $scCO_2$, reducing glutaraldehyde concentration below cytotoxic levels, (3) to design and develop a method for presaturating $scCO_2$ with water and other volatiles to prevent dehydration of model scaffold biomaterials, and (4) to decellularize porcine aorta tissue using a $scCO_2$-based treatment process and determine the relative effects of key process parameters on cell removal and scaffold properties.

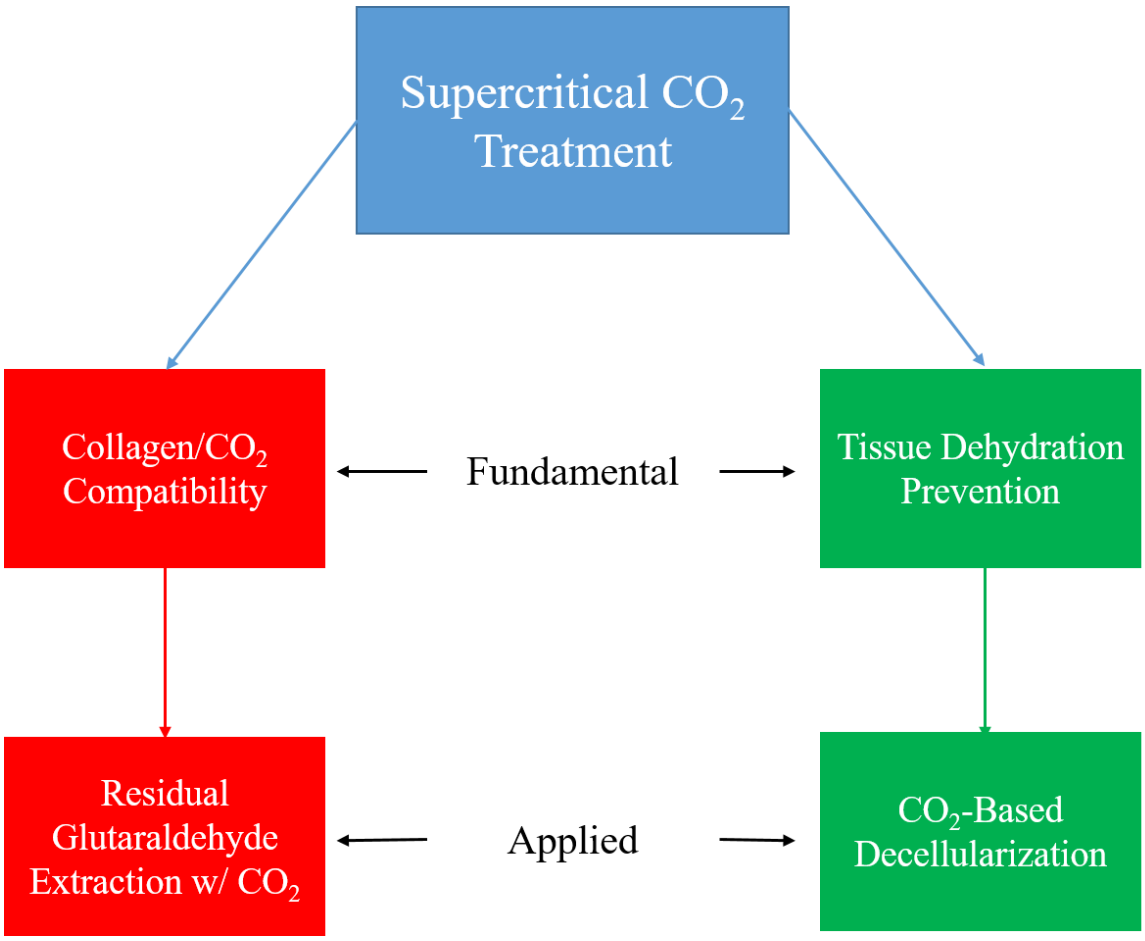

Figure 1.4 – Dissertation Flowchart: Supercritical CO_2 was used to treat both type I collagen and porcine aorta in fundamental and applied studies.

Very little work has been done previously on fabrication of TE scaffolds with $scCO_2$. The findings of this dissertation will elucidate fundamentals of how supercritical fluids and scaffold biomaterials interact. This knowledge can be leveraged into numerous applications for future clinical and industrial benefit in TE and the fields of chemical and biomedical engineering.

Chapter 2 Literature Review

In recent decades, industrial and research interest in supercritical CO_2 technology has seen a considerable increase in a wide variety of applications, including many in the biomedical field [44-46]. In recent years, TE has also seen continual growth and progress in research and development [3, 13, 47]. As this dissertation lies at the intersection of these two important and expanding areas, this chapter includes discussion of current knowledge and critical publications in both $scCO_2$ and TE. The objective of this chapter is to establish where and how this dissertation fits into both fields.

2.1 Supercritical CO_2 Technology

Prior to covering the most prominent applications of $scCO_2$, some background on its unique thermodynamic and chemical properties will be discussed. This subsection will then cover extraction, the primary industrial application of $scCO_2$, with a focus on extraction of biological compounds. It will conclude with discussion of two areas of $scCO_2$ technology highly relevant to this dissertation: sterilization and TE applications.

2.1.1 Supercritical CO_2 Fundamentals

A pressure-temperature phase diagram for a pure substance, such as that of CO_2 shown in Figure 2.1, consists primarily of planar one-phase regions (solid, liquid, and vapor) and two-phase curves where thermodynamic equilibrium exists between the two

phases. These curves on Figure 2.1 are A, the solid-vapor (sublimation) curve; B, the solid-liquid (fusion) curve; and C, the liquid-vapor (vaporization) curve. There also two pressure-temperature coordinate points of interest. Point D is the triple point, where the solid, liquid, and vapor phases exist in three-phase equilibrium. More importantly for this work, point E is the critical point. As the critical point is approached, the liquid and vapor phases approach equal densities and the phase boundary disappears. Once the pressure and temperature of the critical point are exceeded, the substance enters the supercritical fluid phase [48].

Supercritical fluids have a unique combination of properties: densities on the order of liquids but diffusivities and viscosities on the order of gases. Along with having minimal surface tension, these solvent properties allow SCFs to penetrate into pores, films, and surface openings without damaging them. SCFs are green, sustainable replacements for organic solvents in many applications, especially in the area of cleaning materials and surfaces [49]. CO_2 is one of the most commonly used supercritical fluids. It is non-toxic, non-flammable, non-mutagenic, relatively inert, odorless, readily available, and fairly inexpensive [21]. It also has relatively low critical conditions (T_c = 31.1C, P_c = 7.4 MPa), making it particularly well-suited for biological applications. A myriad of molecules have some degree of solubility in $scCO_2$, especially small, non-polar ones [50]. Solubility of polar compounds is sometimes limited, but can be improved in many cases by dissolving a polar additive, such as ethanol, in $scCO_2$, [51].

CO_2 in the liquid phase is also of interest. Liquid CO_2 exists at similar, sometimes greater densities than $scCO_2$, and is therefore also considered a "dense-phase" fluid. Liquid CO_2 can exist at pressures as low as 1 MPa, making it desirable for

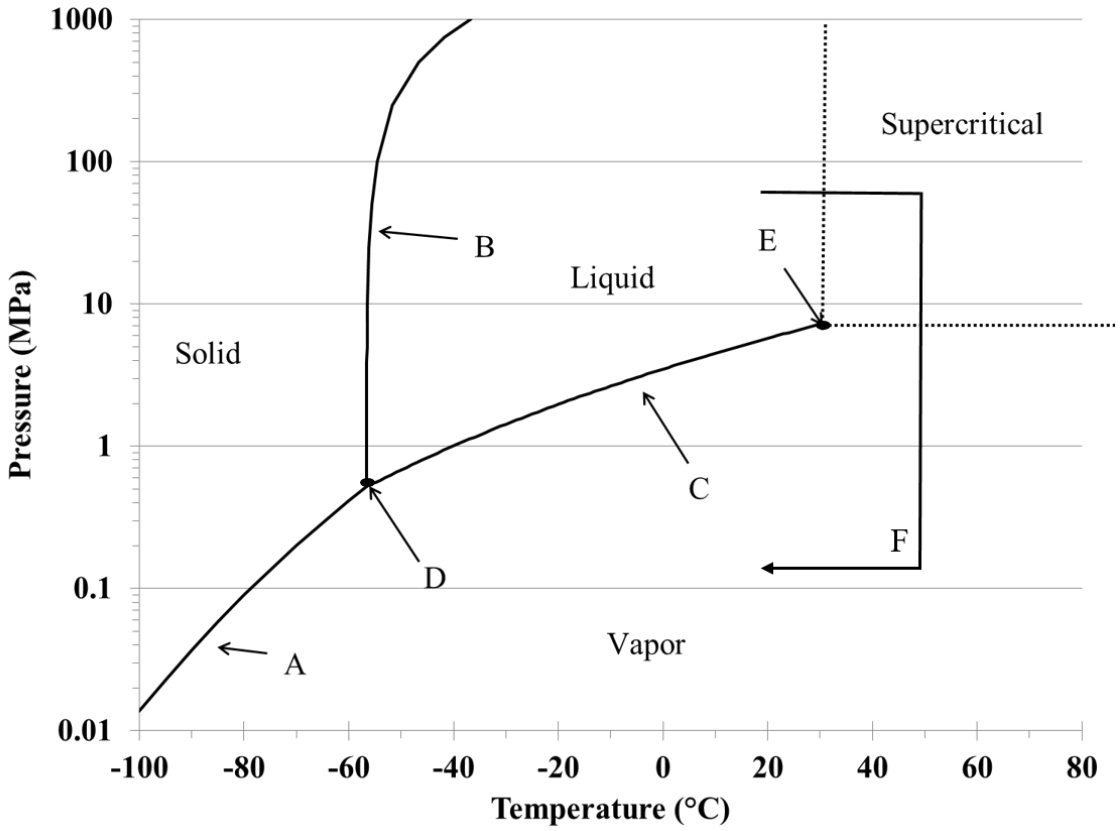

Figure 2.1 – Carbon Dioxide Phase Diagram: A – Sublimation Curve; B – Fusion Curve; C – Vaporization Curve; D – Triple Point; E – Critical Point; F – Critical Point Drying

applications where the higher temperatures and pressures of supercritical CO_2 are detrimental, either physically to the specimen or economically because of the higher equipment cost [52, 53].

One important application of liquid CO_2 is critical point drying (CPD), a process commonly used in TE [54] and other applications, such as electronics processing [55], aerogel formation [56], and scanning electron microscopy [57]. The primary advantage of CPD over conventional evaporative drying is that CPD avoids passing through the vaporization curve of the phase diagram; circumventing the two-phase region is desirable for delicate materials that can be damaged by the surface tension that exists at vapor-liquid phase boundaries [58]. As shown on line F in Figure 2.1, CPD initiates when a liquid solvent, such as ethanol, is removed from a substrate by dissolving it in a second benign solvent, typically liquid CO_2. The mixture is then heated and/or pressurized until CO_2 undergoes a phase transition from the liquid state to the supercritical state. Finally, the pressure is reduced below the critical pressure, allowing the supercritical CO_2 to enter the gaseous state without undergoing the vapor-liquid phase transition. The gaseous CO_2 is removed from the system by depressurizing to ambient conditions.

Dense-phase CO_2 has been utilized in a wide variety of applications, including reaction engineering [59], catalysis [60], polymerization [61], chromatography [62], particle synthesis [63], thin film synthesis [64], jet cutting [65], textile dyeing [66], and as a heat transfer fluid [67]. However, this section will focus on the three realms of CO_2 technology most relevant to this dissertation, which include extraction, sterilization, and tissue engineering.

2.1.2 Extraction

Extraction, the process of separating one component from another using a solvent, is one of the most widespread applications of supercritical CO_2 [21]. One of the oldest and best-known SCF extraction process is the decaffeination of coffee [68], which has more recently been extended to tea and spent coffee grounds [69, 70]. CO_2-based extraction has some inorganic applications, such as removal of metal ions from water and other materials [71, 72], but the main focus of supercritical extraction is on biological molecules. The extraction of oils, lipids, and organic solvents are of particular interest to TE applications.

Supercritical CO_2 extraction of animal and plant oils for supplemental and medicinal use has gained considerable attention in recent years. For example, Ferdosh *et al*. used $scCO_2$ and an ethanol additive to extract and fractionate fish oil, which contains healthy omega-3 fatty acids. The fish oil was extracted from undesired and/or inedible tuna parts in a 2 hr process, though 3 days of pretreatment freeze-drying were required [73]. CO_2 extraction of plant oils has been studied extensively, as well. Plant oils containing fatty acids, one of the two subgroups of lipids, have been traditionally extracted using either a mechanical press or organic solvents, such as hexane or petroleum ether [74]. However, $scCO_2$ has gained popularity in this field because it offers higher yields than a mechanical press without the environmental and safety hazards of organic solvents [75]. Some materials are extracted from plant by-products, such as lycopene from tomato peels [76], but most oils are extracted from seeds. Some types of plant oils successfully extracted with supercritical CO_2 include tea seed [75], sunflower seed [77], and sesame seed [78], among many others.

A key subset of fatty acid-containing oils is those containing conjugated linolenic acids, which may help prevent atherosclerosis and fight some types of cancer [79]. Özkal *et al*. extracted flaxseed oil, an abundant source of α-linolenic acid, in 30-60 minutes of $scCO_2$ treatment with yields of about 0.3 g/seed [80]. $scCO_2$ extraction of *G. Pentaphyllum* (a Chinese herb) seeds for 160 min yielded an oil containing over 88% conjugated linolenic acids, which inhibited the viability of both leukemic and colon cancer cells by about 80% [81]. Another notable subset of fatty acids is phytosterols, which may lower cholesterol and the risk of heart disease [82]. Phytosterols have been extracted from many seed oils using $scCO_2$, as well as other natural sources, such as bee pollen [83].

Along with fatty acids, the other subgroup of lipids is glycerides, which include waxes, triglycerides, and phospholipids [74]. Phospholipids are of particular interest for $scCO_2$-based decellularization, as they are a primary component of cell membranes. However, phospholipids have been studied in much less detail than fatty acids, likely because their high polarity makes them more difficult to extract. Still, some progress has been made in this area. Tanaka *et al*. were able to extract phospholipids from salmon roe with up to 80% purity, though high concentrations of added ethanol were needed [84]. Phosphatidylcholine has been extracted from inedible egg parts with $scCO_2$, but a two-step process was required and yield still was relatively low (< 50 g/kg) [85]. More recently, phospholipids were extracted from activated sludge using $scCO_2$ to assess soil quality [86]. However, more work is needed to determine if extraction of cell membrane components is a viable approach to decellularization.

2.1.3 Sterilization

TE scaffolds must be sterilized before implantation, as hospital patients have an elevated risk of nosocomial infection because of weakened immune systems, close quarters, and the necessity of invasive procedures and implements [87]. This risk is especially high in intensive care units [88]. Thus, sterilization of all medical devices and implants is critical for patient safety. Numerous methods exist to sterilize materials, but most have one or more significant drawbacks for a biomedical application. The high temperature and humidity of steam autoclaving can denature proteins and damage fibrous and polymeric materials [89]. Ethylene oxide is toxic, flammable, and possibly carcinogenic [90]. Gamma irradiation has been shown to cause unwanted changes in the molecular weight, glass transition temperature, and water content of TE biomaterials [91]. Liquid sterilants such as phenols, glutaraldehyde, and peracetic acid are eye and skin irritants with varying degrees of toxicity [92].

Dense-phase CO_2 is often used for sterilization of biomaterials because it does not present any of these drawbacks. Spilimbergo's group has done extensive work on the mechanisms of cell deactivation by $scCO_2$. Through *in situ* fluorescence staining, they have shown that cell death primarily occurs from CO_2 permeation of the lipid bilayer in the cell membrane [93]. CO_2 enters the cell, lowering cellular pH and deactivating enzymes [94, 95]. Bacterial spores are typically more difficult to kill than vegetative bacteria. Our group showed using transmission electron microscopy that $scCO_2$ damages the spore envelope, but a lethal oxidizing additive, such as hydrogen peroxide, must then be absorbed by the cell to complete the deactivation process [35]. Pressure cycling and/or electric pulses also improve spore deactivation [44].

The parameters required to achieve sterilization are or at least high-level disinfection (which does not require removal of spores) are somewhat application-dependent, but usually the supercritical CO_2 phase is used. A temperature of 40°C or above and a pressure of 20 MPa or higher (or a more moderate 8-15 MPa range with pressure cycling) are usually adequate [44]. Deactivation of vegetative bacteria and bacterial spores from biomaterials using $scCO_2$ has been demonstrated numerous times by our group and many others [34, 96, 97], and is also commonly done in pasteurization and food processing [22, 98]. However, comparatively little work has been done on virus deactivation with $scCO_2$. In the late 1990s, Larzul's group used $scCO_2$ to remove viruses from bone allografts, though three additional processing steps were required after $scCO_2$ treatment to achieve high levels of virus deactivation [99]. Recently, nitrous oxide (N_2O) and fluorocarbons have been proven more effective for virus removal under most circumstances, possibly because N_2O is pH neutral instead of acidic [44]. N_2O has similar critical conditions like CO_2, but is often avoided because of safety concerns; it is strong oxidizer that can cause explosions in the presence of an organic fuel source [100].

The microbial removal properties of supercritical CO_2 also extend beyond viruses and bacteria. Exploratory research has shown potential for supercritical CO_2 in pest control during food storage [101]. In our lab, the solubility of tea tree, hinoki, and cedar wood oils in supercritical CO_2 has been utilized to create an acaricidal treatment on household objects for the prevention of asthma [102]. These technologies still have ample room for exploration and development.

Though supercritical is usually the preferred CO_2 phase, liquid CO_2 has been used in some sterilization applications. There are three situations that make liquid CO_2

particularly desirable for an application: (1) when cost of equipment is a limiting factor, (2) when the higher pressures and temperatures required by the supercritical phase would be deleterious, or (3) when surfactant additives are used, since their solubility in CO_2 is often inversely proportional with temperature [53, 103]. In our group, Jimenez *et al*. were able to use liquid CO_2 to completely sterilize a model hydrogel [32], and Tarafa *et al*. successfully removed bacterial endotoxin from titanium disks using water, liquid CO_2, and commercial surfactant Dehypon Ls-54 [104, 105]. Liquid CO_2 has also been used to sterilize textiles [52].

For the purposes of this dissertation, it is worth noting that there are two publications where $scCO_2$ was used to sterilize an acellular material. In 2009, Qiu *et al.* used $scCO_2$ to sterilize acellular porcine dermis [38]. Small pieces of ECM were sterilized using supercritical CO_2 with a peracetic acid additive. In under 30 minutes, 6 log reduction was attained for *Bacillus atrophaeus*, a bacterial spore that has traditionally been analyzed for sterilization effectiveness [31, 35]. They also studied removal of encephalomyocarditis (EMC) and other viruses, and attained complete virus removal in 15 minutes of $scCO_2$ treatment, which was more effective than two hours of treatment in peracetic acid alone. Additionally, $scCO_2$ treatment caused less than a 2% change in matrix weight, showing a relatively mild impact of treatment. Balestrini *et al*. similarly utilized $scCO_2$ to sterilize acellular lung ECM while maintaining key scaffold properties [39]. Supercritical CO_2 appears to have considerable potential for ECM sterilization, but more research is needed, particularly on larger or three-dimensional samples. This research may soon occur given the recent classification of xenogeneic scaffolds as

medical devices by the United States Food and Drug Administration (FDA), thereby requiring terminal sterilization prior to clinical use [106].

2.1.4 Synthetic TE Scaffolds

CO_2 has long been known to create pores in polymeric substances during depressurization, even in the gaseous phase. This process is often called polymer foaming, and it occurs because CO_2 plasticizes the polymer, liquefying it and increasing its density. Upon depressurization, CO_2 nucleates and forms gas bubbles when leaving the polymer, creating a pore network [107]. Two main criteria are necessary for a polymer to undergo this process: (1) moderate to high affinity for CO_2 and (2) a glass transition temperature below the processing temperature [108].

Careful manipulation of process variables, such as pressure, treatment time, and depressurization rate, can lead to predictable porosity and average pore size of the treated biomaterial. A groundbreaking paper demonstrating this was published by Howdle's group in 2007 [29]. They studied $scCO_2$ foaming of poly(lactic acid), PLA, and poly(lactic-co-glycolic acid), PLGA, in considerable depth. Their work included a factorial design of temperature, pressure, molecular weight, glycolic acid concentration, depressurization rate, and treatment time. They found increasing temperature and depressurization rate to be directly proportional to pore size, while increasing pressure, treatment time, molecular weight, and glycolic acid concentration were indirectly proportional to pore size. Porosity was in the acceptably high 70-80% range in most cases, except for very high glycolic acid concentrations, where it decreased considerably. A more uniform pore size distribution was found for $scCO_2$ compared to gaseous CO_2,

likely because the higher diffusivity in the supercritical state creates a more uniform distribution of CO_2 within the plasticized polymer.

Recently, the use of inert particulate additives and CO_2/water/surfactant emulsions has considerably improved pore interconnectivity, overcoming a significant barrier to the viability of scaffolds fabricated using this technique [42]. CO_2 has also been used to augment other scaffold fabrication methods, including emulsion templating [109], microsphere sintering [110], phase inversion [111], electrospinning [112], and biomolecule impregnation [113].

Another concern during any scaffold treatment is loss of bioactivity caused by chemical reactions that alter surface chemistry. Loss of bioactivity could inhibit cellular function or cell adhesion to a scaffold. However, $scCO_2$ is relatively inert and has been shown to not adversely affect bioactivity of both synthetic bone scaffolds and essential oil extracts [114, 115]. Still, establishing bioactivity of a natural scaffold after $scCO_2$ treatment would be an important step.

Since CO_2 also can be used to sterilize TE scaffolds, the amount of processing steps can potentially be reduced by using CO_2 to both form and sterilize the scaffold [33]. Like with extraction and sterilization, the supercritical phase is much more commonly used in scaffold treatment, but liquid CO_2 has been shown to have compatibility with some synthetic polymers, particularly ones with higher crystallinity [116]. CO_2 sorption is so high in amorphous materials that it often causes irreversible effects from extreme amounts of swelling; the compatibility of CO_2 crystalline materials is likely caused by their reduced free volume compared to amorphous materials [117].

Very little work has been done on CO_2 and natural polymers, including potential TE scaffold biomaterials. Though supercritical CO_2 has been applied sparingly to leather processing in the past decade [118, 119], to our knowledge no work has been done prior to this dissertation on the fundamental interactions of collagen and dense-phase CO_2. However, Reverchon's group recently created chitosan aerogels by lyophilization, crosslinked them with glutaraldehyde, and then removed almost all glutaraldehyde (final concentration below 0.1 ppm) using $scCO_2$ and ethanol [41, 120]. This clearly presents an opportunity for $scCO_2$ in crosslinking of naturally-derived scaffold materials. Recent reviews in the decellularization field have also recognized the potential for sterilization ECM with $scCO_2$ and recommend further research in the area [12, 13], but aside from the aforementioned sterilization work [38, 39], no literature is available on the subject.

There is one publication where $scCO_2$ is used in decellularization. Sawada *et al.* used $scCO_2$ and an ethanol additive to decellularize porcine aortas [43]. They reported 100% removal of DNA and 80-90% removal of phospholipids at relatively mild pressures and temperatures. However, problems with tissue dehydration, inability to completely rehydrate, loss of mechanical strength, and residual phospholipids were reported. Though this paper was published in 2008, to our knowledge no follow-up or similar studies have been published since. Chapter 6 of this dissertation includes our efforts to replicate and improve upon Sawada's findings.

2.2 Natural Biomaterial TE Scaffolds

We now turn our attention to the broad topic of TE scaffold design and fabrication. Two main routes exist for the fabrication of TE scaffolds: (1) synthetic

biomaterials, including synthetic polymers and composites, and (2) natural biomaterials. While the former path has scientific merit and does offer some advantages, it is beyond the scope of this dissertation and will not be discussed in greater detail. For further reading on the subject of artificial TE matrices, the reader is encouraged to examine the thorough review by Cho's group [47].

There are two primary avenues for production of TE scaffolds composed of natural biomaterials. The first is scaffolds composed primarily of one major ECM protein, often collagen, which are formed into a desired shape and size by various methods (*e.g.* electrospinning, lyophilization, etc.) [121]. The other subgroup is scaffolds composed of ECM; these are created by decellularization of an animal tissue, with the resulting ECM being used as the scaffold [122]. A great amount of variation exists in the methods by which natural biomaterial TE scaffolds are produced. Some of the most common and most pertinent to this work are explored in this subsection.

2.2.1 Collagen Scaffolds

The extracellular matrix gives structural support to cells, spatial cues for tissue growth, and direction for cell behaviors and functions [123]. These features all make collagen a desirable scaffold material. Collagen is the most abundant protein in the ECM of most tissues; it therefore has numerous sources in the body and is an intuitive candidate for a natural biomaterial scaffold, especially if decellularization of the whole ECM is challenging [124]. Though having the entire ECM is ideal for promotion of constructive tissue remodeling [7, 125], collagen has been shown to regulate cell adhesion, migration, proliferation, and differentiation and is often easier to isolate [126].

The advantages of collagen as a scaffold substrate are numerous. In addition to its role in remodeling, collagen has low immunogenicity and antigenicity, is porous and permeable, and has controllable biodegradability based on its extent of crosslinking. It also biodegrades in a more favorable way than many synthetic materials. While synthetic materials degrade from an immune response mediated by macrophages, ECM proteins like collagen elicit a less aggressive immune response that is mediated by matrix metalloproteinases and growth factors, stimulating natural tissue growth during scaffold degradation [4].

There are also numerous sources of collagen available. Human collagen can be harvested from the placenta [127], but most collagen traditionally comes from mammalian sources, including cow, pig, rat, and sheep. More recently, fish collagen has also been purified from parts that are normally discarded [128]. Finally, studies have been done to produce recombinant collagen; this could be important if collagen scaffolds experience a significant rise in usage, as yields from animal sources are often low [129].

Some scaffolds are made from pure collagen, usually a combination of types I, II, and III, since these are most common in the human body. One common fabrication method is lyophilization, or freeze-drying. Lyophilization protocols involve placing a collagen gel or solution into a specific shape or mold, then freezing it and removing the water. Scaffold properties can be manipulated by changing collagen concentration and freezing time [130]. Another popular approach is electrospinning. In this method, collagen is placed in a syringe or spinneret, charged with high voltage, and a jet eventually shoots at a grounded target once the potential difference is high enough, evaporating the solvent and creating a fiber [131]. These fibers can be manipulated into

various shapes and sizes. Finally, extrusion methods utilize syringe pumps to flow collagen solutions into a desired shape or area. Collagen can be extruded into different geometries based on the design of the extruder, such as the Yost group's tubular design, which has been used to make TE scaffolds for heart, bone, and blood vessel tissues [4, 132-134].

The main disadvantage of collagen as a scaffold material is that it lacks mechanical strength, especially when fully hydrated [121]. Collagen is often physically or chemically crosslinked to improve its mechanical strength. Common physical crosslinking methods include dehydrothermal treatment and ultraviolet or gamma irradiation [135]. Chemical crosslinking has been traditionally done with glutaraldehyde or azides [136], but these chemicals are cytotoxic if not fully removed [18, 137]. Less hazardous crosslinkers have been pursued recently, including EDC [138], genipin [139], and riboflavin [140], but these alternatives may be less potent [141].

Instead of crosslinking, the mechanical strength of collagen can be strengthened by incorporating an additional material into the scaffold to create a collagen blend. These materials include polymers, composites, and ceramics. Some polymers, like poly(ε-caprolactone) (PCL), are synthetic polymers used commonly in TE and add mechanical strength and control over degradation rate [142]. Natural polymers are used as well; for example, silk fibroin adds mechanical strength to collagen and also provides extra adhesion sites during cell seeding. For example, Wei *et al*. used a collagen/PCL/silk fibroin blend to create a bladder scaffold that promoted proliferation of epithelial cells [143]. Other common blending materials include hydroxyapatite, a ceramic often used in bone tissue scaffolds for its osteoinductivity [144], and carbon nanotubes, which can

increase scaffold stiffness and promote cell differentiation [145]. Growth factors can also be incorporated into collagen scaffolds, particularly during electrospinning [146].

2.2.2 Decellularized ECM Scaffolds

Decellularized scaffolds are fabricated by removing DNA and cellular matter from an animal tissue and using the recovered ECM as a TE scaffold. The primary benefits of ECM scaffolds are low immunogenicity and the capacity for constructive remodeling after recellularization [5-7, 125]. Constructive remodeling involves the development of nerves, vasculature, and proper tissue function after a scaffold is implanted. It occurs as a result of an anti-inflammatory immune response mediated by Th2 helper cells and M2 macrophages, rather than the pro-inflammatory Th1 cells and M1 macrophages normally observed in the deposition of scar tissue [106]. This type of response is associated with ECM scaffolds specifically [147, 148].

Decellularization has been performed on almost every tissue in the body, including adipose [149], bladder [150], blood vessel [151], bone [152], brain [153], cornea [154], esophagus [155], heart [156], intestine [157], kidney [158], liver [159], lung [160], nerve [161], skin [162], trachea [163], and others. Decellularized tissues originate from several different mammalian sources, most commonly porcine, bovine, ovine, or murine, among others [13]. There are numerous decellularization methods and agents, but decellularization techniques are usually categorized as physical, chemical, enzymatic, or a combination of the three [12].

Chemical treatment often involves removal of cells with chemical detergents (surfactants). The two most common detergents are sodium dodecyl sulfate (SDS) and

Triton X-100; they are nearly ubiquitous in the field. SDS is an ionic detergent and functions by solubilizing DNA and lipid membranes, as well as disrupting covalent protein-protein bonds. The main drawbacks of SDS are residual cytotoxicity and disruption of glycosaminoglycans (GAGs) and other ECM molecules [122, 164]. Triton X-100 is a non-ionic detergent that solubilizes proteins; it is less disruptive to ECM, but fails to decellularize denser tissues [165]. Zwitterionic detergents, such as tributyl phosphate [166] and CHAPS [160], maintain the native charge and state of proteins and are often effective in decellularizing thin tissues. Any detergent will eventually cause ECM degradation, so they are usually limited to very low concentrations and/or short treatment times [167]. Chemical treatment can also include acids, bases, or organic solvents, though these can significantly alter ECM mechanical properties and chemical composition and are less common [155, 168]. Of particular note for this study is Lumpkins' use of ethanol in decellularization. As in Sawada's work, considerable dehydration was reported, with ECM stiffness increasing threefold [168].

Biological agents can destroy and remove cellular material from tissues. In particular, certain enzymes can break the bonds in large organic molecules, such as peptides and nucleotides. For example, in adipose decellularization, Choi *et al.* used DNase and RNase in conjunction with SDS to achieve more complete decellularization than SDS alone [149]. Chelating agents, such as EDTA, can aid cell removal by increasing membrane permeability and by breaking adhesions between cells and the ECM via disruption of calcium transfer [169].

Finally, physical treatment can be used to detach cells from the ECM. Agitation and sonication are used to burst cells or dislodge them from the ECM [15, 170]. High

hydrostatic pressure (HHP) followed by extended washing has been used to decellularize aortic tissue [171], suggesting potential for $scCO_2$ in decellularization, as its pressure is far lower than HHP. Another common physical treatment is electroporation, where cell membranes are lysed by electrical pulses [172, 173]. These and other physical decellularization methods, such as temperature treatment and pressure gradients, are described in greater detail by Keane *et al.* [13].

Of particular note for this dissertation is the decellularization of blood vessels by Simionescu's group [151, 174, 175]. In particular, they have had considerable success with immersion decellularization of aorta and aortic roots using a 16-day treatment of SDS, Triton X-100, sodium deoxycholate, and EDTA followed by 4 days of enzymatic treatment. The resulting ECM was acellular and responded well to biaxial mechanical testing [17]. The group also created elastin scaffolds for arterial TE in diabetic patients by decellularizing in sodium hydroxide, which removed most of the collagen [9]. Though these scaffolds are of excellent quality, they are time-consuming to produce. If successful, $scCO_2$ decellularization would offer a significant reduction in treatment time.

The term "decellularization" once referred primarily to the treatment of tissues, small layers of cells that compose part of an organ. Now, much research is being done on whole-organ decellularization. This potentially represents a great improvement in fabrication efficiency because macroscopically large volumes can be decellularized using just one treatment process, with the ultimate objective being the ability to engineer and mass-produce entire organs for patients in need of organ transplants [176]. Most whole-organ decellularization processes use a technique called perfusion to apply the decellularizing agent. A perfusion system involves connecting a small tube to the native

vasculature (*e.g.* Baptista *et al.* chose the portal vein in whole liver decellularization [159]) and then applying a small flow (usually on the order of 1 mL/min) of one or more decellularizing agents throughout the organ's vasculature for several hours or days [177]. This can uniformly decellularize a three-dimensional structure. Recellularization has proven extremely challenging, but is usually attempted using a perfusion bioreactor with cell media.

Because of the many different treatment types and the lack of universal standards for both decellularization and ECM properties, it is difficult to compare different decellularization protocols and results. The characteristics of a successfully decellularized tissue or organ are generally agreed upon in the field – the material should be (1) acellular, (2) sterile, and of the same (3) mechanical strength (4) biochemical composition and bioactivity as before treatment. Yet, there is little-to-no agreement on quantitative standards to determine if these criteria have been met, and the ability to confirm decellularization is critical given the severe inflammation and rejection caused by implantation of an incompletely decellularized construct [10].

Crapo *et al.* addressed this lack of a universal standard in their 2011 decellularization review [12], and suggested the following characteristics to define a fully decellularized material:

1. Less than 50 ng of double-stranded DNA per mg ECM (dry weight)
2. DNA fragment length of less than 200 base pairs
3. No "visible nuclear material" after DAPI and/or H&E staining

However, this has yet to become a widespread standard, and in their words the standard "may be too stringent, sufficient, or too liberal." Furthermore, this decellularization

standard only addresses the first of the four points mentioned above. Desired sterility of implanted medical devices, including xenogeneic scaffolds, has been established by the FDA at 6 log reduction of pathogens [37]. However, quantitative standards on the mechanical and biochemical properties of decellularized scaffolds are still needed.

Chapter 3 Fundamental Interactions of Type I Collagen and Dense-Phase CO_2

3.1 Introduction

Collagen is the most abundant protein in the human body and has been studied at length as a biomaterial for TE scaffolds [121]. Some common methods for fabricating collagen scaffolds include electrospinning [146], lyophilization [130], extrusion [8], and gelation [178]. The advantages of collagen scaffolds are numerous. Collagen is a key player in tissue growth and remodeling, having been shown to direct cell adhesion, migration, and proliferation [126]. Collagen has low immunogenicity and antigenicity, is porous and permeable, and its biodegradation rate can be controlled by the extent of crosslinking [123]. It also elicits an anti-inflammatory immune response rather than the pro-inflammatory response of many synthetics [4]. There are numerous sources of collagen available, including mammalian [179], fish [128], and recombinant [129].

The main disadvantage of collagen as a scaffold material is that it lacks adequate mechanical strength, especially when hydrated [121]. For this reason, collagen is often treated improve its mechanical strength; in fact, collagen has been treated ever since the first production of leather many decades ago [180]. One approach is material blending, the addition of a second biomaterial to improve mechanical strength. The primary advantage of material blending is that it allows the engineer to tailor the properties of the scaffold based on the properties of the material chosen. Materials commonly added include natural polymers like silk fibroin [181], synthetic polymers like

poly(ε-caprolactone) [142], carbon fibers or nanotubes [182], and ceramics such as hydroxyapatite [144].

Collagen is also commonly processed using solvents. One reason for such treatment is crosslinking, which improves the mechanical strength of collagen without the need of material blending. Physical crosslinking is accomplished by ultraviolet irradiation or dehydrothermal treatment [135]. Also quite common is chemical crosslinking, often done with glutaraldehyde [136]. However, glutaraldehyde is cytotoxic if not fully removed [18], and the removal process is often difficult. Less hazardous crosslinkers have also been pursued recently, including carbodiimides [138], genipin [139], and riboflavin [140]. Collagen is treated with alcohols and phenols in other applications, but these compounds can affect the thermal and conformational stability of the collagen triple helix [183].

Given the extensive amount of collagen processing that occurs, novel solvents could significantly benefit the field. One solvent that we feel has been overlooked is supercritical CO_2. Below its critical temperature and pressure, a pure fluid can exist in two-phase vapor-liquid equilibrium. But upon exceeding the critical values, a pure fluid exists as a one-phase supercritical fluid. Supercritical fluids have low diffusivities and viscosities like gases, but high densities like liquids; these properties make them desirable solvents [21]. Supercritical CO_2 is of particular interest because of its unusually low critical temperature of 31.1°C, allowing treatment of biomaterials at physiologic temperature (37°C). CO_2 is also non-toxic, non-flammable, chemically inert, and readily available. Supercritical CO_2 has already been utilized in a number of other biomedical applications, including extraction of biomolecules [25, 73, 80], polymer foaming [28,

29], decellularization [43], and sterilization, a focus area for our group [30-37, 104, 116]. Additionally, Reverchon's group recently used $scCO_2$ to extract residual glutaraldehyde from a crosslinked chitosan aerogel [41]; the same is almost certainly possible for collagen scaffolds.

Very few published reports of $scCO_2$ treatment of collagen exist, and they are very development-oriented, such as sterilization of collagen sponges [184] and infusion of transglutaminase into leather [185]. To our knowledge, no one has studied the fundamental interactions between collagen and $scCO_2$ or assessed their chemical compatibility. Chemical compatibility exists if two molecules do not react when one is exposed to the other, and if exposure does not cause thermal phase changes in one or both species (in the specific case of proteins, the phase change is denaturation) [186, 187]. Additionally, there has been no published study on treatment of collagen with liquid CO_2. CO_2 in the liquid phase can be desirable for applications constrained by equipment cost or the higher temperatures or pressures needed for $scCO_2$. [32, 33, 104]. Liquid CO_2 is known to be compatible with crystalline synthetic polymers [116], making collagen a likely candidate for liquid CO_2 compatibility given its high crystallinity.

The objective of this study is to observe how the native collagen triple helical structure responds to treatment with liquid and supercritical CO_2. This will be done by analysis of three properties before and after CO_2 treatment: (1) thermal stability, (2) molecular weight distribution, and (3) changes in secondary structure. After establishing how dense-phase CO_2 and collagen interact, viable applications for CO_2 processing of collagen will be elucidated.

3.2 Materials and Methods

The experiments performed were chosen to determine how liquid and supercritical CO_2 affect the physical and biochemical properties of type I collagen.

3.2.1 Collagen Fiber Extrusion

A 1% (w/v) type I bovine corium collagen dispersion in water was obtained from the Yost group (Medical University of South Carolina, Charleston, SC), prepared in their lab as described previously [4]. The collagen was extruded into fibers based on the method of Dunn's group [181]. An aliquot of collagen was thawed overnight at 4ºC and the pH was reduced to 2.4 using 1 M hydrochloric acid. The collagen was vortexed once every 10 min for 30 min (3 times total) and then centrifuged at 5000 rpm for 15 min to degas. During vortexing and centrifugation, a fiber formation buffer (FFB) was prepared. This buffer consisted of 0.135 M NaCl, 0.03 M N-[Tris(hydroxymethyl)methyl]-2-aminoethanesulfonic acid (TES), and 0.03 M sodium phosphate dibasic heptahydrate (SPDH). The buffer was heated to 37ºC and sodium hydroxide pellets were added to increase the pH to 7.5.

After collagen centrifugation, the FFB was poured into a Pyrex container with large surface area and the collagen dispersion was loaded into a syringe pump attached to 1.59 mm (1/16 inch) diameter polyethylene tubing. The collagen was then extruded through the tubing and into the FFB at a 0.1 mL/min flow rate. The self-assembled fibers, usually 10-15 cm in length and 1.5 mm in diameter, rose to the surface from buoyancy forces. After 10 minutes, the FFB was siphoned and replaced with isopropanol and the fibers were soaked for 4 hr to remove residual buffer. Finally, fibers were

removed from the isopropanol and dried overnight under the tension of their own weight. Dried collagen fibers were stored at room temperature until CO_2 treatment.

3.2.2 Dense-Phase CO_2 Treatment

Collagen fibers were placed in a 25 mL cylindrical stainless steel pressure vessel with threaded endcaps (Waters Corp., Milford, MA) and secured in an upright position using small rare earth magnets prior to treatment with CO_2. Fibers were treated with dense-phase CO_2 in one of two states: the liquid phase, 8 MPa and 10°C (ρ_{CO2} = 0.903 g/mL), or the supercritical phase, 20 MPa and 37°C (ρ_{CO2} = 0.856 g/mL), under dynamic conditions (1 mL CO_2/min).

A schematic of the apparatus used can be viewed in Figure 3.1. Bone-dry grade carbon dioxide (1) (99.8% purity with siphon tube, Airgas National Welders, Charlotte, NC) was compressed in a chilled syringe pump (3) (500 HP Series, ISCO Inc., Lincoln, NE) and slowly injected into the pressure vessel (4), which was maintained at the desired temperature by the environmental chamber (5) (ESPEC Corp. LU-113, Osaka, Japan). The pressure in the vessel was maintained by a back-pressure regulator (6) (TESCOM, Elk River, MN). After 1 hr of exposure to CO_2, the system was depressurized at a controlled rate of 0.34 MPa/min (50 psi/min) using a manual hand pump (7) (High Pressure Co., Erie, PA). Valves and fittings rated for pressures up to 68.9 MPa (2) (High Pressure Co., Erie, PA) were used throughout the system.

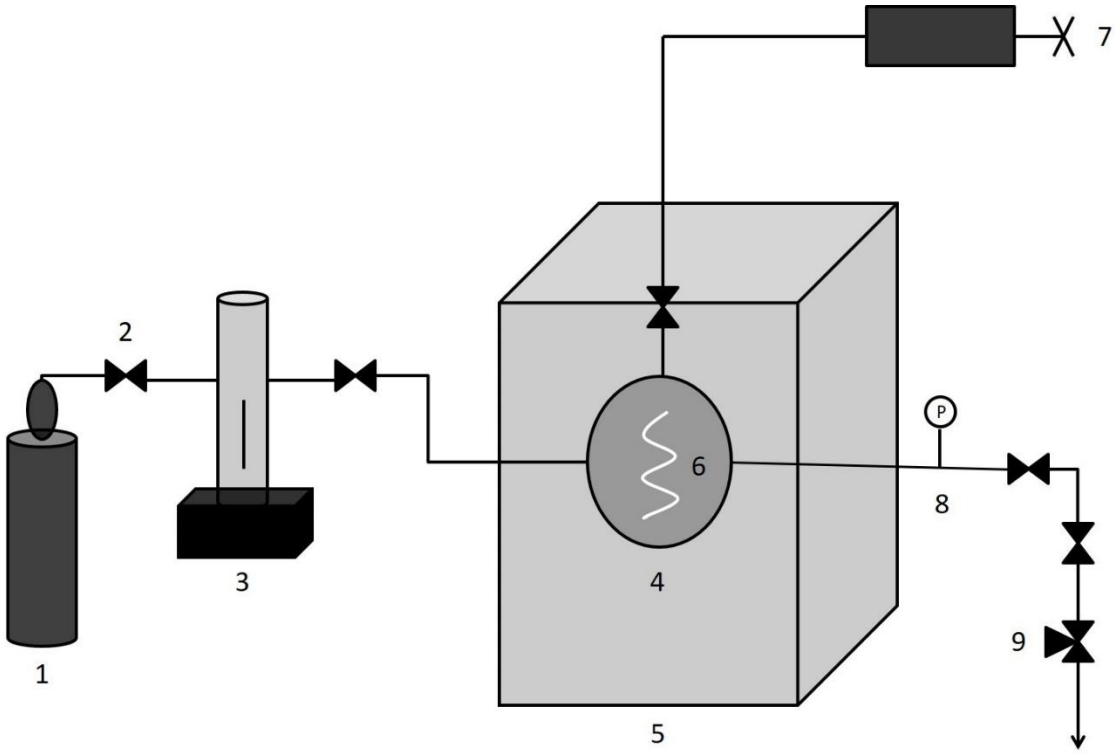

Figure 3.1 – Collagen Fiber Testing Schematic: 1 – CO_2 Supply; 2 – High Pressure Valve; 3 – Syringe Pump; 4 – Environmental Chamber; 5 – Presaturation Chamber; 6 – Collagen Fiber; 7 – Manual Hand Pump; 8 – Pressure Gauge; 9 – Back-Pressure Regulator

3.2.3 Bicinchonic Acid Assay

Protein concentrations of solutions used in the following sections were determined using the bicinchonic acid (BCA) assay. To perform the BCA assay, 25 μL of a solution of unknown protein concentration was loaded into one or more wells in a 96-well plate and mixed with 200 mL of the BCA working reagent (Thermo Scientific, Waltham, MA). The unknown samples and a set of known bovine serum albumin (BSA) standards were scanned at 562 nm with microplate reader. Optical density readings of the BSA standards were used to create a standard curve, which was subsequently used to determine the concentration of the collagen solution.

3.2.4 Differential Scanning Calorimetry (DSC)

Collagen fibers were characterized using DSC to ascertain possible changes in thermal stability caused by CO_2 treatment. After CO_2 treatment, collagen fibers were dissolved in 4% v/v (0.7 M) acetic acid to create a collagen solution with 1 mg/mL collagen concentration. Each solution was degassed for 15 min using a vacuum desiccator and magnetic stirring bar before testing. After doing a baseline scan of acetic acid, the degassed collagen solution was carefully added to the sample port of the Nano DSC (TA Instruments, New Castle, DE). The instrument was pressurized to 3 atm (gauge) and the sample was heated from 15 to 100°C at a rate of 2°C/min. Data were recorded and analyzed with the NanoAnalyze software accompanying the instrument.

3.2.5 Sodium Dodecyl Sulfate Polyacrylamide Gel Electrophoresis (SDS-PAGE)

After CO_2 treatment, collagen fibers were dissolved in 4% acetic acid. Laemmli sample buffer (Bio-Rad, Hercules, CA), which contained 62.5 mM Tris-HCl (pH 6.8), 2% SDS, 0.01% bromophenol blue, and 25% glycerol, was reduced with β-mercaptoethanol (βME) to a βME concentration of 5% and then mixed with the four collagen solutions: untreated, liquid CO_2-treated, scCO_2-treated, and thermally denatured collagen (used as a control). The solutions were heated for 10 min at 80˚C using a water bath. After cooling to ambient temperature, 10 μg of protein was loaded into the wells of a 4-15% acrylamide Mini Protean TGX gradient gel (Bio-Rad). Running buffer (Tris-Glycine buffer, Bio-Rad) was added and electrophoresis was conducted at a constant 100 V until the dye front approached the bottom of the gel. Precision Dual Color Standards (Bio-Rad) were used as molecular weight markers in the leftmost well.

After electrophoresis, the gel was separated from the plastic cover and washed three times with deionized water for 5 min each. The water was decanted and the gel was stained for 1 hr on an orbital shaker using 50 mL of Coomassie Brilliant Blue R-250 stain (Bio-Rad). The gel was washed for 30 min in deionized water and then photographed to observe protein bands.

3.2.6 Circular Dichroism (CD)

The same collagen treatments studied in SDS-PAGE were dissolved in 10 mM sodium phosphate and studied using a CD spectropolarimeter (Jasco J-815, Oklahoma City, OK). Collagen solutions were analyzed at concentrations of 10, 15, and 20 μg/mL, and a thermally-denatured collagen solution was used as a negative control. Nitrogen

flow set to 10 L/min. After waiting 30 minutes for the xenon lamp to reach full power, 1 mL of each collagen solution was added to a quartz cuvette. CD scans were run at scan rates of 20 and 50 nm/sec over a 250-190 nm wavelength range. Data were exported to Excel and saved to a USB drive.

3.2.8 Statistical Analysis

Graphs and tables show the mean value plus or minus one standard deviation. A Student's *t*-test was used to determine statistical differences between groups. 95% confidence ($p < 0.05$, indicated by *) was considered statistically significant, while 99% confidence ($p < 0.01$, indicated by **) was considered extremely significant.

3.3 Results and Discussion

Though collagen processing and compressed CO_2 have each garnered attention in the TE field, little is known about the fundamentals of how the two interact. In this study, chemical compatibility of type I collagen with liquid and $scCO_2$ was assessed by studying changes in thermal stability (DSC), molecular weight (SDS-PAGE), secondary structure (CD), and water content (vacuum drying). If native collagen is chemically compatible with either or both CO_2 treatments, then applied processing can be explored. Though chemical compatibility is studied directly, mechanical compatibility can also be inferred given the temperatures and pressures required for dense-phase CO_2 to exist.

3.3.1 Thermal Stability

For CO_2 to be practical in collagen processing, maintaining the thermal stability of the protein is crucial. If collagen is denatured by heat, the crystalline regions collagen melt and it loses functionality like any other protein [188, 189]. Native collagen at mildly acidic pH is reported to denature at temperatures as low as 39-40°C [183]. This makes $scCO_2$ treatment a concern because treatment at physiologic temperature (37°C) approaches this threshold.

The thermal stability of treated and native collagen was assessed by DSC. A sample DSC thermogram of untreated collagen is shown in Figure 3.2. This thermogram shows two characteristic peaks: a minor peak at 32-33°C and a major peak at 38-40°C, that were consistently observed in collagen denaturation. This suggests a bimodal denaturation process, as recently observed by Staicu *et al*. under similar conditions [190]. They propose that the initial small peak is caused by the disassembly of supramolecular complexes (*i.e.* separation of collagen molecules from one another) and the large second peak indicates the unfolding of each triple helical molecule into a random coil formation.

Table 3.1 shows that $scCO_2$ treatment does not have a significant impact on the height or temperature of either peak, indicating that the thermal stability of collagen is not substantially altered by $scCO_2$ treatment. This result indicates thermal compatibility, likely because the uncharged and nonpolar $scCO_2$ does not disrupt the polar and charged amino acids in collagen. However, Table 3.1 shows that liquid CO_2 treatment significantly reduces the height of both peaks, and sometimes the smaller peak is not even observed. This indicates considerable denaturation during treatment.

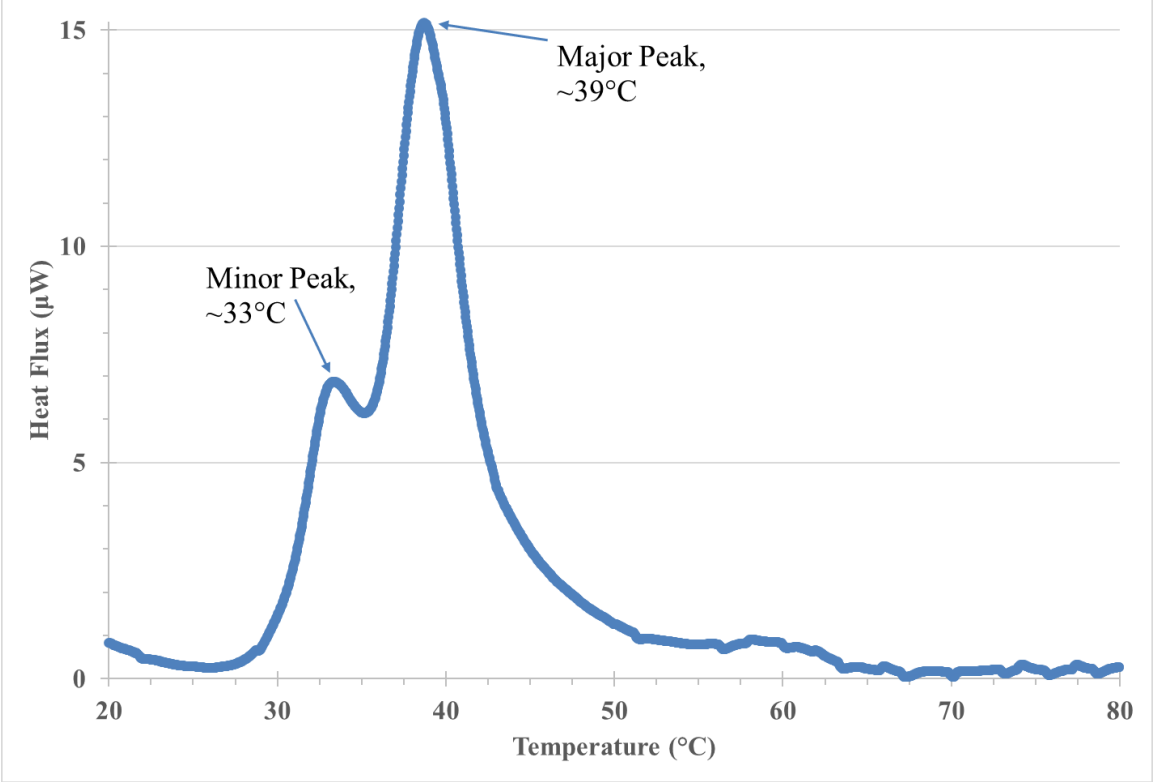

Figure 3.2 – Sample Thermogram of Collagen DSC: Thermogram of native collagen in 4% acetic acid, 0.25 mg/mL. The smaller initial peak represents the unfolding of supramolecular complexes, while the larger peak is the unfolding of the collagen molecule itself.

Table 3.1 – Collagen DSC – Native Collagen

Treatment	Minor T (°C)	Minor Ht. (uW)	Major T (°C)	Major Ht. (uW)
Native	33.1 ± 1.0	8.6 ± 2.5	38.5 ± 0.5	58.6 ± 12.0
Supercritical	33.3 ± 0.3	10.4 ± 3.8	38.3 ± 0.6	47.5 ± 9.7
Liquid	34.2^ ± N/A	3.9^ ± N/A	39.1 ± 0.3	10.5** ± 6.6

^Peak only observed once; the height value of zero was used for other runs.
** $p < 0.01$ compared to native collagen

This finding is surprising, as our previous work with liquid CO_2 at room temperature indicated that crystalline polymers tend to be compatible with liquid CO_2 [116]. Furthermore, the liquid CO_2 treatment was done at milder conditions than $scCO_2$. However, the temperature in this work was 10-15°C below room temperature. At first glance, a temperature difference of only 10-20°C seems unlikely to cause such a drastic change in thermal stability, but further consideration of collagen chemistry reveals several consequences of the temperature difference. Temperature is the most notable factor in protein denaturation, but pH and salt concentration also play a role [191, 192]. Since water is present internally within the collagen structure [179, 193], CO_2 forms carbonic acid in the presence of water, causing a significant pH reduction. Recent studies have shown that collagen is stable at mild pH but denatures readily at high acidity or basicity [194]. pH depression by CO_2 may be exacerbated at lower temperatures because the solubility of CO_2 in water is inversely proportional with temperature.

Although protein denaturing by heating is done routinely, a similar phenomenon by cooling, called cold denaturation, also exists for many proteins [195]. Other studies have shown that long-term freezing of collagen negatively affects its thermal properties, including reducing its heat denaturing temperature by over a degree Celsius [196]. CO_2 density also increases at lower temperatures. However, the liquid CO_2 temperature used in this study was above freezing, and cold denaturation is more commonly observed in globular proteins [197], so internal pH drop is more likely to be the driving force of the observed denaturation during liquid CO_2 treatment.

It was hypothesized that repeating liquid CO_2 treatment at a higher temperature would significantly reduce or even eliminate collagen denaturation, and preliminary

research indicates that this is the case. DSC of a collagen fiber treated with liquid CO_2 at 25°C indicated much less denaturation (see Appendix A). If raising the process temperature is not feasible, a basic additive, such as ammonia, could also counteract the pH drop caused by the interaction of liquid CO_2 and water.

3.3.2 Molecular Weight

The effect of CO_2 treatment on the molecular weight of collagen was determined by gel electrophoresis. Native type 1 collagen would be expected to show a doublet at 139 and 129 kDa, indicating the presence of the α-1 and α-2 helices, and possibly to show a double helix β-band at 258-288 kDa [198]. On Figure 3.3, a band between 150 and 125 kDa is clearly observed for untreated collagen and both CO_2 treatments. There is no Clear band visible above 250 kDa, which indicates that the collagen is broken down into individual α-helices during the preparation step. Comparison of lanes 3, 5, and 7 to the large smear (rather than bands) in lane 9 shows that neither CO_2 treatment completely denatures the protein.

Though an α-helix band is clearly observed in Figure 3.3, it is unclear in the figure if there is one band or two in the 130-140 kDa region. Magnified images of lane 7 are shown in Figure 3.4. A doublet is somewhat observable in image (a), but becomes very clear upon image enhancement in image (b). As expected, the first band, for the α-1 helix at 139 kDa, is about twice the size of the α-2 band at 129 kDa. Overall, the SDS-PAGE results show that both supercritical and liquid CO_2 treatment do not have a significant effect on the molecular weight distribution of collagen.

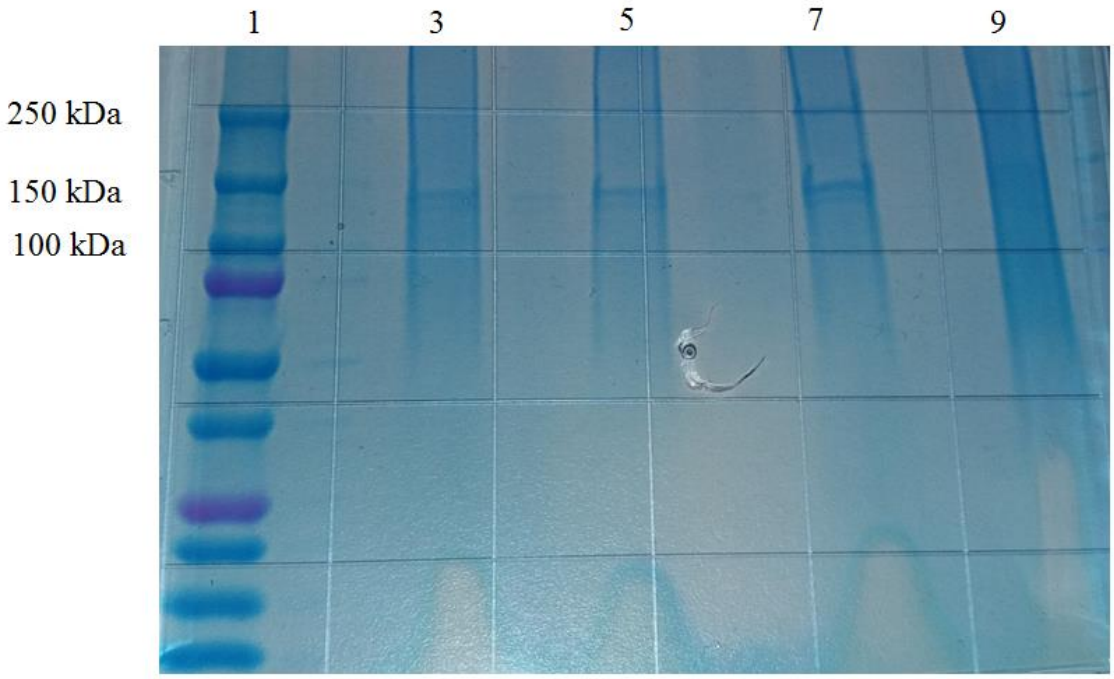

Figure 3.3 – SDS-PAGE Gel Stained with Coomassie Blue: Lane 1 – Protein Standards; Lane 3 – Untreated Collagen; Lane 5 – Supercritical CO_2 Treatment; Lane 7 – Liquid CO_2 Treatment; Lane 9 – Thermally-Denatured Collagen

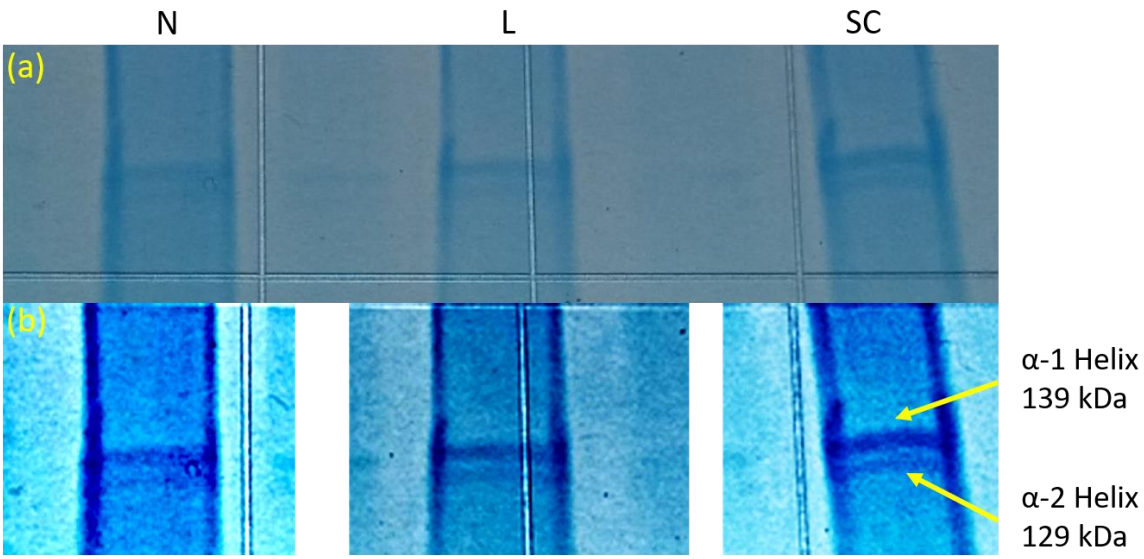

Figure 3.4 – SDS-PAGE Doublet Close-Up: (a) Original photograph, (b) Enhanced photograph. N is native collagen, L is liquid CO_2 treatment, and SC is scCO_2 treatment. Image (b) was enhanced by adjusting the contrast and color saturation levels in Adobe Photoshop. Bands are observed for both the α-1 and α-2 helix present in type I collagen in native collagen and both CO_2 treatments. The α-1 band is roughly twice as large because type I collagen contains two α-1 helices and one α-2 helix.

3.3.3 Secondary Structure

The effects of CO_2 treatment on the secondary structure of collagen were determined using circular dichroism (CD). Normally, triple-helical collagen has a CD spectrum with a positive peak at 225 nm and a negative peak at 205 nm [183]. As collagen denatures, it shifts from helix conformation to a random coil. The same four treatments used for SDS-PAGE were analyzed by CD in the ultraviolet range (190-250 nm); CD spectra for each treatment at the 15 μg/mL concentration are shown in Figure 3.5 (spectra at other concentrations are available in Appendix B). For native collagen (blue), a positive peak is observed at 225 nm and a negative peak at 205 nm, as expected. In contrast, denatured collagen (red) is simply a flat line because denatured collagen has no secondary structure. Mirroring the DSC findings, $scCO_2$ treatment (green) has very little impact on the secondary structure, with very similar peak magnitudes and wavelengths to native collagen. On the other hand, liquid CO_2 treatment (yellow) causes significant changes to the CD spectrum: the magnitude of the positive peak is considerably less, and the negative peak is barely observable. These changes suggest a conformational shift toward random coil, since the random coil conformation has a positive peak near 210 nm that would counteract with the negative peak observed at 205 nm in native collagen [199].

The finding that liquid CO_2 disrupts collagen secondary structure may appear to contradict the SDS-PAGE findings, which indicated no protein damage by liquid CO_2 treatment, but this is not the case. CD measures secondary structure, which is clearly disrupted by liquid CO_2 treatment. Proteins studied in SDS-PAGE, however, must be linearized for bands to form; *i.e.* their secondary structure must be fully removed

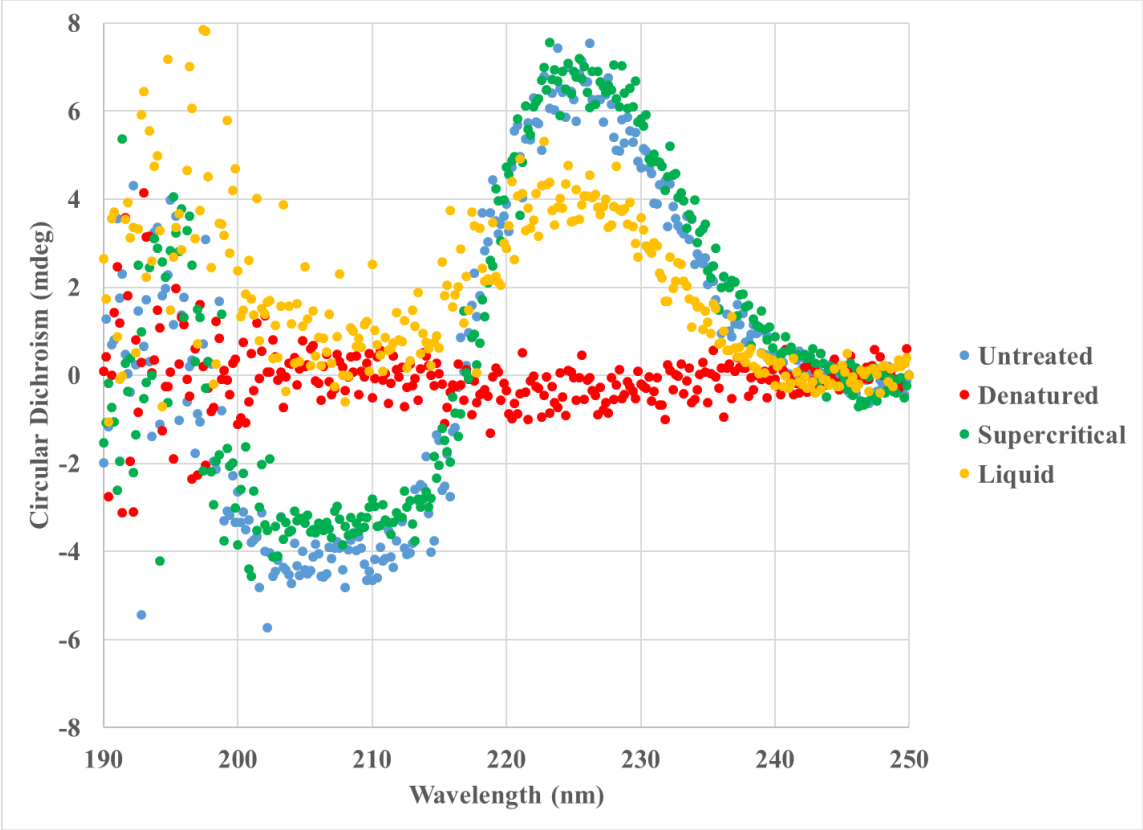

Figure 3.5 – Circular Dichroism Spectra of Collagen CO_2 Treatments: In untreated triple helical collagen, a positive peak is observed at 225 nm and a negative peak at 205 nm. Similar results are observed for supercritical CO_2 treatment, but response is dampened for liquid CO_2 treatment. Denatured collagen shows no peaks, as expected.

(this is done with βME and the 10-minute heating step; see section 3.2.5). Therefore, one can conclude that liquid CO_2 treatment partially denatures collagen – *i.e.* it is disruptive enough to affect the secondary structure, but not enough to affect the primary structure.

It is worth noting the large amount of CD scatter observed at wavelengths below 200 nm. This is a common problem with some CD buffer solutions, where a considerable amount of noise is encountered in the high frequency part of the ultraviolet region (usually between 180 and 200 nm). Several attempts were made to reduce this noise, but they were unsuccessful in reducing the noise while still maintaining sharp peaks. Fortunately, no characteristic collagen CD peaks are found in the low wavelength region for either the triple helix or random coil conformations, so the noise did not meaningfully affect data collection or results interpretation.

3.4 Conclusions

In this chapter, the effects of supercritical and liquid CO_2 treatment on the chemical and physical properties of type I collagen fibers were investigated. Analysis by differential scanning calorimetry found minimal alteration of collagen thermal stability by $scCO_2$ treatment, but significant denaturation from liquid CO_2 treatment. This surprising result may be attributable to internal pH drop caused by the low temperature used during this treatment; preliminary data indicate better compatibility at higher temperatures.

SDS-PAGE showed no significant changes in collagen molecular weight during either CO_2 treatment, as the characteristic α-helix doublet was observed in both. CD

spectra of $scCO_2$-treated collagen showed only a small effect on peak height and no change in peak wavelength, but liquid CO_2 treatment caused a significant reduction in peak height and also shifted the negative peak toward a higher wavelength, indicating a transition from helical conformation to random coil structure. Again, this finding may be caused by the treatment temperature used.

In summary, it can be concluded from this study that $scCO_2$ and type I collagen are chemically compatible, and it would be sensible to consider utilization of $scCO_2$ in more practical collagen processing applications, such as sterilization, scaffold production, and extraction of residual crosslinking agents. Liquid CO_2 partially denatures collagen at the conditions studied, though preliminary data indicates that increasing the temperature could improve compatibility. Since the supercritical phase is generally preferred because of its superior transport properties, only $scCO_2$ was studied for the remainder of this dissertation.

Chapter 4 Extracting Glutaraldehyde from Crosslinked Collagen with $scCO_2$

4.1 Introduction

Since the emergence of TE as a scientific field, collagen has been utilized in TE scaffolds [180]. Collagen is found ubiquitously throughout the human body and has very low immunogenicity and antigenicity. Collagen can be molded into scaffolds of various sizes and morphologies in both the solid and liquid/gel state; some examples of this include electrospun scaffolds [200], lyophilized collagen [130], and collagen hydrogels [198]. These methods allow collagen scaffolds to be tailored to have a desired porosity and permeability. Furthermore, collagen has been proven influential in orchestrating the adhesion, migration, and proliferation of cells during tissue growth [126]. Collagen scaffolds also evoke an anti-inflammatory wound healing immune response [4].

However, collagen does have one major weakness as a TE scaffold material: its lack of mechanical strength. Because of this deficiency, untreated collagen is rarely used as the sole material in fabrication of TE scaffolds. There are two approaches commonly utilized to circumvent this problem. The first is blending collagen with another biomaterial [121]. A number of biomaterials have been used for this purpose, including natural polymers [201], synthetic polymers [142], carbon nanotubes [145], and ceramics [144]. This approach increases the mechanical strength, but risks increasing immunogenicity. It also increases the complexity of scaffold design and post-fabrication processing steps, such as sterilization and removal of residuals.

The other approach is crosslinking collagen to augment its mechanical strength. Crosslinks are covalent bonds formed between adjacent polymer chains that increase the mechanical strength of a polymer. Such bonding can be photo-activated using ultraviolet (UV) irradiation, but UV crosslinking can denature proteins and is ineffective for thick samples because of its non-uniform penetration depth [135]. Chemical crosslinking is often more effective; in particular, glutaraldehyde is a reagent that has been shown to achieve a high degree of crosslinking at relatively low concentrations [202]. However, residual glutaraldehyde is extremely cytotoxic. Speer's group showed that as little as 3 ppm of glutaraldehyde in cell media can kill over 99% of fibroblasts [137], and glutaraldehyde is also a known carcinogen [203]. Crosslinked TE structures often must undergo a rigorous heating process to remove residual reagents; this can be unsuitable for the physical and biochemical properties of collagen scaffolds [204]. Recently, more attention has been given to alternative crosslinking agents, such as EDC [138], genipin [139], and riboflavin [140], but these are relatively unexplored and may be less potent than glutaraldehyde [141].

If residual glutaraldehyde were removed using a faster and less disruptive method, it could significantly benefit collagen TE research. The objective of this study was to develop a process to extract residual glutaraldehyde from crosslinked collagen films using $scCO_2$. $scCO_2$ is formed when pure CO_2 is heated and pressurized above the critical conditions of 31.1°C and 7.38 MPa. These relatively mild conditions are suitable for processing biomaterials. In particular, $scCO_2$ has been used to extract numerous biomolecules, including essential oils [26], caffeine [69], and fatty acids [205]. It has

also been used in several other biomedical applications, including critical point drying [57], pasteurization [23, 93], and sterilization [30-32, 34-37].

Recently, Reverchon's group used $scCO_2$ with an ethanol additive to extract residual glutaraldehyde from crosslinked chitosan aerogels [41]. They found that an 8 hour CO_2 treatment could reduce glutaraldehyde levels below 1 ppm, and in some cases even below 0.1 ppm. This is a critical finding for gel TE, as the standard heating process to remove residual glutaraldehyde would exceed the glass transition temperature of the biomaterial and cause collapse of the aerogel structure. An analogous finding for collagen TE would be of similar benefit.

Additionally, it was desired to quantify any possible effects or alterations to the chemical and physical properties of crosslinked collagen caused by $scCO_2$ treatment. This was accomplished by comparing the thermal stability and mechanical properties of treated films to untreated films. Maintaining the thermal and mechanical properties of collagen during glutaraldehyde extraction is important for preserving scaffold functionality in downstream applications.

4.2 Materials and Methods

4.2.1 Fabrication of Collagen Films

A 1% (w/v) type I collagen dispersion was obtained from the Yost lab; it was prepared by their group as described previously [4]. Collagen films were prepared according to the protocol of Weadock *et al* [206]. 1 M hydrochloric acid was added to 2 mL aliquots of collagen until reaching pH 2. The acidified collagen was poured into a 35 mm diameter petri dish (BD Falcon, Tewksbury, MA), covered with aluminum foil, and

air-dried in a chemical fume hood for 48 hr. The resulting dried film was then carefully removed using fine forceps, cut into 2 cm x 0.5 cm rectangular strips, and stored at room temperature pending further experimentation.

4.2.2 Glutaraldehyde Crosslinking

To crosslink the films, a 25% (v/v) glutaraldehyde solution (TCI America, Portland, OR) was diluted with deionized water to either 0.25% or 1%, as desired. The solution was vortexed for 1 min at high speed to ensure uniform mixing, then a collagen film strip was carefully immersed in the solution. The film and glutaraldehyde solution were left undisturbed for 72 hr, then the film was removed and washed several times with deionized water before further treatment.

4.2.3 Glutaraldehyde Extraction using $scCO_2$

Crosslinked collagen films were loaded into the treatment chamber of a two-chamber $scCO_2$ flow system, shown in Figure 4.1. The main difference from Figure 3.1 is the addition of a second high-pressure vessel (5). Here, ethanol was mixed with $scCO_2$ until it was fully dissolved (no more than 1 min). Then, the valve to the treatment chamber (6), which contains the collagen film to be treated (7), was opened, and $scCO_2$ flow was set to 2.5 mL/min (residence time: 4 min). Design of the presaturation system is discussed in greater detail in Chapter 5.

As done previously, the temperature was maintained at 37°C by the environmental chamber, (4), and the pressure of the $scCO_2$ in the vessels was maintained at 20 MPa (2900 psi) using a back-pressure regulator (10). A manual hand pump (8) was

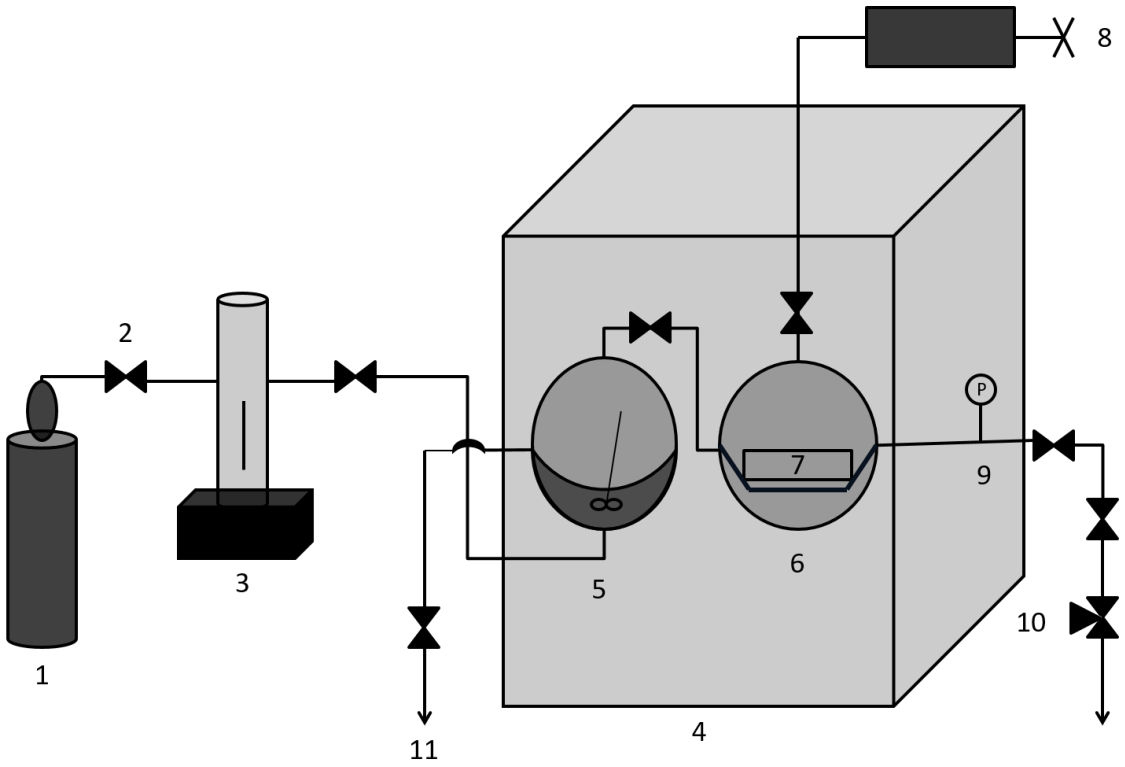

Figure 4.1 – Glutaraldehyde Extraction Schematic: 1 – CO_2 Supply; 2 – High Pressure Valve; 3 – Syringe Pump; 4 – Environmental Chamber; 5 – Presaturation Chamber and Stirring Bar (ethanol additive); 6 – Treatment Chamber; 7 – Collagen Film; 8 – CO_2 Hand Pump; 9 – Pressure Gauge; 10 – Back Pressure Regulator; 11 – Emergency Vent

used to depressurize the system at a rate of 0.34 MPa/min (50 psi/min). Valves and fittings rated for pressures up to 68.9 MPa (2) were used throughout the system.
As a control, glutaraldehyde was separately removed from crosslinked collagen films by heat treatment for 12 hr at 120°C using a vacuum oven according to the protocol of Yang *et al* [204].

4.2.4 Measurement of Residual Glutaraldehyde

The concentration of residual glutaraldehyde was measured using a spectrophotometric method first performed by Bigi *et al*. [207]. Crosslinked collagen films were placed in a quartz cuvette (VWR, Radnor, PA) before and after $scCO_2$ treatment. The cuvette contained 3 mL phosphate buffered saline (PBS) with 0.1 M glycine. The presence of glycine has been shown to counteract the gradual pH drop normally observed with proteins in PBS solutions.

The cuvette was immediately placed into a UV/visible spectrophotometer (Beckman-Coulter DU 730, Brea, CA), which was utilized in Kinetic/Time mode to measure the optical density of the solution at 260 nm every 1 min. Typically, glutaraldehyde was released from the film over the course of 2-4 hr. Separately, a standard curve was generated for known concentrations of glutaraldehyde in the PBS/glycine solution; the standard curve was used to determine the unknown concentration of residual glutaraldehyde in each collagen film.

4.2.5 Differential Scanning Calorimetry

Crosslinked collagen films were studied before and after $scCO_2$ treatment using DSC to analyze their thermal stability. Films were dissolved in 4% acetic acid overnight under gentle stirring. Collagen solutions were next degassed for 15 min using a vacuum desiccator and magnetic stirring bar. The degassed collagen solution was pipetted into to the sample port of the DSC instrument after performing a baseline scan with acetic acid as the reference solution. The instrument was pressurized to 3 atm (gauge pressure) and the sample was heated from 10 to 90°C at 2°C/min. Data were obtained using instrument-associated RunDSC and NanoAnalyze software and then were exported to Excel for further analysis.

4.2.6 Tensile Testing

A uniaxial tensile test to failure was used to analyze the modulus of elasticity (MOE) and ultimate tensile strength (UTS) of collagen films before and after $scCO_2$ treatment. Collagen films were loaded onto a Bose 3230 Electroforce Biomechanical Tester (Bose Corp., Farmingham, MA) and one end was stretched at a rate of 0.01 mm/s until failure. The accompanying Wintest 4.1 software was used to control the experiment and collect data, which was exported to Excel for further analysis.

4.2.7 Statistical Analysis

Graphs and tables display the mean value plus or minus one standard deviation. A Student's *t*-test was used to determine statistical differences between groups. 95% confidence ($p < 0.05$, *) was considered statistically significant, while 99% confidence

was considered highly statistically significant ($p < 0.01$, **). All experiments were performed in triplicate ($n = 3$) unless stated otherwise.

4.3 Results and Discussion

Collagen films were prepared, crosslinked with glutaraldehyde, then either used as controls or treated with $scCO_2$ for 1 hour to extract unreacted glutaraldehyde. Treated films were examined for extent of glutaraldehyde removal and for any changes in their physical properties effected by $scCO_2$ treatment.

4.3.1 Glutaraldehyde Extraction

Figure 4.2 shows an example of transient glutaraldehyde release from collagen films before and after $scCO_2$ treatment. The concentration of glutaraldehyde plateaus after all residual glutaraldehyde has leached into the glycine solution. In this example, it is clear that the glutaraldehyde concentration is far greater than the cytotoxic level prior to $scCO_2$ treatment, but well below it afterwards. Similar behavior was observed in all other runs. Glutaraldehyde extraction with $scCO_2$ was effective at both crosslinking concentrations, 0.25% and 1%, as seen in Figure 4.3. Two key findings are noted. First, and most importantly, $scCO_2$/ethanol treatment removes over 95% of residual glutaraldehyde at both crosslinking concentrations. The residual glutaraldehyde concentration after $scCO_2$ treatment is below the reported cytotoxic threshold of 3 ppm in our experiments, though it should be noted that the magnitude of residual glutaraldehyde concentration is dependent on the mass of collagen and volume of PBS/glycine solution

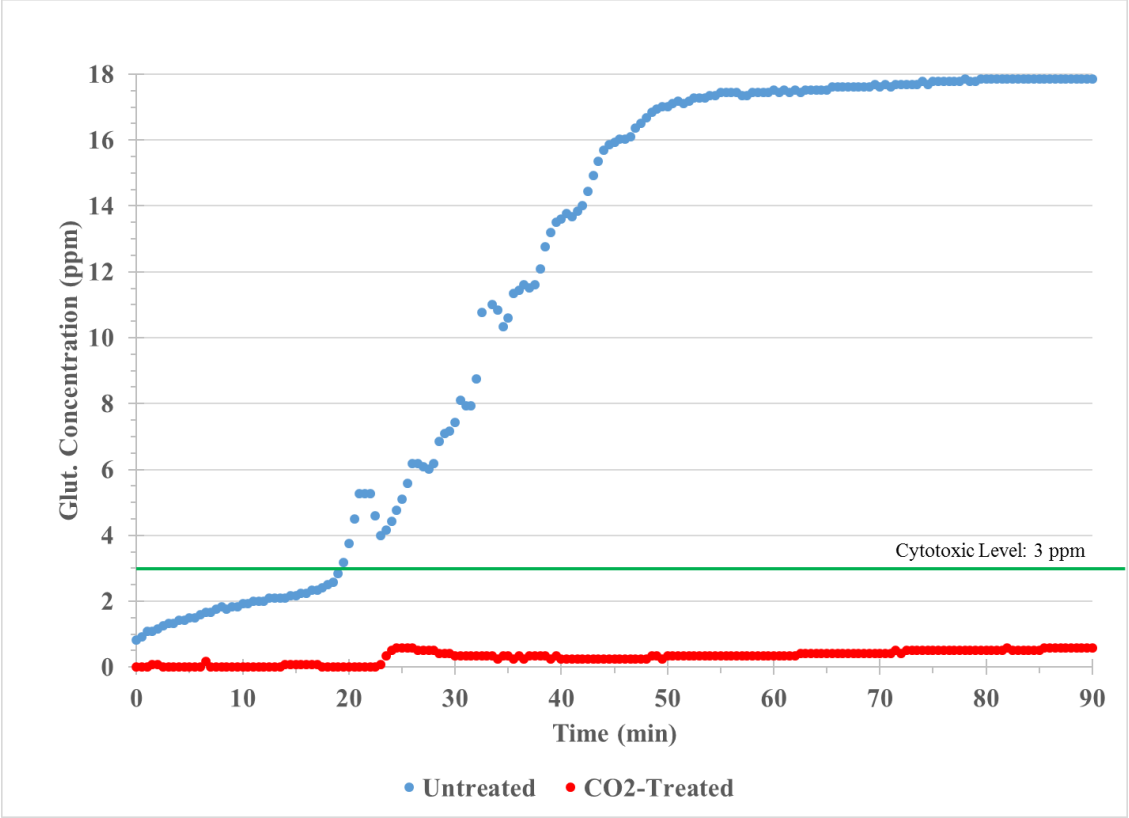

Figure 4.2 – Example Glutaraldehyde Release Curves: Glutaraldehyde leaches from the collagen films at a linear rate until the concentration plateaus. Far less glutaraldehyde is present in the collagen film after $scCO_2$ treatment.

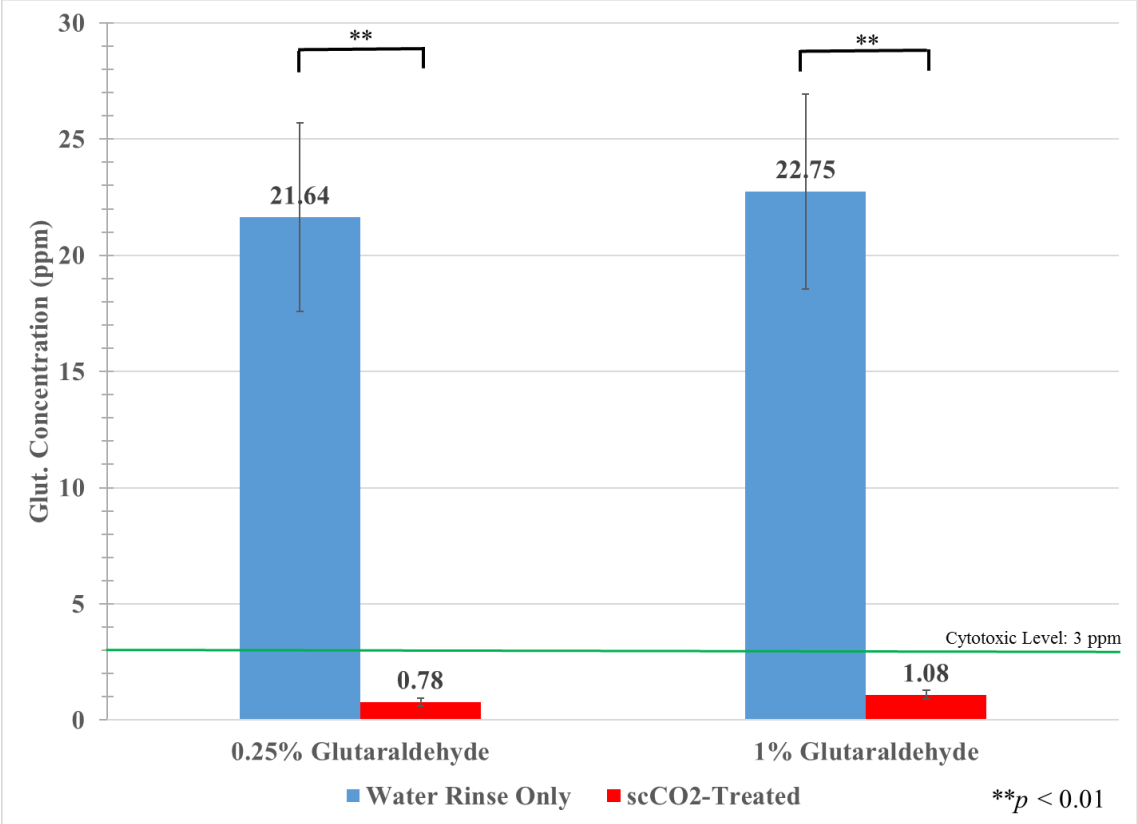

Figure 4.3 – Quantitation of Residual Glutaraldehyde: At both concentrations used, $scCO_2$ extraction of glutaraldehyde reduces the residual concentration by over 95%.

used in the experiment. Another interesting observation is that the similarity between the results observed for 0.25% and 1% glutaraldehyde crosslinking solutions.

One would intuitively expect larger residual glutaraldehyde concentration when a larger concentration is used during crosslinking, but there are several possible explanations for this result. For example, there may be surface porosity and/or mass transfer limitations. Also, the results may be related to extent of crosslinking. It is possible that all of the glutaraldehyde reacts for both solutions, *i.e.* neither 0.25% nor 1% glutaraldehyde is a high enough concentration to fully crosslink collagen. Conversely, the opposite could also be true – the number of amine crosslinking reaction sites on collagen are limited [208], so if 0.25% glutaraldehyde fully crosslinks collagen, then increasing the concentration to 1% will have minimal effect.

In their similar study, Baldino *et al*. found that increasing the mass of glutaraldehyde used during crosslinking led to more residual glutaraldehyde in the matrix after $scCO_2$ treatment (pre-treatment glutaraldehyde concentrations were not reported) [41]. However, this increase was not significant until an extreme excess of glutaraldehyde was used, which could indicate incomplete crosslinking at higher glutaraldehyde concentrations or complete crosslinking even at low glutaraldehyde concentrations. The validity of these theories, particularly those regarding reaction sites and extent of crosslinking, are elucidated by studying the physical properties of the collagen films after $scCO_2$ treatment, especially DSC.

Another result worth further consideration is the rapid glutaraldehyde leaching observed in this work. For example, Figure 4.2 depicts a trial where most of the residual glutaraldehyde leaches into the PBS/glycine solution in 60 minutes. This calls into

question using $scCO_2$ at all when glutaraldehyde can be removed just as quickly by the leaching method. However, the duration of the leaching process is abnormally fast compared to other accounts. Glutaraldehyde leaching is very slow when the residual concentration is below 1 ppm, sometimes taking 24 hr or longer [41, 207]. Such low glutaraldehyde concentrations are likely necessary to avoid cytotoxicity, as media concentrations above 3 ppm inhibit 99% of cells and concentrations as low as 0.5 ppm cause some amount of inhibition [137]. Also, the effects of exposing collagen to PBS and glycine are not confirmed to be benign; salt in particular can affect the thermal stability of collagen [192], whereas $scCO_2$ is non-toxic and highly inert. Finally, leaching of other crosslinking agents, such as genipin or riboflavin, would be even slower since they are larger molecules than glutaraldehyde. For all these reasons, we believe $scCO_2$ has future viability as a crosslinking aid.

4.3.2 Physical Property Analysis

The effect of $scCO_2$ treatment on collagen film properties was studied using two analytical methods: DSC to assess changes in thermal stability, and uniaxial tensile testing to measure alterations in stiffness and tensile strength.

The thermal stability of crosslinked collagen films was studied using DSC; peak heights and denaturing temperatures of crosslinked collagen in 4% acetic acid are listed in Table 4.1. Compared to native collagen, crosslinked collagen has a much higher denaturation temperature and a reduced denaturing peak height. The crosslinking process increases the thermal stability of the protein by introducing covalent bonds, thereby requiring a higher temperature to denature the protein. However, the peak height is

reduced because breaking covalent crosslinks is an exothermic process, while protein unfolding is endothermic [202]. Table 4.1 reveals that $scCO_2$ treatment does not affect the thermal stability of crosslinked collagen, but heat treatment reduces both peak height and denaturation temperature, the former being statistically significant. It is noteworthy that after crosslinking, thermal collagen denaturation is no longer bimodal and only one peak is observed. This is observed because in the crosslinked state, the collagen molecules do not separate from each another before unfolding because they are covalently bonded by the crosslinks, instead of being associated by electrostatic forces only [209].

Uniaxial tensile testing was performed to determine the effects of crosslinking and $scCO_2$ treatment on the mechanical properties of collagen films. The MOE and UTS for each treatment can be found in Table 4.2. Compared to native collagen, crosslinking caused a major increase in UTS and a lesser but still significant increase in MOE – this is expected and confirms the DSC findings that suggest a high extent of crosslinking. The more interesting result is that for $scCO_2$-treated films, the UTS greatly increased with a lesser but still significant increase in MOE. A likely explanation for this is dehydration is the addition of ethanol during $scCO_2$ treatment. Ethanol increases $scCO_2$ polarity, improving solubility of the polar glutaraldehyde molecule (to our knowledge, solubility of glutaraldehyde in pure $scCO_2$ is not documented, but chemistry of similar molecules suggests it is minimal). Though ethanol improves glutaraldehyde solubility, it is also known to substantially increase extraction of water from biomaterials [43, 54].

The implications of biomaterial dehydration vary considerably depending on the material treated and the application. In Baldino's work with chitosan aerogels, for

Table 4.1: Collagen DSC – Crosslinked Collagen

Film Type	Denaturation Temp. (°C)	Peak Height (μW)
Native	39.1 ± 0.4	30.1 ± 8.4
Crosslinked	63.2** ± 0.2	10.0*± 1.9
Crosslinked + $scCO_2$	63.3** ± 0.5	10.6* ± 2.5
Crosslinked + 12 hr heat	59.7** ± 2.7	3.9^ ± 1.8

* $p < 0.05$ compared to native collagen
** $p < 0.01$ compared to native collagen
^ $p < 0.05$ compared to crosslinked control

Table 4.2: Collagen Film Tensile Test Data

Treatment	Modulus (kPa)	UTS (kPa)
Native Collagen	838 ± 141	12.0 ± 2.7
Glut. Crosslinked (72 hr)	1113 ± 220	281** ± 30
Glut. + SC-CO_2	1584* ± 404	1067** ± 211
Glut. + 12 hr heating	N/A^	N/A^

* $p < 0.05$ compared to native
**$p < 0.01$ compared to native
^Heat-treated samples were too damaged to be tested

example, dehydration is probably not a major concern (no mechanical testing was reported in their study), since air is used to purposely remove water from the gels. In other applications, such as scaffold production for long-term storage, a dry product is acceptable or even desirable [210]. However, in a water-rich substrate like a hydrogel, this drying effect is potentially a major hindrance to scaffold function and/or mechanical properties [168]. We have developed a method to prevent dehydration of biomaterials during $scCO_2$ treatment that could be applied to this system to prevent the drying phenomenon [211]; this method will be discussed in considerable detail in Chapter 5 in the context of tissue decellularization.

It should be noted that the mechanical test performed has some limitations. The assumption of a perfectly rectangular geometry used in calculations is not fully accurate for treated films; the crosslinking and CO_2 treatment processes can cause warping around the edges of the films, distorting the original shape. Also, most tissues undergo more complex stressed *in vivo* than the static uniaxial forces applied in this work. Blood vessels, for example, undergo dynamic biaxial forces in both the axial and longitudinal directions that vary with regular changes in blood pressure [212]. Therefore, it is important to assess the mechanical properties of a tissue engineering scaffold or biomaterial based on the intended application.

4.4 Conclusions

In this chapter, a novel $scCO_2$ method for extracting residual glutaraldehyde from crosslinked type I collagen films was presented. In one hour of $scCO_2$ treatment, over 95% of unreacted glutaraldehyde was removed from the films, reducing residual

glutaraldehyde levels below 1 ppm. Very similar results were obtained when 0.25% and 1% glutaraldehyde solutions were used to crosslink the films, likely because all possible reaction sites were utilized at both concentrations.

After $scCO_2$ treatment, DSC and tensile testing were performed to determine any potential effects of $scCO_2$ treatment on the thermal and mechanical properties of the collagen films. The DSC response was essentially unchanged before and after CO_2 treatment in terms of both peak height and denaturation temperature, indicating that CO_2 treatment did not disrupt the thermal stability of the films. Tensile testing caused a significant increase in stiffness compared to the control and an even greater increase in UTS, indicative of supercritical drying caused by the ethanol additive. However, this finding may not be problematic in some applications, and recent work in our lab indicates that biomaterial dehydration is easily preventable if desired. The availability of a fast, innocuous method for removing residual glutaraldehyde from crosslinked collagen films overcomes a significant problem presented in the collagen TE literature. Moving forward, it will be important to assess scaffold biocompatibility after $scCO_2$ treatment and to determine the efficacy of this method for substrates of varying composition, thickness, and morphology.

Chapter 5 Preventing Biomaterial Dehydration with $scCO_2$ Presaturation

5.1 Introduction

Currently in the United States, over 120,000 people are on the national waiting list for an organ transplant, and that number is rapidly increasing [1]. One way to address this problem is the implantation of artificial tissues and organs fabricated via tissue engineering (TE), which would reduce wait times and alleviate the current necessity for tissue and organ donors. However, tissues, organs, and their corresponding extracellular matrices (ECM) are highly complex and differ considerably throughout the body, making the development of functional, biocompatible, and sterile biomaterials very challenging. Potential barriers in the development of both synthetic and naturally-derived scaffolds include dehydration, loss of mechanical strength, chemical alteration of the matrix structure, and residual cytotoxicity when some detergents are used [10, 20, 213].

One promising but underexplored method of fabricating TE scaffolds involves using a SCF as a solvent. In particular, $scCO_2$ is promising for biomedical applications. It is inexpensive, readily available, chemically inert, nontoxic, and nonflammable [21]. It has mild critical conditions of 31.1°C and 7.4 MPa, so processing biological materials can take place at or near physiologic temperature (37°C). Equipment and processes utilizing $scCO_2$ have already been demonstrated in extraction of biological compounds [25, 26, 76-78, 80-83], decellularization [43], pasteurization [22-24, 93-95], and in sterilization of medical devices [33, 104], hydrogels [32], and decellularized ECM [38, 39]. Additionally, $scCO_2$ has been used to aid in hydrogel and polymer foaming [29, 40,

42], crosslinking of chitosan hydrogels [41], and several other TE scaffold fabrication methods [109-113].

Because the $scCO_2$ platform has such versatility, it is important to explore the fundamentals and mechanisms behind the various processes. One issue reported has been undesired dehydration of biomaterials during $scCO_2$ treatment. Water has a small but appreciable solubility in $scCO_2$, around 0.01 mole fraction at mild supercritical conditions [214], which causes gradual dehydration of a material in a dynamic $scCO_2$ system. For example, Sawada *et al.* used $scCO_2$ to decellularize porcine aorta [43]. They reported DNA and cellular removal that would be adequate for the preparation of a naturally-derived TE scaffold, but SCF extraction of volatile substances (primarily water) during treatment caused embrittlement of the ECM, potentially endangering its viability as a scaffold. Because hydrogels also have very high water content, understanding and preventing unwanted water extraction from occurring is of great importance in processing both synthetic and naturally-derived biomaterials with $scCO_2$.

The reported extraction of volatiles during CO_2 treatment is not surprising. In fact, this phenomenon is well-known and is the basis of critical point drying (CPD), a process commonly used in tissue engineering [54] and other applications, such as electronics processing [55] and scanning electron microscopy [57]. The primary advantage of CPD over conventional evaporative drying is that CPD avoids passing through the two-phase vapor-liquid region of the phase diagram. Avoiding this region is desirable for delicate materials that can be damaged by the surface tension that exists at vapor-liquid interfaces [58]. However, in this application, it is desired to avoid any kind of drying.

In this chapter, we address a challenge that will be common to any process, namely, the unwanted removal of water and volatiles from soft biomaterials. We hypothesize that dehydration caused by $scCO_2$ treatment can be significantly reduced or even eliminated by presaturating $scCO_2$ with water prior to treatment. Establishing thermodynamic equilibrium between water and $scCO_2$ will prevent volatile substances from being extracted. The objectives of this chapter are as follows: (1) to construct an apparatus that can presaturate $scCO_2$ with water (*i.e.* achieve dynamic total solubility of water), and (2) to compare the amount of water extracted from two model scaffolds, a poly(acrylic acid-*co*-acrylamide) hydrogel and porcine aorta tissue, using dry and presaturated $scCO_2$. Achieving these objectives will enable further development of $scCO_2$-based TE and decellularization processes.

5.2 Materials and Methods

To prevent water extraction from porcine tissue it is necessary to first achieve dynamic thermodynamic equilibrium (*i.e.* complete saturation) between CO_2 and water. The saturated CO_2 phase is subsequently suitable for treating a TE matrix. The first experimental objective was to ensure that the CO_2 was being fully saturated during the mixing process. Achieving this goal is critical before attempting to decellularize a tissue.

5.2.1 Apparatus Development and Validation

A schematic of the presaturation apparatus used is shown in Figure 5.1. The essential function is to contact flowing $scCO_2$ with liquid water in a temperature-controlled, high pressure vessel. The vessel (5) shown in Figure 5.1 is a 25 mL high pressure stainless steel view cell (Waters Corp., Milford, MA). 10 mL of deionized water

was added to the vessel prior to the start of each run. The vessel was continuously agitated using a stirrer plate and magnetic stirring bar. Temperature was maintained at 50°C by the environmental chamber, (4). The pressure of $scCO_2$ in the view cell was maintained at 13.8 MPa (2000 psi) using a back-pressure regulator (7).

To validate apparatus function, liquid carbon dioxide (1) was compressed in a chilled syringe pump (3) and slowly bubbled into the high pressure vessel. After waiting 15 minutes for thorough mixing, the humidified $scCO_2$ was then flowed at various rates (controlled by the syringe pump) through the vessel and then a cold trap (8), which was maintained at -70°C using an ethanol/dry ice bath to condense dissolved water as the CO_2 exited the system.

The mass of the cold trap was measured after each experiment using an analytical mass balance (Mettler Toledo, Columbus, OH) to determine the amount of water dissolved in the $scCO_2$ at each flow rate. This process is called the dynamic solubility method, where one stream is continuously fed into the system and the temperature and pressure are controlled externally and kept constant [215]. Calibration of this apparatus required validation that $scCO_2$ would be saturated at sufficiently low $scCO_2$ flow rates. It is known that as the flow rate of CO_2 increases in a dynamic flow apparatus, the residence time becomes too short for complete presaturation. Trials were conducted at varying CO_2 mass flow rates (1, 2.5, 5, 10, 15, and 20 mL CO_2/min; n = 4 for each flow rate) measured at the pump inlet (0°C, 13.8 MPa; ρ_{CO2} = 0.994 g/mL). Treatment time was varied for each flow rate to ensure the same mass of $scCO_2$ was used in each trial. The equilibrium solubility of water in supercritical CO_2 at 50°C and 13.8 MPa (ρ_{CO2}

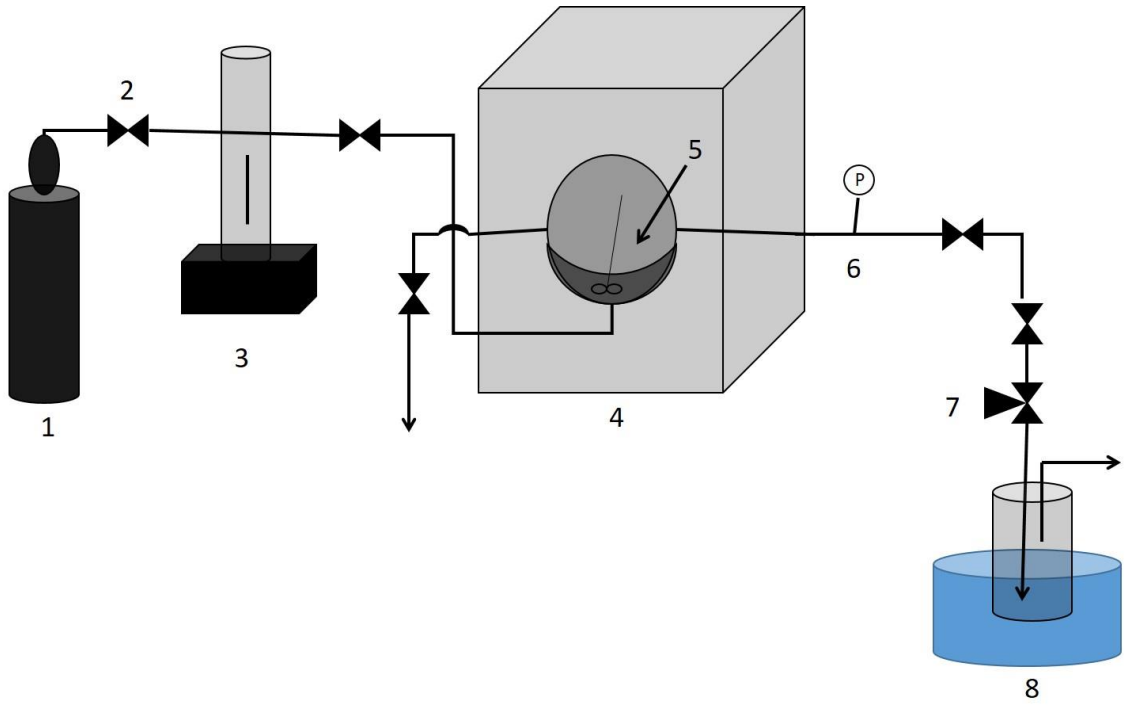

Figure 5.1 – Presaturation Test Schematic: 1 – CO_2 Supply; 2 – High Pressure Valve; 3 – Syringe Pump; 4 – Environmental Chamber; 5 – 25 mL High Pressure Vessel; 6 – Pressure Gauge; 7 – Back-Pressure Regulator; 8 – Cold Trap

=0.665 g/mL) was found to be 0.00837 mole fraction by interpolation of known data [214], and compared to the mole fraction of water dissolved in CO_2 at each flow rate to calculate an observed mole fraction, y_{obs}.

5.2.2 Biomaterial Selection and Preparation

To further investigate presaturation, we studied both a synthetic hydrogel and a natural tissue, porcine aorta. The hydrogel was poly(acrylic acid-*co*-acrylamide) potassium salt (Sigma-Aldrich, St. Louis, MO), a hydrogel used previously to establish the ability of dense-phase CO_2 to achieve sterilization within a porous matrix [32]. Hydrogel powder was hydrated in excess water at 4°C for 24 hr. Excess water was removed from each hydrogel specimen by drying for 15 minutes under a light vacuum, using filter paper and a Buchner funnel to remove free saline prior to weighing and treatment. Each hydrogel specimen was blotted onto a nylon filter and sealed inside the treatment chamber prior to exposure to $scCO_2$. The weight of each gel specimen was approximately 0.2 g.

Porcine heart was obtained from a local slaughterhouse, and the aorta was isolated and surrounding fatty tissue removed. The aortic tissue was cut into rectangles (approximately 3 cm x 2 cm) and stored in phosphate-buffered saline (PBS) at 4°C for up to 48 hours prior to use. Each specimen was dried for 15 minutes under a light vacuum using filter paper and a Buchner funnel. The treatment ratio and other conditions used (including temperature, pressure, and depressurization rate) were chosen to be very similar to the conditions used by Sawada *et al.* to allow for comparison [43]. Drying in a

vacuum oven (37°C, 38.1 cm Hg vacuum) was used as a negative control; changes in mass were recorded after 1, 2, 3, 6, and 24 hr.

5.2.3 Treatment of Hydrated Tissue Matrices

All biomaterial treatments were performed using the apparatus shown in Figure 5.2. Compared to Figure 5.1, the primary addition is a second pressure cell, the 10 mL treatment chamber (6), which contained the biomaterial. Also, a manually-operated pump (8) (Pressure Generator 62-6-10, High Pressure Equipment Co., Erie, PA) was connected to the treatment chamber; the manual pump enabled a slow, controlled depressurization rate of 0.34 MPa/min (50 psi/min) after treatment.

Two treatments were conducted on each biomaterial: one using dry $scCO_2$ (no water in the presaturation chamber) and the other using $scCO_2$ presaturated with water (n = 4 for both treatments). All treatments were performed at 13.8 MPa (2000 psi). The temperature was held constant at either 37°C (ρ_{CO2} = 0.769 g/mL) or 50°C (ρ_{CO2} = 0.665 g/mL, for hydrogel only). Four runs were made at each temperature and state of $scCO_2$ hydration. All biomaterials, regardless of initial mass, were subjected to a treatment ratio of 60 minutes of $scCO_2$ flow (1 mL CO_2/min) per 0.2 g of gel or tissue to account for small differences in individual masses.

5.2.4 Statistical Analysis

Graphs of data show the mean value plus or minus one standard deviation. A Student's *t*-test was used to determine statistical differences between groups. 95%

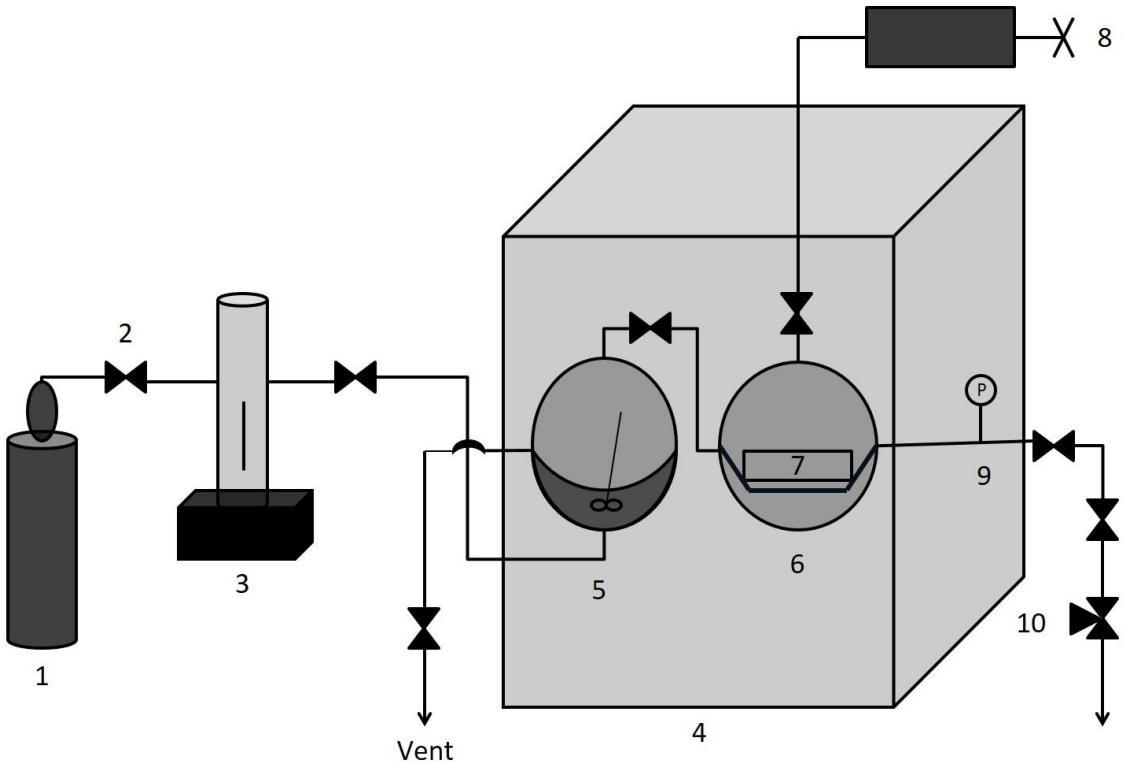

Figure 5.2 – Hydrogel and Tissue Dehydration Test Schematic: 1 – CO_2 Supply; 2 – High Pressure Valve; 3 – Syringe Pump; 4 – Environmental Chamber; 5 – Presaturation Chamber; 6 – Treatment Chamber; 7 – Sample; 8 – Hand Pump; 9 – Pressure Gauge; 10 – Back Pressure Regulator

confidence ($p < 0.05$, indicated by *) was considered to be statistically significant; 99% confidence ($p < 0.01$, indicated by **) was considered extremely significant.

5.3 Results and Discussion

5.3.1 Verification of Thermodynamic Equilibrium

Validation of the apparatus was demonstrated by using a cold trap to collect dissolved water in the effluent stream. Validation data are presented in Figure 5.3. For each CO_2 flow rate, an observed water mole fraction (y_{obs}) was calculated from the moles of water collected in the cold trap and the moles of $scCO_2$ pumped by the syringe pump. The y_{obs} value was compared to the known equilibrium solubility at the conditions studied, 0.00837 mole fraction. Complete thermodynamic equilibrium between $scCO_2$ and water was achieved at flow rates of 5 mL CO_2/min and below, as measured at the syringe pump. At flow rates 5 mL/min and below, the effluent water mole fractions approach the equilibrium limit. As the flow rate increases, the observed mole fraction decreases, indicating failure to equilibrate. CO_2 flow rates of 1 mL/min were used for the remainder of this work.

5.3.2 Hydrogel Treatment

An important characteristic of tissues and organs is that they are highly hydrated. Hydrogels have long been studied as a biomaterial for the fabrication of TE scaffolds because of their high water content, three-dimensional structure, and their ability to be crosslinked and functionalized [216]. Hydrogels were chosen as a model scaffold for this study because they are composed primarily of water. Treating a hydrogel with $scCO_2$

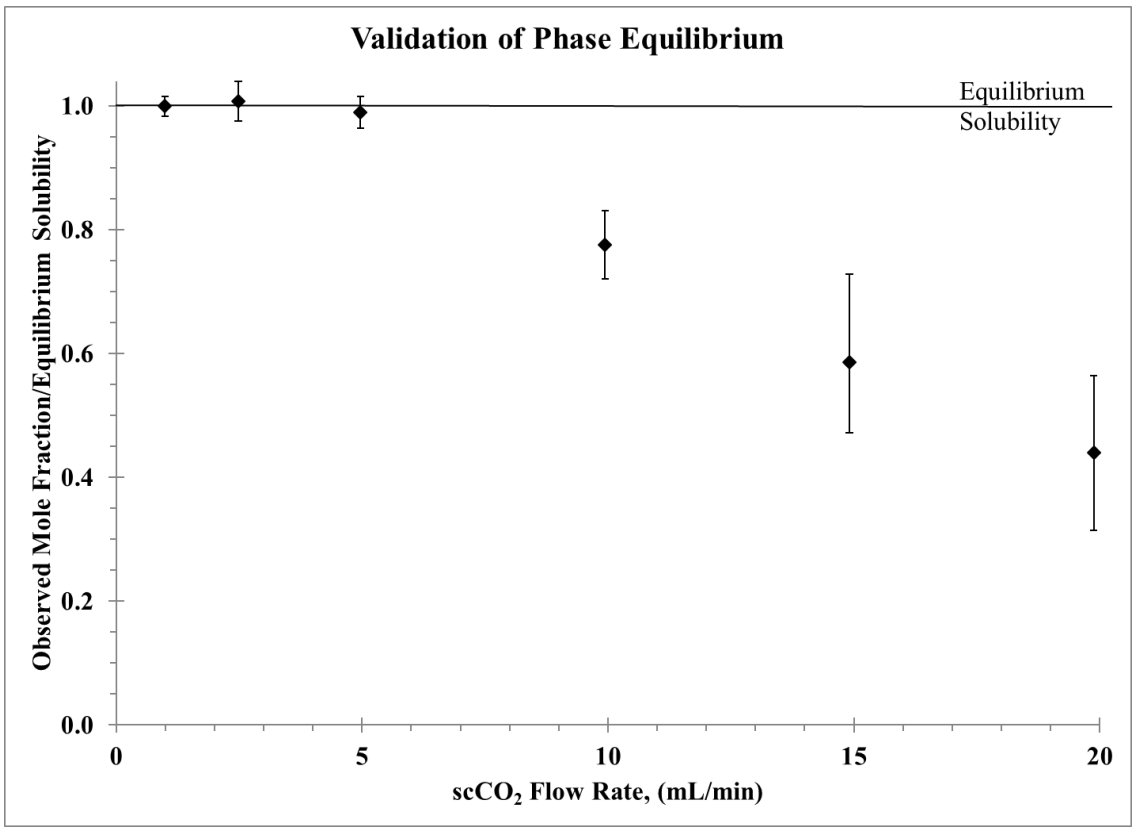

Figure 5.3 – Validation of Phase Equilibrium: Complete presaturation is achieved at flow rates less than 5 mL/min.

allowed us to study the behavior of water and $scCO_2$ in the system without potential interference from other compounds or variables.

Hydrogels were treated with dry (control) and water-presaturated $scCO_2$ at 13.8 MPa and either 37 and 50°C. Data from these experiments are summarized in Figure 5.4. At both temperatures, the average water retention was over 99% when $scCO_2$ was presaturated with water, but only about 50% when dry $scCO_2$ was used.

Results from treating the hydrogel with $scCO_2$ confirm the initial hypothesis. The hypothesis was also observed visually, as the hydrogels appeared shrunken and partially collapsed after treatment with dry CO_2, as shown in Figure 5.5. The mass retention with dry $scCO_2$ is slightly lower at 50°C, likely because both water vapor pressure and solubility in CO_2 increase with temperature. With presaturated $scCO_2$, gel mass is maintained at both temperatures.

One noticeable feature of Figure 5.4 is that the error bars for dry $scCO_2$ treatment of the hydrogels are relatively large. This is likely related to structural changes in the hydrogel as it dries. Porous hydrogels like poly(acrylic acid-*co*-acrylamide) do not dry uniformly; surface tension effects change the shape of the gel as water molecules are lost [217]. Additionally, drying curves for this hydrogel were produced by our group in a previous CO_2 sterilization study [32], and a period of sharp mass decline during the drying process was observed. However, regardless of the specific amount of water lost during dry $scCO_2$ treatment, Figure 5.4 clearly indicates that presaturating $scCO_2$ prevents water from being extracted from the hydrogels.

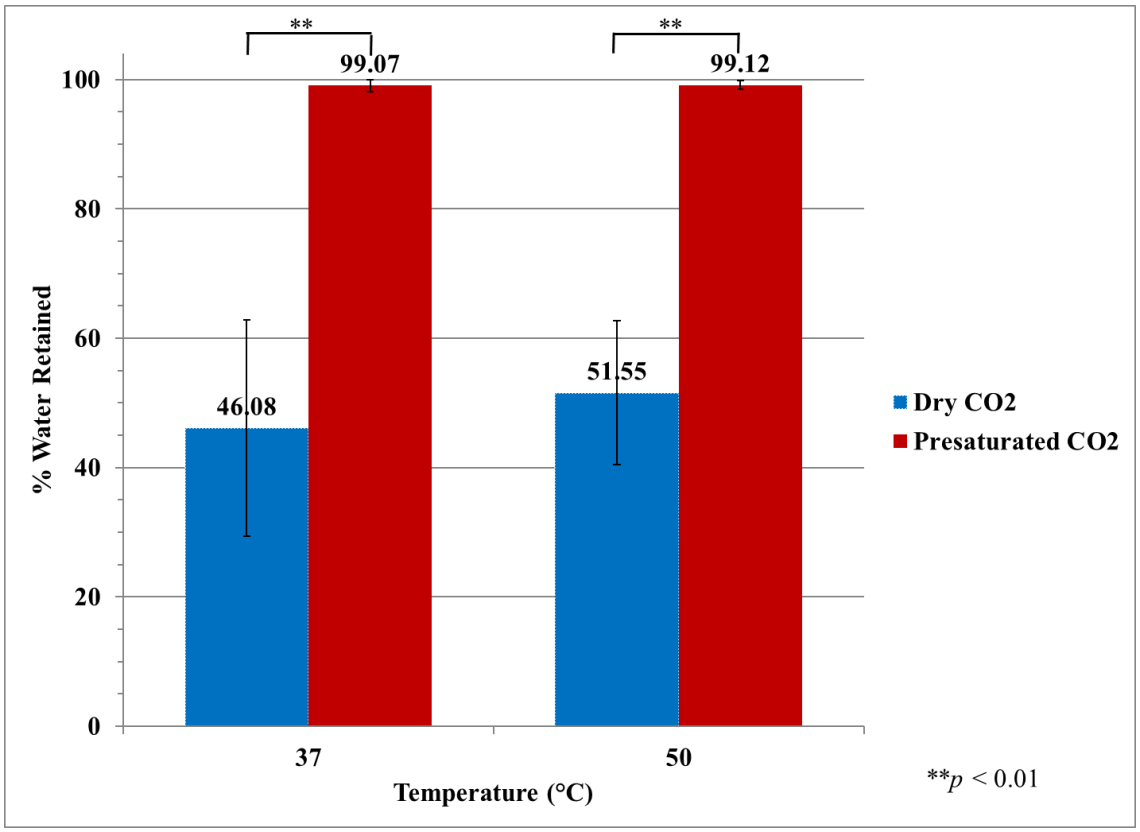

Figure 5.4 – $scCO_2$ Treatment of Hydrogels at 13.8 MPa: Dry $scCO_2$ (blue) extracted a substantial amount of water, while presaturated $scCO_2$ (red) removed very little.

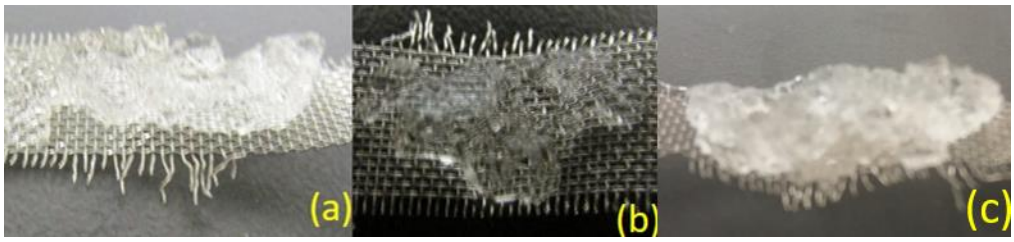

Figure 5.5 – Visual Appearance of Treated Hydrogels: (a) untreated hydrogel, (b) hydrogel treated with dry $scCO_2$, (c) hydrogel treated with presaturated $scCO_2$

5.3.3 Porcine Aorta Treatment

Vacuum drying was used to produce a complete drying curve for porcine aorta tissue (n = 6), as shown in Figure 5.6, where dimensionless mass on the y-axis is the ratio of the mass measured at each time point to the original mass of the tissue. Substantial water loss occurred during the first six hours, but afterward the loss of mass was insignificant. Vacuum drying of the native tissue removed over half of the initial mass in the first hour, with a continually more gradual decline in mass over the next five hours until reaching slightly above 20% of the initial mass. This is consistent with the known water content of porcine aorta, which is about 75% [218].

Results for control (dry $scCO_2$) and presaturated $scCO_2$ treatments of porcine aorta are shown in Figure 5.7. The average mass retentions are 78.6% ± 4.6% with dry CO_2 and 97.3% ± 1.4% with presaturated $scCO_2$; this difference is highly significant. It is evident from these results that using presaturated $scCO_2$ considerably reduces the amount of mass lost during treatment, again confirming the initial hypothesis. Visually, in Figure 5.8, the samples treated with presaturated $scCO_2$ (image b) maintained the beige color of the native tissue (a), while specimens treated with dry $scCO_2$ (c) experienced considerable darkening, particularly around the edges of the specimen.

There is still some mass loss using presaturated $scCO_2$, which indicates that a small amount of volatile substances other than water are extracted from the tissue. This mass loss may be attributed to other extractable materials in the tissue. While the aorta is primarily composed of water and polymeric materials like collagen and elastin, there are other materials present in trace amounts that may be extractable by $scCO_2$. Like most tissues, porcine aorta is known to contain lipids such as cholesterol [218]; these may

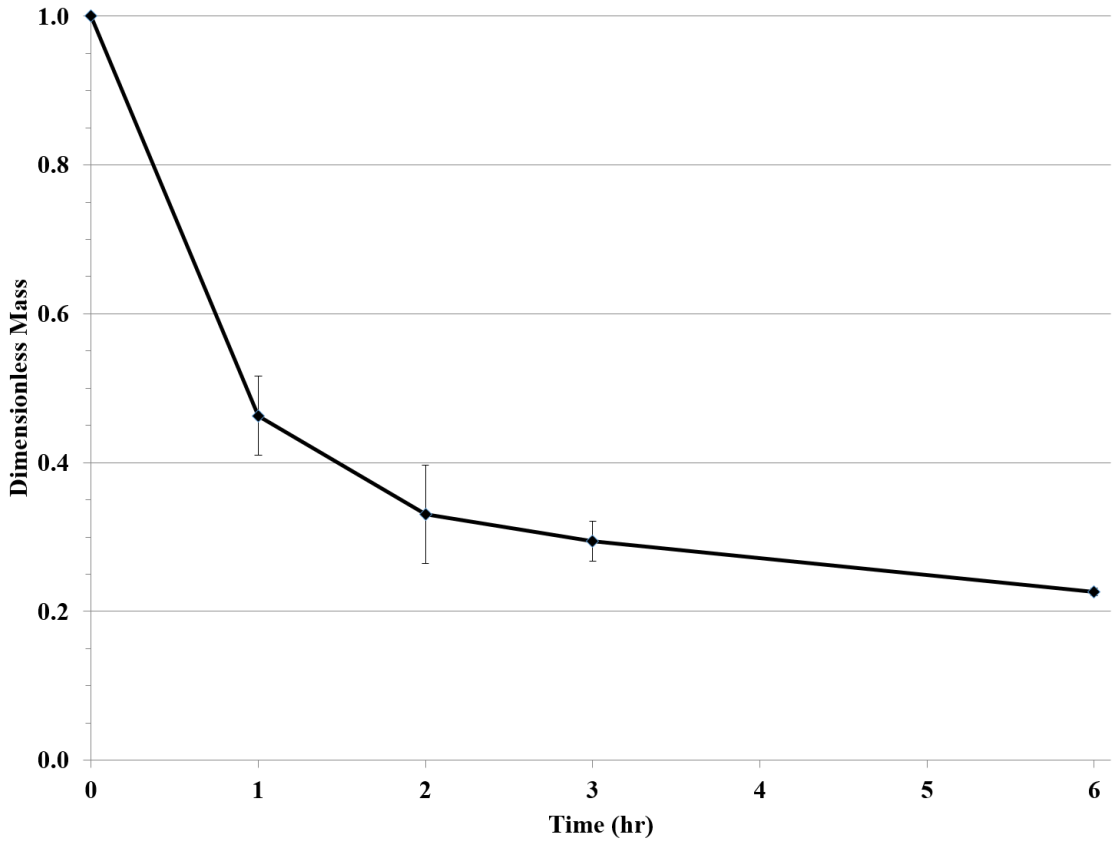

Figure 5.6 – Vacuum Drying of Porcine Aorta: Conditions were 37°C, 38.1 cm Hg (15 in. Hg) vacuum; over half the tissue mass was lost in the first hour.

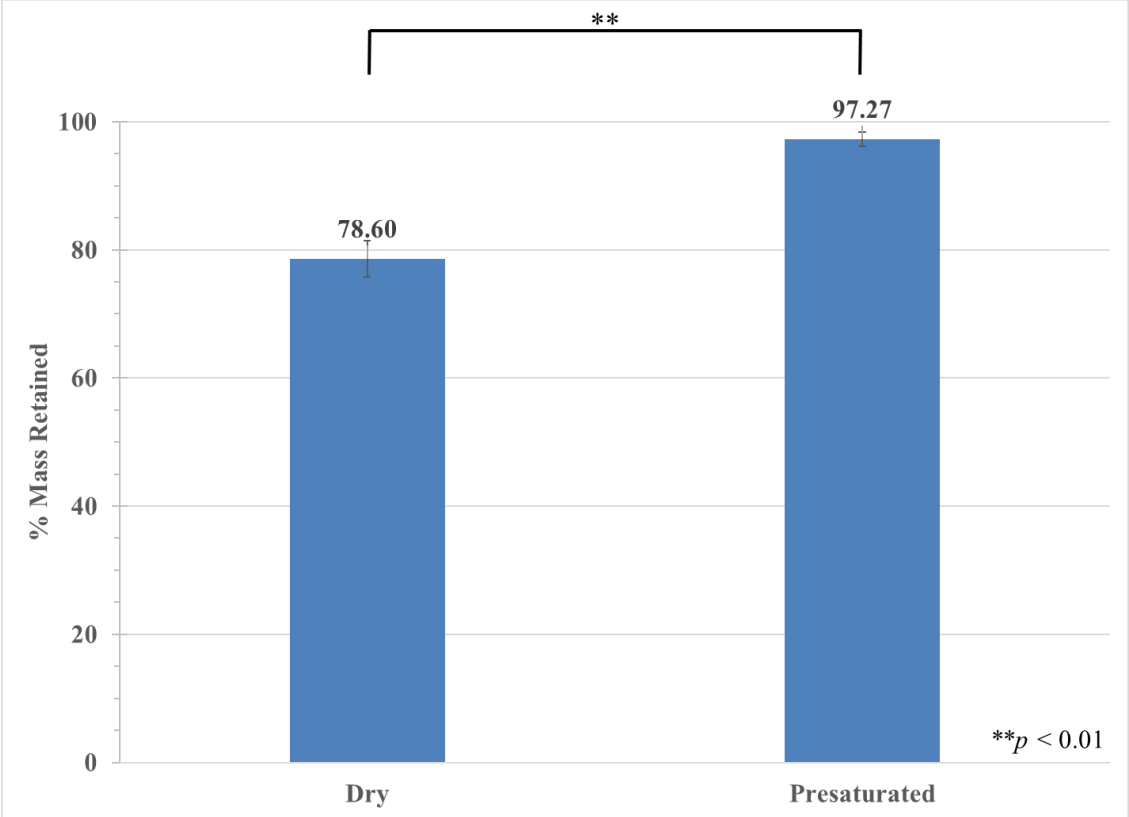

Figure 5.7 – $scCO_2$ Treatment of Porcine Aorta at 37°C, 13.8 MPa: Using presaturated CO_2 significantly increases mass retention.

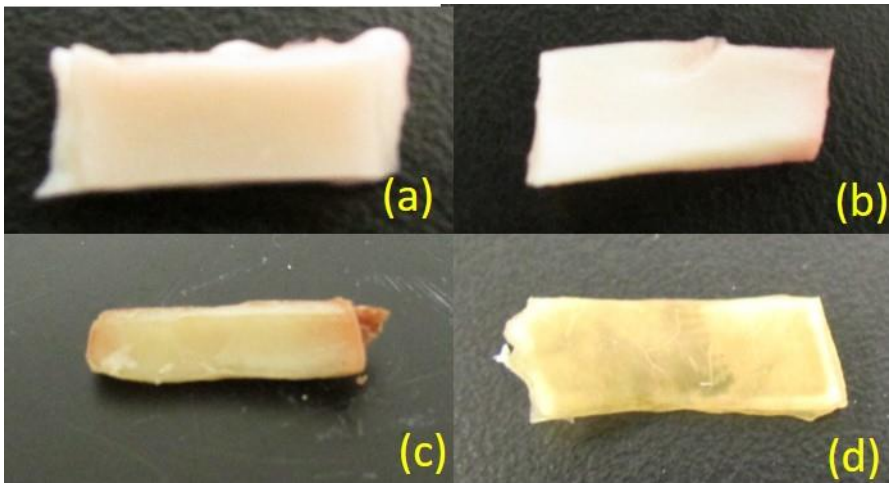

Figure 5.8 – Visual Appearance of Treated Porcine Aorta. (a) untreated aorta; (b) aorta treated with presaturated CO_2; (c) aorta treated with dry CO_2; (d) vacuum-dried aorta

TE scaffold. However, this has been done either with a scaffold material other than a decellularized tissue [41], and/or was done with the intention of long-term scaffold storage [120, 210]. After long-term storage, a scaffold would require rehydration before comprise the non-water extracted volatiles in the tissue, as $scCO_2$ has been shown to be efficacious for the extraction of fatty acids and other lipids [205]. For further development, any additional volatiles of interest could be identified and, if maintaining their presence is important, removal could be prevented by pre-equilibration of $scCO_2$, analogous to pre-equilibration with water.

$scCO_2$ treatment was found to cause less water removal than vacuum drying – Figure 5.9 shows where dry and presaturated $scCO_2$ treatment lies on the vacuum drying curve. Even dry $scCO_2$ treatment causes much less drying than a vacuum treatment over the same time interval. This finding was also confirmed visually, as shown in image (d) of Figure 5.8. Vacuum drying caused tissues to become significantly darker in color, similar to dry $scCO_2$ (image c), but also made the tissue far more brittle and translucent.

As indicated by the square on Figure 5.9, only about one-third of the native water was extracted by dry CO_2 treatment. $scCO_2$ drying is less severe than oven drying for two reasons. First, the flowing $scCO_2$ never allows equilibrium to be established between the fluid phase and the tissue matrix. There is also mass transfer resistance within the tissue, which slows transfer of water from the tissue to the flowing $scCO_2$. However, though $scCO_2$ drying is less pronounced than vacuum drying, unintentional water extraction on this level could still significantly hamper the effectiveness of a TE scaffold, so minimizing any drying caused by $scCO_2$ is very important.

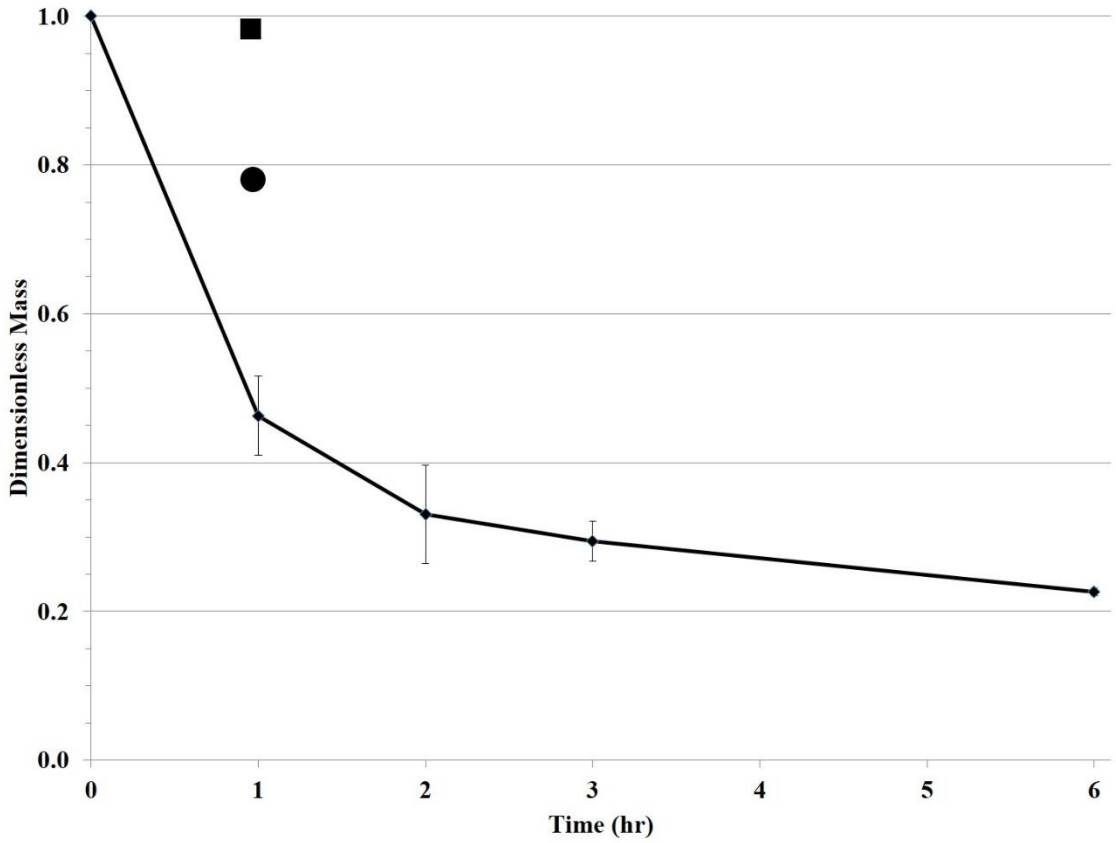

Figure 5.9 – Comparison of Vacuum Drying and $scCO_2$ Treatment of Porcine Aorta. The square represents the average tissue dehydration run with 1 hour of presaturated $scCO_2$ treatment (0.97), while the circle represents the average tissue dehydration run with 1 hour of dry $scCO_2$ treatment (0.78). Both values are significantly larger than 1 hour of vacuum drying (0.46).

Finally, it should be noted that this work is focused on preventing unintentional drying during $scCO_2$ treatment, and we are not making the claim that any scaffold dried during a $scCO_2$ process or otherwise is immediately invalid or nonviable. In fact, work has recently been published by other groups where $scCO_2$ is used to intentionally dry a seeding and implantation. In addition to adding another processing step, the rehydration process has been shown to not fully restore the original water content of the matrix because of irreversible changes in ECM microstructure [43, 210]. Therefore, we maintain that in producing a decellularized tissue for immediate use as a TE scaffold, it would be preferable to retain the original hydration state of the tissue after treatment.

5.4 Conclusions

A novel method for treating hydrogels, tissues, and other hydrated biomaterials with presaturated $scCO_2$ is presented. The method eliminates or heavily reduces the extraction of water and other volatiles that has been observed during $scCO_2$ treatment of biomaterials. In the model biomaterial studies, it was determined that dry $scCO_2$ extracts considerably more water from hydrogels and tissues than presaturated $scCO_2$. It was also determined that dry $scCO_2$ treatment removes water from tissues more slowly than vacuum drying, but that the amount of water extracted by dry $scCO_2$ is still enough to potentially alter the properties of a hydrated TE scaffold. Even presaturated $scCO_2$ does extract some volatile components from the tissue, though further analysis is required to verify this.

From these observations, we conclude that presaturation of $scCO_2$ can be used to prevent undesired dehydration of biomaterials for TE applications, allowing treated biomaterials to be used immediately instead of requiring a rehydration step. Having

overcome this obstacle, further investigation into $scCO_2$-based fabrication of tissue engineering scaffolds is warranted, including decellularization of natural tissues. Maintaining properties such as porosity and mechanical strength will be important as this technology is further developed.

Chapter 6 Decellularization of Porcine Aorta Using Supercritical CO_2

6.1 Introduction

Over 8,000 Americans die annually while awaiting an organ transplant, and currently over 120,000 Americans are on the national waiting list. Furthermore, the average wait time to obtain an organ transplant is several years [1]. One way to address this problem is by replacing damaged tissues and organs with ones created by tissue engineering (TE), which could greatly reduce transplant wait times and also alleviate the current dearth of available organ donors. However, tissues and organs are extraordinarily nuanced and complicated structures, which creates numerous criteria for developing effective biomimetic materials.

Whether derived from synthetic or natural materials, TE scaffolds must be sterile, porous, mechanically strong, biocompatible, and of appropriate stiffness and surface chemistry for the application at hand [2]. Additionally, scaffold fabrication can introduce numerous mechanical and biochemical deficiencies, including loss of mechanical strength, loss of surface activity, denaturation of extracellular matrix (ECM) proteins, scaffold dehydration, and residually cytotoxic solvents, detergents, and/or crosslinking agents [47]. All of these challenges require novel and innovative TE scaffold fabrication methods to be continually developed and refined.

Additionally, TE scaffolds must direct cell proliferation and differentiation during tissue growth. This is a particular strength of naturally-derived biomaterials, which have recently been shown to promote constructive remodeling during tissue growth [7]. In

particular, scaffolds prepared from decellularized tissues are uniquely able to receive and transmit signals to cells, an interaction called dynamic reciprocity [125]. Acellular ECM scaffolds have also been shown to elicit an anti-inflammatory immune response, which may be related to a reduced risk of immune rejection [5].

Decellularization is accomplished using a variety of different techniques, including physical [15], chemical [219], and enzymatic treatment [163]. Treatment with aqueous detergents, such as sodium dodecyl sulfate (SDS) and Triton X-100, is most common. Detergents lyse cell and nuclear membranes, but also denature proteins, which often leads to thorough cell removal but can also disrupt glycosaminoglycans (GAGs), growth factors, and ECM ultrastructure [13]. Because of these hazards, it has become common for protocols to use detergents at very low concentrations over several days or even weeks, minimizing ECM damage while eventually removing all cells [17]. Though this approach is effective, novel methods are desired to decellularize tissues as effectively but with shorter treatment times and without using harsh chemicals or solvents for long periods.

One relatively unexplored method worthy of consideration is treatment with supercritical carbon dioxide ($scCO_2$). $scCO_2$ is non-toxic, non-flammable, and relatively inert. Its mild critical temperature (31.1°C) makes it viable physiologic temperatures, and it has desirable transport properties such as high diffusivity, relatively high density, and low viscosity [21]. $scCO_2$ has been used extensively in TE applications that involve synthetic materials, particularly in polymer foaming, where CO_2 is used to fabricate TE scaffolds from synthetic polymers [27-29]. $scCO_2$ has also been utilized in other biomedical applications, including extraction of biologically-relevant molecules [25, 26],

critical point drying [57], pasteurization [22-24], and sterilization of biomaterials and medical devices [30-37].

A novel decellularization technique using $scCO_2$ offers considerably faster decellularization, on the order of hours instead of days. The absence of harsh chemicals or solvents could also mitigate damage to the ECM. In 2008, Sawada *et al*. used $scCO_2$ to decellularize porcine aorta, but dehydration of the scaffold during treatment prevented further progress [43]. In Chapter 5, we presented a method, presaturation of $scCO_2$ with water, that greatly reduces tissue dehydration during $scCO_2$ treatment [211].

Our broad aim is to develop a novel $scCO_2$ decellularization method that also maintains the hydration state of the treated tissue. The objectives of this chapter are: (1) to examine the extent of decellularization in porcine aorta using $scCO_2$ with different additives, pretreatments, and thermodynamic conditions; and (2) to present a hybrid detergent/$scCO_2$ treatment that decellularizes the tissue more quickly and as effectively as a standard detergent treatment. Achieving these objectives will enable further development of CO_2-based decellularization and TE processes.

6.2 Materials and Methods

6.2.1 Tissue Procurement and Standard Detergent Treatment

Porcine aorta was obtained from a local abattoir, rinsed with PBS and cut into ring-shaped sections measuring about 1 cm in length. Specimens were stored at -20°C for up to 48 hr until being treated with $scCO_2$ or a standard SDS treatment.

The standard SDS treatment (treatment "S"; all treatments are listed in Table 6.1) was performed according to the protocol of Funamoto *et al* [171]. Tissues were

Table 6.1: List of Decellularization Treatments

Treatment Name	Treatment Description
A	1 hr $scCO_2$ with added water
B	1 hr $scCO_2$ with added water & Ls-54
C	1 hr $scCO_2$ with added ethanol
D	1 hr $scCO_2$ with added water & ethanol
S	48 hr SDS/enzymes + 24 hr PBS wash (“standard treatment”)
H	48 hr SDS/enzymes + 1 hr $scCO_2$ “wash” (“hybrid treatment”)

pretreated for 1 hr in a solution containing 0.2% (w/v) EDTA and 10 mM pH 8 Tris buffer to increase cell membrane permeability. They were then decellularized for 48 hr under light agitation in 0.1% (v/v) SDS, 10 mM Tris buffer, 0.2 mg/mL DNase I, and 0.02 mg/mL RNase A. Specimens were washed with PBS several times over the course of 24 hr to remove cell debris and residual detergent; thus the total time required for decellularization was 72 hours.

6.2.2 Decellularization with Supercritical CO_2

The aorta specimen (8) was loaded into the treatment chamber (7) of the $scCO_2$ apparatus, shown in Figure 6.1. The apparatus contained valves and fittings rated for high pressures up to 68.9 MPa (2). Liquid carbon dioxide (1) was compressed in a chilled syringe pump (3) and slowly bubbled into the presaturation chamber (5) to maximize mass transfer. In this chamber, the additive and $scCO_2$ were stirred vigorously until reaching thermodynamic equilibrium (10-15 min with water and water solutions, 1-2 min for pure ethanol). Four different additive solutions were used to determine whether aqueous additives enhanced decellularization: (treatment “A") water, (“B”) water + Dehypon Ls-54 surfactant (BASF America, Florham Park, NJ), (“C”) ethanol, and (“D”) water + ethanol.

Once equilibrium was reached, the valve to the treatment chamber was opened, and $scCO_2$ flow was programmed to 1 mL/min at the pump inlet. During treatment, the environmental chamber (4) was used to maintain the temperature at either 10 or 37°C, and a back-pressure regulator (11) was used to keep the pressure of the $scCO_2$ in the vessels constant at either 10.3 or 27.6 MPa (1500 or 4000 psi, respectively). A manual

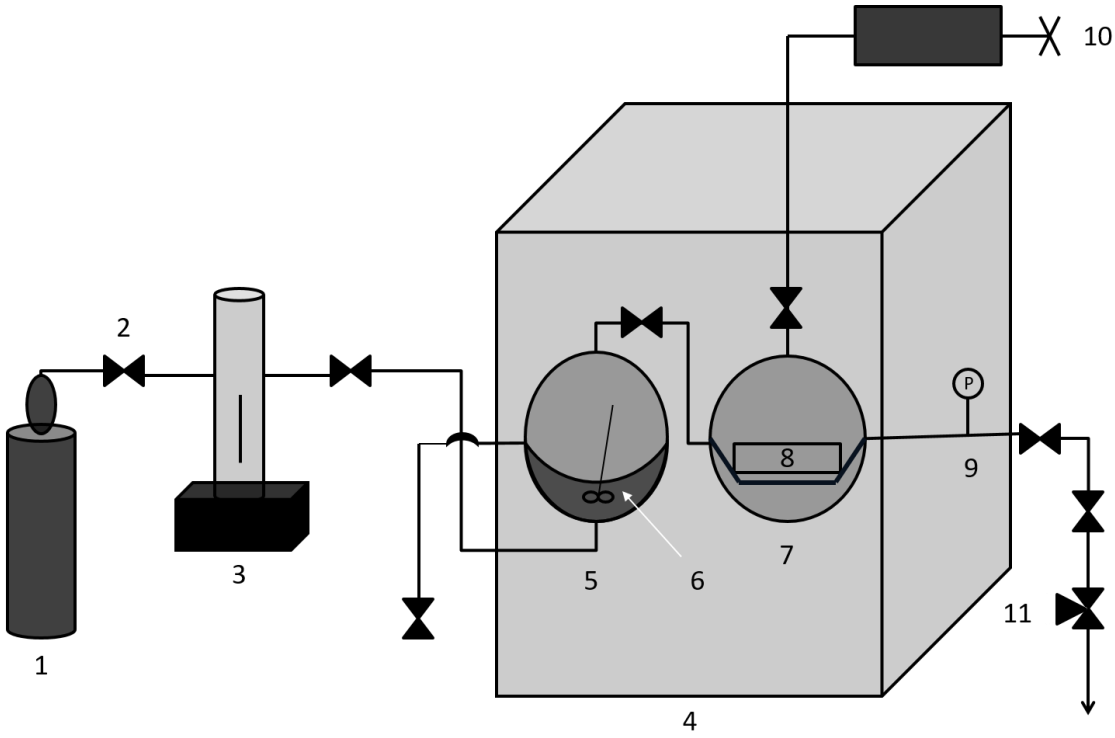

Figure 6.1 – Supercritical CO_2 Decellularization Schematic: 1 – CO_2 Cylinder; 2 – High Pressure Valve; 3 – Syringe Pump; 4 – Environmental Chamber; 5 – Presaturation Chamber; 6 – Stirring Bar & Additive Solution 7 – Treatment Chamber; 8 – Aorta Specimen; 9 – Pressure Gauge; 10 – Hand Pump; 11 – Back Pressure Regulator

hand pump (10) was used to depressurize the system at a rate of 0.34 MPa/min (50 psi/min).

6.2.3 Hematoxylin and Eosin (H&E) Staining

After treatment, tissues were fixed in 10% neutral buffered formalin for at least 24 hr and embedded in paraffin. Tissues were then cut into 5 μm sections using a microtome and deparaffinized by immersion in xylene (3 times), 100% ethanol, 95% ethanol, 80% ethanol, and finally water. The tissues were stained with hematoxylin for 7 minutes, washed with water and ammonia, and then stained with eosin for 2 minutes before being dehydrated by immersion in 80% ethanol, 95% ethanol, 100% ethanol, and finally xylene (3 times). A coverslip was mounted on slides, which were then viewed using a light microscope (Nikon E600, Tokyo, Japan) after waiting at least 24 hr for the slides to dry.

6.2.4 DNA Quantitation

DNA was quantified using the DNAzol reagent kit (Invitrogen, Carlsbad, CA) according to the prescribed protocol with minor changes. 25 mg of dry aorta were flash-frozen in liquid nitrogen and ground with a mortar and pestle. Specimens were then placed in a 2 mL tissue homogenizer (VWR International, Radnor, PA) with 0.5 mL of DNAzol reagent and ground for 5-10 strokes or until fully dissolved. The solution was then centrifuged at 10,000 x g for 10 minutes and the supernatant was recovered. 0.25 mL of 100% ethanol was added to precipitate the DNA, which was recovered and washed twice with 70% ethanol for 1 min per wash. DNA was air-dried for 5 sec and re-dissolved in 4 mM sodium hydroxide (pH 9). Optical density was measured at 260 nm

using a spectrophotometer (DU 730 model, Beckman-Coulter, Brea, CA) and the DNA concentration was calculated based on the absorbance measurement and initial mass of the tissue

6.2.5 Basic Physical Characterization

Aorta specimens from treatments A, B, C, and D were weighed before and after $scCO_2$ treatment using an analytical mass balance (Mettler Toledo, Columbus, OH) and compared to the mass of untreated samples and to each other. Additionally, samples were photographed with a digital camera (PowerShot SX500, Canon Inc., Tokyo, Japan) and analyzed for changes in size, color, and overall appearance.

6.2.6 Scanning Electron Microscopy (SEM)

After treatments C and D, samples were crosslinked with 2% glutaraldehyde (TCI America, Portland, OR) in 0.1 M sodium cacodylate buffer, pH 7.2 (Fisher Scientific, Hampton, NH), overnight at 4°C. The sample was then washed 5 times in 0.1 M cacodylate buffer (pH 7.2) for 1-2 min each and then post-fixed in 1% osmium tetroxide (Fisher) for 1 hr at 4°C. After secondary fixing, the specimen was washed 3 times in cacodylate buffer and then dehydrated in gradually increasing ethanol rinses (50%, 70%, 80%, and 95%) for 10 min each and finally rinsed twice in 100% ethanol for 10 min per wash to fully dehydrate the specimen.

Specimens were then transferred into microporous vials, immersed in ethanol, and placed in a critical point dryer (CPD3 – Ladd Research Industries, Williston, VT). During critical point drying, the sample was submerged in liquid CO_2 at 6.2 MPa (900

psi) at 10°C and the temperature was gradually increased to 40°C, reaching the supercritical CO_2 state. The pressure was then decreased to atmospheric at a rate of 0.69 MPa/min (100 psi/min). Dried specimens were mounted on a stub and coated with gold twice using a sputter coater (Denton Vacuum, Moorestown, NJ) and then loaded into the SEM. The SEM used was the Vega3 SBU (Tescan, Brno, Czech Republic) and was used at a working voltage of 10 kV.

6.2.7 Hybrid SDS/CO_2 Treatment

After analyzing the results of the above treatments, development of a hybrid detergent/$scCO_2$ treatment was desired. The hybrid treatment ("H") involved exposure of tissue to the standard detergent treatment solution described in section 6.2.1, followed by 1 hr $scCO_2$ treatment described in section 6.2.2 in lieu of the PBS wash. Water and ethanol were used together as additives.

6.2.8 Mechanical Testing

The mechanical properties of aorta specimens from treatments S, C, and H were examined using a uniaxial ring test as described by Twal *et al*. [220]. Annular samples were mounted onto a Bose Electroforce 3230 Biomechanical Tester (Bose Corp., Farmingham, MA) using two parallel cannulas. Specimens were subjected to three preconditioning cycles at a rate of 0.05 mm/s with a maximum stretch ratio of 1.2 during each cycle. Samples were kept moist with PBS during preconditioning to prevent dehydration. At the start of the identical fourth cycle, load and displacement data were recorded at a rate of 50 points/sec using the accompanying Wintest software.

6.2.9 Residual SDS Quantitation

Residual SDS from the standard and hybrid treatments was quantified using an SDS Detection and Estimation Kit (G Biosciences, St. Louis, MO). The assay involved mixing 1 mL methylene blue dye with 0.5 mL extraction buffer and 5 μL of aqueous solution containing SDS, then vortexing for 30 seconds. 1 mL of chloroform was then added, then the mixture was vortexed again for 30 seconds. Methylene blue is extracted into the organic phase if SDS is present. After waiting 5 minutes, the bottom chloroform phase was sampled and optical density was measured at 600 nm. SDS concentration was calculated by comparison to a standard curve.

6.2.10 Statistical Analysis

Numerical data is presented as mean values plus or minus one standard deviation. A Student's *t*-test was used to analyze confidence in statistical differences between groups. 95% confidence ($p < 0.05$, indicated by *) was considered to be statistically significant, while 99% confidence ($p < 0.01$, **) was considered highly significant.

6.3 Results and Discussion

The objective of decellularization is to maximize removal of cells and cellular debris while minimizing alteration done to the ECM during treatment [13]. A successful decellularization protocol utilizing $scCO_2$ would quicken the process considerably and could do so using a benign solvent that leaves no residual material in the matrix.

Currently, there is no universally-accepted standard for evaluating the extent of decellularization. This is not surprising, because tissues vary greatly in stiffness, cell

density, ECM composition, and numerous other characteristics. Therefore, decellularization processes must be tailored to the specific tissue of interest [122]. However, Badylak's group recently proposed a list of three criteria that can adequately describe a decellularized tissue of any kind. They are [12]:

1. Lack of visible nuclear material in H&E and/or DAPI-stained sections
2. Total amount of double-stranded DNA less than 0.05 μg/mg dry tissue
3. No individual DNA fragment longer than 200 base pairs

In this study, we focused on the first two criteria by performing H&E staining and DNA quantitation on porcine aorta after $scCO_2$ treatment.

Six different treatments of porcine aorta were undertaken to determine the extent of decellularization. They included two controls: SDS treatment and treatment with dry $scCO_2$, and treatment with presaturated $scCO_2$ using four different additive mixtures: water, water/Ls-54, ethanol, and water/ethanol. The thermodynamic conditions chosen were based on the factorial design and process optimization performed in Sawada's work [43].

6.3.1 Extent of Decellularization with $scCO_2$ – Histology

Tissue sections from each treatment were stained with hematoxylin and eosin (H&E) and observed under an optical microscope. Hematoxylin is a basic, positively charged stain that binds to the acidic, negatively charged nuclear envelope and chromatin, staining it black or purple. Eosin is an acidic, negatively charged stain that binds to positively-charged ECM proteins like elastin and collagen. There were three controls in this study: the untreated tissue as a negative control, and the SDS-treated tissue and dry

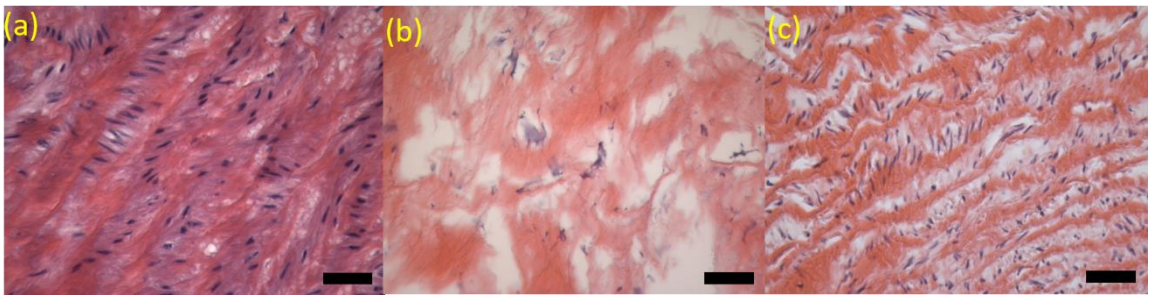

Figure 6.2 – Histology of Control Specimens: H&E stained sections of untreated (a), SDS-treated (b), and dry $scCO_2$-treated (c) porcine aorta. Scale bars represent 50 μm.

CO_2-treated tissue as positive controls.

Sections from the tunica media of each of the controls can be seen in Figure 6.2. In the native tissue (image a on the figure), the elastic fibers of the ECM are parallel with regular spacing between them. Round or elliptical whole smooth muscle cells are attached to the elastic fibers. The middle image on the figure (b) shows the same tissue after treatment with SDS and a PBS wash. Few intact cells are visible, indicating some degree of disruption. However, dark, irregularly-shaped areas of cellular debris are observed, indicating incomplete cell removal. Additionally, significant damage to the ECM fibers is evident based on their widespread breakage and deformation. Tissue treated with dry (pure) $scCO_2$ (image c) primarily has intact, undisturbed cells like the native tissue, though a few cells appear to be shriveled or completely removed based on the empty space in the micrographs. Elastic fibers are disturbed somewhat, as some shrinkage is observed and the spacing between fibers is less uniform, but unlike the SDS treatment, the fibers are not entirely broken.

These findings can be explained by considering the known mechanisms of how detergents and supercritical fluids interact with cells and proteins. The SDS results mirror the literature; it is well-known that most ionic detergents, including SDS, can disrupt both the cell and nuclear membranes by replacing molecules in the lipid bilayer via the micelle effect [13]. This effect leads to intracellular contents exiting the confines of the cell and leaving the black, irregular areas of cellular debris found in the micrographs. However, SDS alone does not remove the cellular debris from the matrix; debris is usually removed by prolonged washing with a saline solution. In this work, washing with PBS was done for a relatively brief 24 hr according to Funamoto's protocol

[171], but Simionescu's group and others have shown that saline rinses often require several days or even weeks to remove all residual cellular material and detergent from a decellularized blood vessel [17]. It is also well-documented that SDS denatures proteins, so the shrinkage and cleavage of elastic fibers is not surprising.

Treatment with dry $scCO_2$ was much less disruptive to elastic fibers in the ECM than SDS treatment. Though no breakage was observed, there is still a clear loss of uniformity in both fiber size and spacing. This is a reasonable outcome, given that tissue dehydration is a known effect of dry $scCO_2$ treatment. However, pure $scCO_2$ was ineffective at removing cells from the matrix. This outcome matches previous observations by Sawada's group that $scCO_2$ is ineffective at cell removal without an additive [43]. Though there is a currently a clear lack of experimental proof, it has been proposed that the mechanism of $scCO_2$ decellularization is extraction of both whole cells and cellular debris [12]. Because these materials are charged, dissolution in pure $scCO_2$ is minimal because carbon dioxide is a nonpolar molecule. This suggests using a polar, CO_2-soluble additive to aid in decellularization, as described in the following.

Four different additives were used to presaturate $scCO_2$ in an attempt to improve cell removal: water (A), water + Ls-54 (B), ethanol (C), and water + ethanol (D). H&E sections from treatments A and B are shown in Figure 6.3 alongside the untreated tissue. With regard to decellularization, there appears to be no more removal than with dry $scCO_2$ (Figure 6.2c). This is not surprising, because although water is polar, it has relatively low solubility in $scCO_2$ (less than 0.01 mole fraction at the conditions studied) [214], meaning that the humidified CO_2 still is highly nonpolar and unlikely to extract polar components. Using water as an additive does appear to improve the continuity and

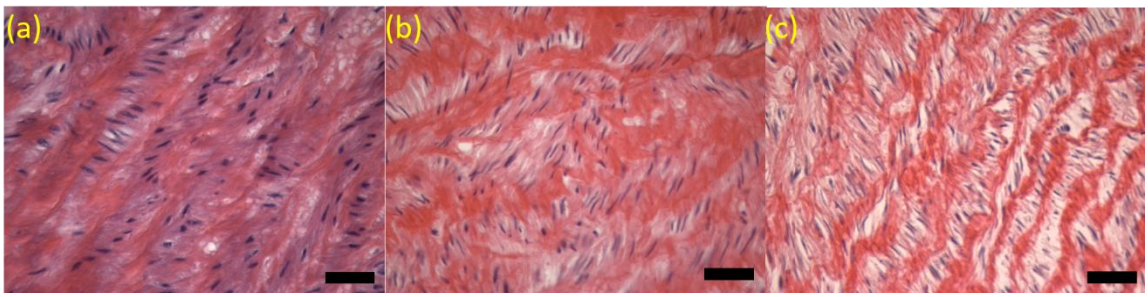

Figure 6.3 – Histology of Water and Water/Ls-54 Additives: H&E stained sections of untreated (a), water/scCO$_2$-treated (b), and water/Ls-54/scCO$_2$-treated (c) porcine aorta. Scale bars represent 50 μm.

uniformity of elastic fibers, which makes sense since the tissue is not dehydrated by this treatment.

Figure 6.3 also shows the effect of adding Ls-54 to the solution to be minimal. Ls-54 is a non-fluorinated surfactant that has been shown to have solubility in dense-phase CO_2 and water (about 0.001-0.005 mole fraction) and to be an effective additive for removing bacterial endotoxin from a solid surface [103, 104]. However, it appears to be ineffective in enhancing decellularization, probably because its chemistry differs from SDS despite them both being surfactants. Though their alkyl chain lengths are similar, Ls-54 contains a hydroxyl group at the end of its chain rather than the highly dissociative sodium ion of SDS. Ls-54 also contains several ethoxyl and propoxyl groups, whereas SDS has a long, nonfunctionalized alkyl chain. These characteristics give SDS amphiphilic properties that interact with the lipid bilayer in cell membranes much more readily than Ls-54.

The ineffectiveness of Ls-54 could also be related to treatment temperature. Past work has shown an inverse proportionality between temperature and Ls-54 solubility in CO_2, including into the liquid CO_2 phase [105]. Treatment B was also conducted at 10°C, where CO_2 is more dense and exists in the liquid phase at the treatment pressure, but no significant changes in extent of decellularization were observed (Figure 6.4). While it is generally expected that thermodynamic conditions will affect the extent of decellularization, it is likely that this particular treatment is so far from achieving complete decellularization that these effects cannot be ascertained at this magnification.

To further increase the polarity of the $scCO_2$ mixture, two final treatments were investigated, using ethanol and ethanol/water as additive solutions. Figure 6.5 displays

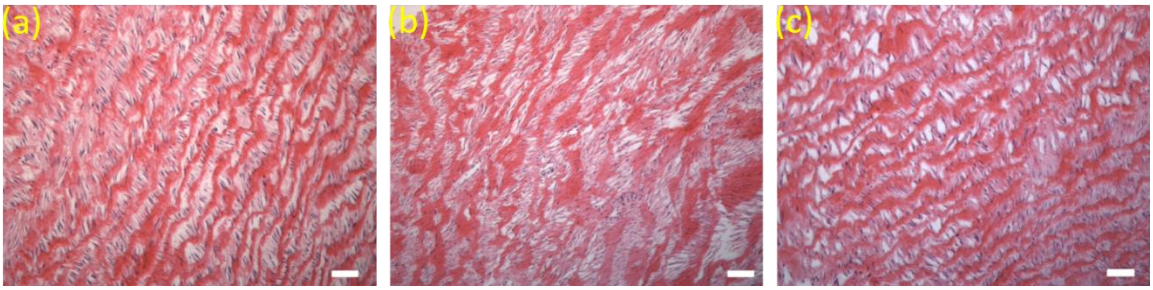

Figure 6.4 – Effect of Thermodynamic Conditions on Extent of Decellularization: H&E stained sections with water/Ls-54 as the additive solution at the three different thermodynamic conditions: (a) low density (10.3 MPa, 37°C), (b) medium density (27.6 MPa, 37°C), and (c) high density (27.6 MPa, 10°C). No significant changes in extent of decellularization were observed between treatments. Scale bars represent 50 μm.

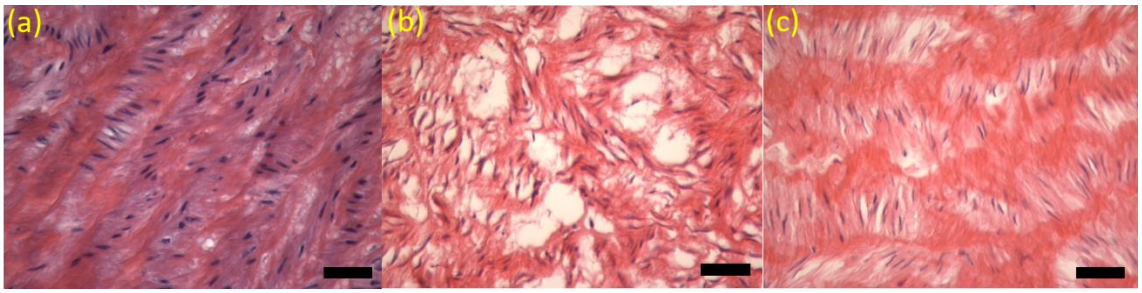

Figure 6.5 - Histology of Ethanol and Ethanol/Water Additives – H&E stained sections of untreated (a), ethanol/scCO$_2$-treated (b), and ethanol/water/scCO$_2$-treated (c) porcine aorta. Scale bars represent 50 μm.

H&E-stained sections from these treatments. Treatment with ethanol alone shows considerable shriveling and branching of the elastic fibers, as was expected. However, the use of ethanol does not aid considerably in cell removal. Though some of the areas where the ECM is damaged have fewer cells, the intact elastic fibers have numerous intact cells attached to them. The addition of water to the ethanol does not markedly change the extent of decellularization, but does significantly improve the condition of the elastic fibers. This finding is expected based on Figure 6.3 and the findings of Chapter 5; the primary objective of using water as an additive is to prevent dehydration, not to remove cells. Overall, the three treatments that included water as an additive were notably more effective in maintaining the alignment of the elastic fibers than ethanol alone. This supports findings in our previous work, which showed that presaturating $scCO_2$ with water before treatment prevents dehydration of the ECM during $scCO_2$ treatment.

On the contrary, when ethanol is the only additive, shriveling and fraying of the ECM fibers is observed, as in Sawada's paper. These findings were also confirmed visually and by manual handling, as treatment clearly increased the rigidity of the matrix when water was not added, while the addition of water maintained the apparent flexibility and pliability of the material. Though interesting, the prevention of tissue dehydration is made impractical by the lack of cell removal in any of the experiments.

The physical properties of treatments A, B, C, and D were analyzed by mass measurement, photography, and scanning electron microscopy (SEM). These findings were rendered impractical by the lack of decellularization, but have been preserved in Appendix C for the sake of completeness.

6.3.2 Extent of Decellularization with $scCO_2$ – DNA Quantitation

Ultimately, microscopy indicates only very limited cell removal with the four $scCO_2$ + additive treatments, and not nearly enough to indicate decellularization. To confirm visual microscopy results, we employed quantitation of DNA as a measure of decellularization; one of the proposed criteria for establishing decellularization is a double-stranded DNA concentration below 0.05 μg DNA/mg dry tissue [12]. For each treatment in this study, DNA was extracted and its concentration was calculated based on spectrophotometric absorbance readings. Results of DNA quantitation are shown in Figure 6.6. All treatments show some amount of DNA removal compared to the untreated tissue. However, no treatments aside from the standard SDS method approach the target maximum concentration of 0.05 μg DNA/mg dry tissue.

The results of DNA quantitation follow the histological findings, where SDS was required in some capacity to rupture cell membranes and attain at least an appreciable amount of cell removal. The four $scCO_2$ additives do reduce the DNA content compared to the untreated tissue, though none of the treatments approach complete decellularization, as with the H&E findings.

The failure of the $scCO_2$/ethanol mixture to decellularize is the most surprising result, given that this finding is in direct opposition to the findings of Sawada's group and that the experiments and the apparatuses used in both studies are both similar. While there may be unknown differences in equipment or specimens that create a significant difference between the studies, our results lead us to question Sawada's findings. When analyzing the results of an experiment, particularly one where mechanistic steps cannot be viewed *in situ*, it is imperative to consider the underlying mechanisms to glean

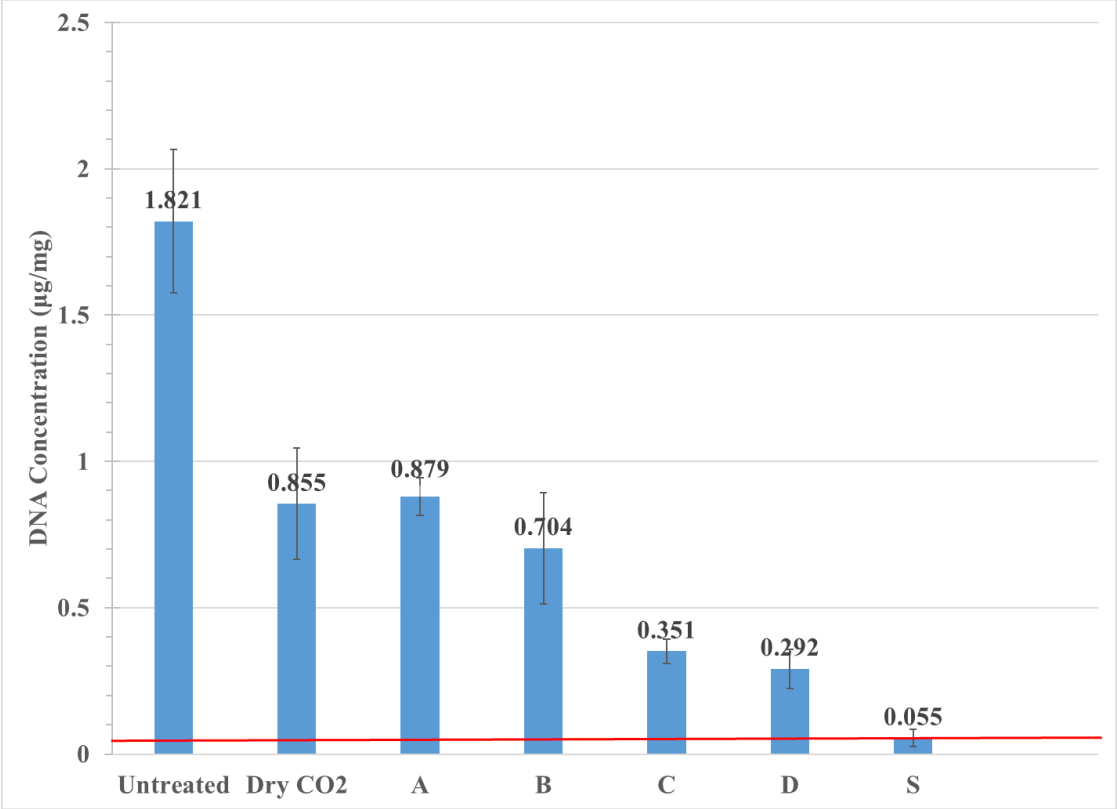

Figure 6.6 - DNA Quantitation: Standard & $scCO_2$ Treatments: Values below the red line (0.05 µg DNA/mg dry tissue) would indicate complete decellularization. All treatments showed significant DNA removal compared to the control, but none neared adequate decellularization except for the SDS treatment.

information about what is physically occurring during the experiment.

The limited discussion in the literature on $scCO_2$ interaction with cell membranes includes two possibilities: supercritical extraction of cells or cellular debris as a primary mechanism, and physical dislodging of cells from the ECM caused by high pressure. Based on our findings, we do not expect the high pressure alone to remove cells; other work has been published where blood vessels have been decellularized with high hydrostatic pressure – pressures on the order of several hundred MPa – and cells still require long-term continuous washing to be removed in these applications [171]. This suggests renewed focus on the extraction mechanism.

6.3.3 SDS/$scCO_2$ Hybrid Treatment for Decellularization

Earlier in this chapter, the ineffectiveness of Ls-54 surfactant in decellularization was discussed, possibly because of its inability to permeate the cell membrane. We theorized that $scCO_2$ in general may suffer from this same problem. To test this hypothesis, a two-step hybrid SDS/CO_2 decellularization treatment was investigated. With this treatment, tissues were treated with SDS as described in section 6.2.1, but without the subsequent PBS wash. Instead, tissues were then treated (washed) for 1 hr with $scCO_2$ presaturated with ethanol and water at the same thermodynamic conditions used previously.

The effect of the hybrid treatment can be seen in Figure 6.7. Using this hybrid approach, there are no visible intact cells or cellular debris. Therefore, it is likely that the tissue is fully decellularized. This is an exciting and intriguing result that suggests polar

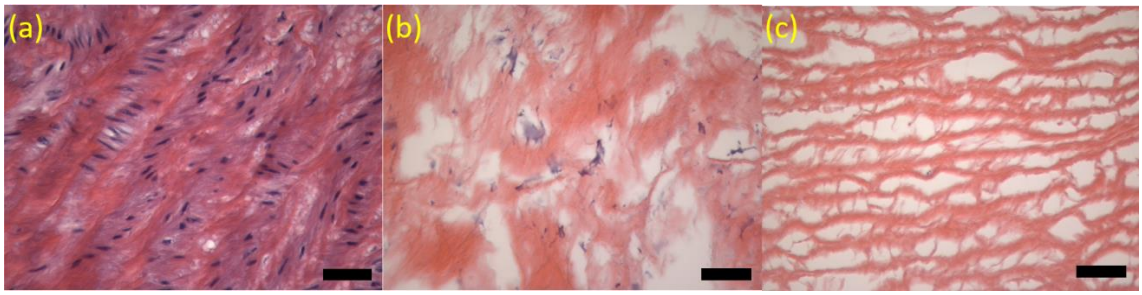

Figure 6.7 – Histology of Hybrid Treatment: H&E stained sections of untreated (a), SDS-treated (b), and SDS/scCO$_2$-treated (c) porcine aorta. Image (c) shows complete decellularization. Scale bars represent 50 μm.

supercritical CO_2 will extract intracellular debris, but cannot do so unless another agent is used to enhance membrane permeation or rupture. Significantly, the ECM fibers appear to be intact and mostly undisturbed compared to the complete SDS treatment. Maintenance of fiber integrity may be a result of shorter exposure time to SDS; the $scCO_2$/water + ethanol "wash" takes only an hour instead of the day or more required for PBS washing.

DNA quantitation from the hybrid method, along with the results of the other treatments, can be seen in Figure 6.8. The figure shows a level of DNA removal similar to the standard SDS treatment, below the threshold for decellularization with a concentration of 0.036 μg DNA/mg dry tissue. This is a very exciting result, as the hybrid method is able to achieve the original objective: to decellularize effectively while avoiding dehydration of the tissue.

It should be noted that the DNA test performed has sensitivity limitations with the spectrophotometer used. Optical density near the decellularization threshold is very low, approaching the tolerance of the instrument. Thus, some error may be present in the numerical value of the DNA concentration for SDS-containing treatments. However, the histological results and statistical comparison to the other treatments confirm the efficacy of the method.

To analyze the physical properties of treated aorta, uniaxial tensile testing was performed on samples from selected $scCO_2$ treatments (S, C, and H). Stress responses for each treatment are plotted against stretch ratio on Figure 6.9. The bimodal stress response seen for each treatment in the figure is normally observed when blood vessel tissue is subjected to a uniaxial ring test [220, 221]. The first linear segment, observed

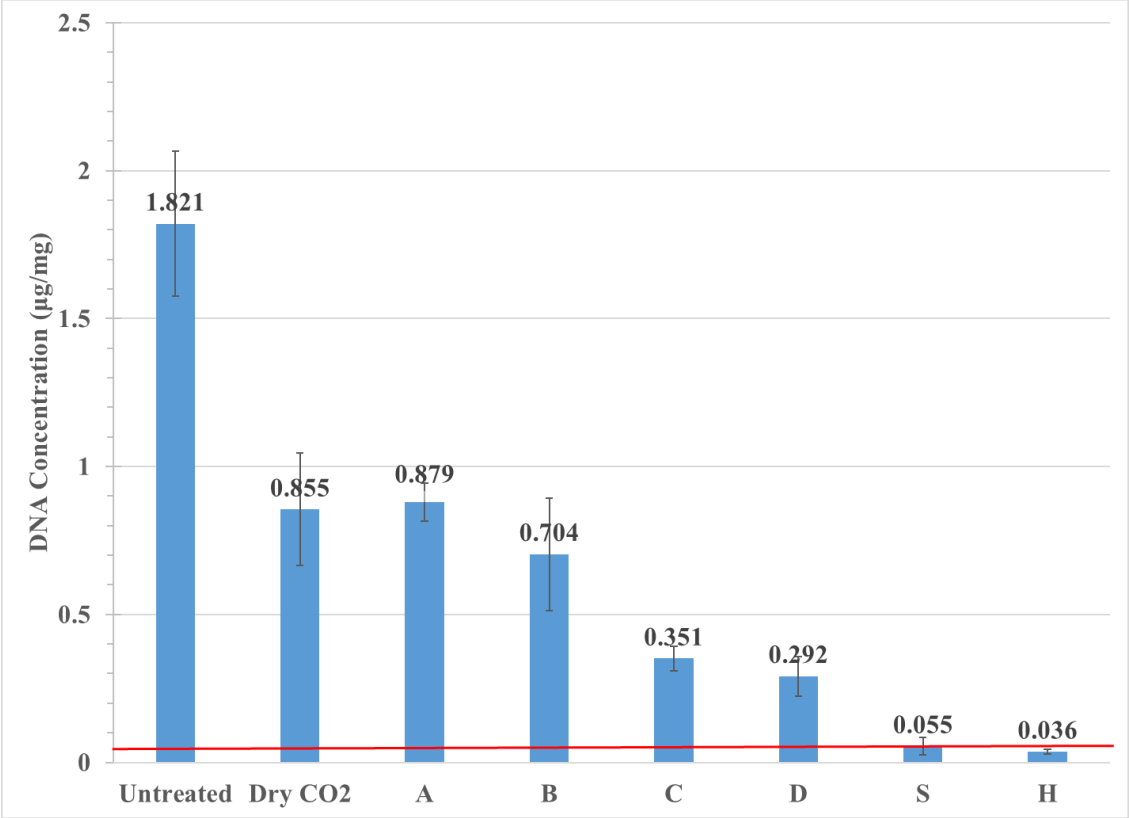

Figure 6.8 – DNA Quantitation including Hybrid Treatment: Bar chart displaying the DNA content of each detergent and $scCO_2$ additive treatment. Values below the red line (0.05 µg/mg) indicate adequate decellularization according to Crapo's standard.

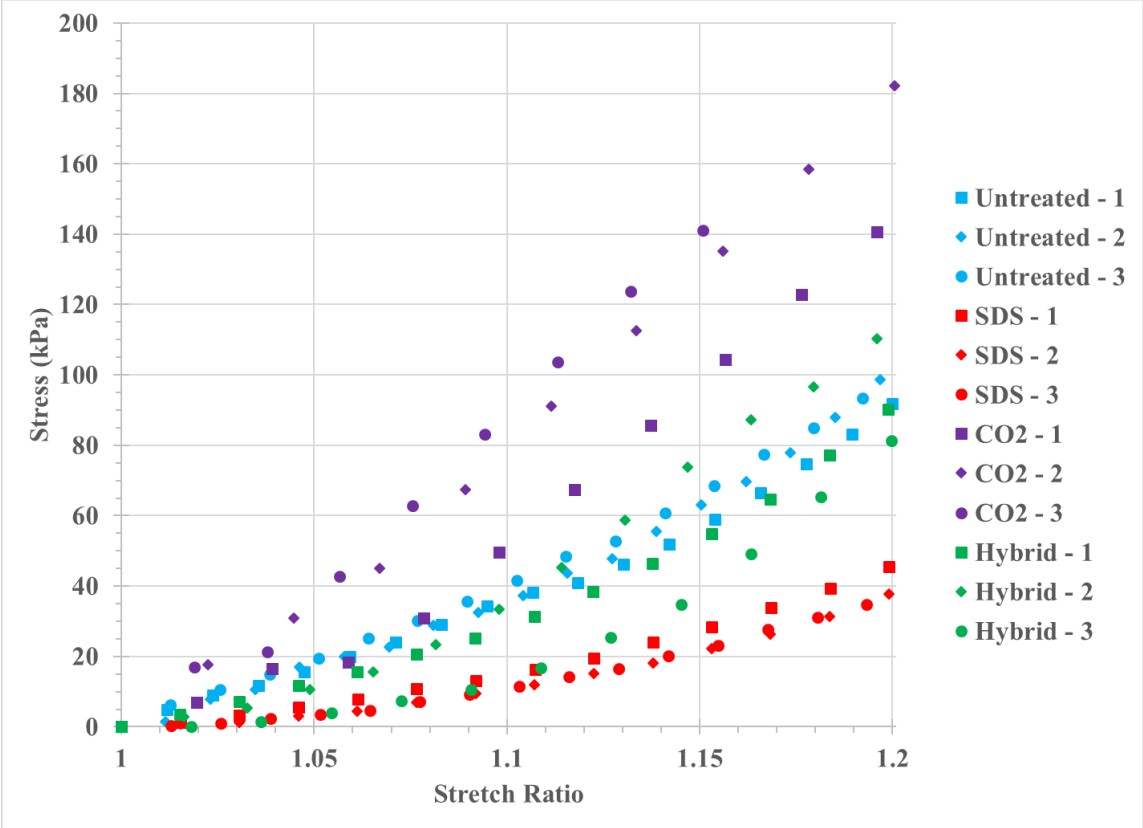

Figure 6.9 – Uniaxial Ring Test of Treated Aortas: Compared to native aortas (blue), C treatments ($scCO_2$ plus ethanol, purple) have a sharper stress response while the response after standard SDS treatments (red) have a flatter slope. The SDS/$scCO_2$ hybrid treatments (green) are most similar to the untreated aorta.

for stretch ratios from about 1.0-1.08, is primarily governed by elastin. The response of the second linear segment, observed for stretch ratios from 1.12-1.2, is governed by collagen. Contributions to modulus of elasticity by both collagen and elastin were calculated for each treatment and are listed on Table 6.2. As expected, SDS exposure denatures proteins and reduces stiffness, while treatment with $scCO_2$ and ethanol causes a significant increase in stiffness because of dehydration. Both of these extremes are mitigated by the hybrid treatment: faster treatment reduces protein denaturation and presaturation with water prevents matrix dehydration. However, the hybrid treatment does cause a significant decrease in $MOE_{elastin}$, though the decrease is less dramatic than that caused by the standard SDS treatment.

It should be noted that the uniaxial ring test has some limitations. First, a uniaxial test does not accurately represent the stresses applied to blood vessels *in vivo*, as those stresses are biaxial and vary with time and blood pressure. Additionally, blood vessels are highly anisotropic, so using globalized values of stretch ratio and strain can introduce error for specific locations on the specimen, especially those near the clamps on each end. A more robust approach would include biaxial testing with monitoring of local stresses and strains using a digital camera or other imaging device, as others have demonstrated. [222, 223].

Removal of SDS is another consideration for scaffold viability, as cytotoxicity is observed for many cell types at concentrations greater than about 0.002% SDS [164]. Residual SDS was quantified for the standard SDS treatment and the SDS/$scCO_2$ hybrid treatment, Figure 6.10. The figure shows that one hour of $scCO_2$ treatment removes about as much SDS as 24 hours of washing with PBS, a significant time savings. PBS

Table 6.2 – Elastic Moduli for Uniaxial Ring Tests

Treatment	$MOE_{Elastin}$ (kPa)	$MOE_{Collagen}$ (kPa)
Untreated	350.8 ± 18.8	717.1 ± 49.3
SDS w/ PBS Wash (S)	106.2 ± 24.2**	306.0 ± 23.5**
$scCO_2$ + ethanol (C)	715.0 ± 61.9**	988.3 ± 50.6**
SDS/$scCO_2$ Hybrid (H)	232.4 ± 59.5*	743.4 ± 49.5

*$p < 0.05$ compared to native aorta
**$p < 0.01$ compared to native aorta

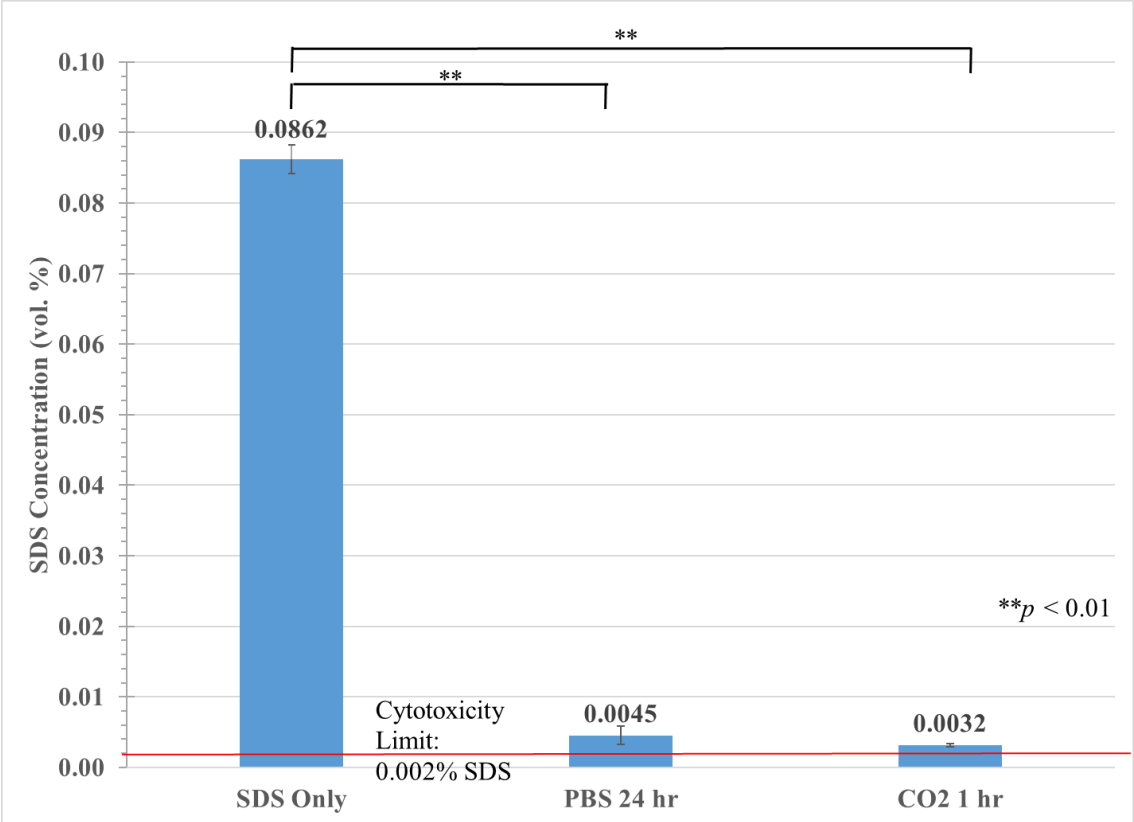

Figure 6.10 – SDS Quantitation Assay: SDS was quantified before and after washing with either PBS or $scCO_2$. 1 hour of $scCO_2$ treatment compares similarly to 24 hours of PBS washing, though neither reduces SDS concentration below the cytotoxic level of 0.002%.

washes also have diminishing returns, making the wash step last several days in many protocols to reduce SDS below cytotoxic levels [224]. Thus, $scCO_2$ could compare even more favorably over longer time periods. This finding also indicates some solubility of SDS in the $scCO_2$ treatment solution; solubility may be low because SDS a charged molecule, but SDS does have similar molecular weight to other molecules extracted by $scCO_2$ in this dissertation, such as glutaraldehyde and Ls-54.

6.4 Conclusions

A novel $scCO_2$ method for decellularizing porcine aorta without compromising its hydration state. This method offers considerably faster decellularization of tissues without requiring long-term exposure to detergents or organic solvents. As anticipated, nonpolar $scCO_2$ solutions were proven ineffective for decellularizing porcine aorta by both histology and DNA quantitation, though presaturating $scCO_2$ with water did better maintain the hydration state of the matrix, even in the presence of other additives. More surprisingly, the addition of ethanol to increase $scCO_2$ polarity did not substantially intensify the extent of decellularization, suggesting that $scCO_2$ alone is unable to lyse the cell membrane and that the previously proposed mechanism of whole-cell extraction is unlikely to be valid.

The inability of $scCO_2$ alone is unable to disrupt cell membranes was further tested by the development of a hybrid decellularization protocol that utilized an SDS pretreatment step before washing with $scCO_2$ and water plus ethanol as additives. This treatment shows that $scCO_2$ can extract intracellular material if the cell membrane is lysed beforehand. Complete decellularization was achieved using this method, which

was about 24 hr faster than the standard method and maintained the hydration state of the native tissue. Mechanical response of ECM decellularized by the hybrid treatment was similar to that of the native tissue, and most residual SDS was removed. Still, further study is required to determine the capabilities and limitations of this method and to fully assess the effects of decellularization on the mechanical and biochemical properties of the matrix.

Chapter 7 Final Conclusions and Future Perspectives

Natural biomaterials present several advantages as TE scaffold materials. However, fabricating safe and effective biomimetic scaffolds challenging, and novel methods continue to seek improvements in functionality, safety, and fabrication efficiency. Though $scCO_2$ is commonplace in synthetic TE, its use in the fabrication of naturally-derived TE scaffolds, including collagen and decellularized ECM, is still in its infancy. More research and development is required before the technologies presented in this dissertation become clinically viable or can be directly used for other practical applications. In this brief chapter, some recommended avenues of future research are discussed.

In Chapter 3, biochemical compatibility was demonstrated between type I collagen and $scCO_2$ on both a chemical and physical level. This discovery is a gateway for numerous practical applications going forward. For example, in Chapter 4, $scCO_2$ was used as a crosslinking aid to remove residual glutaraldehyde from collagen films, avoiding the undesirable long treatment times and high temperature exposure normally required to remove unreacted glutaraldehyde. Future research should include assessment of bioactivity, removal of other crosslinking agents, treatment of other types of collagen (type II, type III, etc.), and also to three-dimensional collagen constructs, as the morphologies explored in this dissertation, collagen fibers and films, are relatively simplistic. Many other applications are possible beyond crosslinking, such as scaffold

fabrication and sterilization with $scCO_2$; some preliminary research exists on the latter [96, 225].

$scCO_2$ was also explored as a novel decellularization agent. Though previously-reported tissue dehydration was prevented using a novel presaturation method presented in Chapter 5, studies in Chapter 6 showed that $scCO_2$ alone is ineffective for decellularization. Based on evidence that $scCO_2$ is unable to penetrate the cell membrane, a hybrid treatment was designed using SDS to first lyse cell membranes followed by $scCO_2$ extraction of intracellular debris. Complete decellularization of porcine aorta was achieved with the hybrid method. Furthermore, the hybrid method was faster than the standard method and did not compromise mechanical properties or deposit large amounts of residual SDS.

These results are exciting, but much more study is still needed. The logical next step for this work is a factorial design on the parameters of the hybrid method (*e.g.* SDS concentration and treatment time, $scCO_2$ pressure, treatment time, and depressurization rate). This would elucidate which parameters are critical for successful decellularization and allow the process to be optimized for faster treatment or tuning of specific scaffold properties. Moving forward, it is imperative to verify scaffold bioactivity after $scCO_2$ treatment. Bioactivity can be studied with an *in vitro* cell assay, such as Alamar blue or MTT. More scaffold characterization should also be performed, including more robust biaxial mechanical testing and electron microscopy, which can determine the effect of $scCO_2$ decellularization on surface properties and elastic fiber alignment. Finally, recellularization and *in vivo* study using an animal model is required to determine the

efficacy of this decellularization method for clinical TE use. Once the hybrid method is better understood, this technology can be extended to tissues other than blood vessels.

Additionally, $scCO_2$ should be investigated further regarding ECM sterilization. Xenogeneic scaffolds were recently classified as medical devices by the US Food and Drug Administration and therefore require terminal sterilization prior to clinical use [106]. Research on the effects of sterilization methods on ECM scaffolds has only recently begun [226], but $scCO_2$ sterilization has been proven effective in this application and may offer several advantages over other methods [13, 30, 38, 39]. The ultimate prize for this research is an effective $scCO_2$-based decellularization process that simultaneously sterilizes; such a process would greatly improve scaffold fabrication efficiency by eliminating an entire processing step.

References

1. **Introduction**. *American Journal of Transplantation* 2014, **14**(Suppl. 1).

2. Berthiaume F, Maguire TJ, Yarmush ML: **Tissue Engineering and Regenerative Medicine: History, Progress, and Challenges**. In: *Annual Review of Chemical and Biomolecular Engineering, Vol 2.* Edited by Prausnitz JM, vol. 2. Palo Alto: Annual Reviews; 2011: 403-430.

3. Wobma H, Vunjak-Novakovic G: **Tissue Engineering and Regenerative Medicine 2015: A Year in Review**. *Tissue Engineering Part B-Reviews* 2016, **22**(2):101-113.

4. Yost MJ, Baicu CF, Stonerock CE, Goodwin RL, Price RL, Davis JM, Evans H, Watson PD, Gore CM, Sweet J *et al*: **A novel tubular scaffold for cardiovascular tissue engineering**. *Tissue Engineering* 2004, **10**(1-2):273-284.

5. Brown BN, Londono R, Tottey S, Zhang L, Kukla KA, Wolf MT, Daly KA, Reing JE, Badylak SF: **Macrophage phenotype as a predictor of constructive remodeling following the implantation of biologically derived surgical mesh materials**. *Acta Biomaterialia* 2012, **8**(3):978-987.

6. Badylak SF, Taylor D, Uygun K: **Whole-Organ Tissue Engineering: Decellularization and Recellularization of Three-Dimensional Matrix Scaffolds**. In: *Annual Review of Biomedical Engineering, Vol 13.* Edited by Yarmush ML, Duncan JS, Gray ML, vol. 13. Palo Alto: Annual Reviews; 2011: 27-53.

7. Reing JE, Zhang L, Myers-Irvin J, Cordero KE, Freytes DO, Heber-Katz E, Bedelbaeva K, McIntosh D, Dewilde A, Braunhut SJ *et al*: **Degradation products of extracellular matrix affect cell migration and proliferation**. *Tissue Engineering Part A* 2009, **15**(3):605-614.

8. Oliveira SM, Ringshia RA, Legeros RZ, Clark E, Yost MJ, Terracio L, Teixeira CC: **An improved collagen scaffold for skeletal regeneration**. *Journal of Biomedical Materials Research Part A* 2010, **94A**(2):371-379.

9. Chow JP, Simionescu DT, Warner H, Wang B, Patnaik SS, Liao J, Simionescu A: **Mitigation of diabetes-related complications in implanted collagen and elastin scaffolds using matrix-binding polyphenol**. *Biomaterials* 2013, **34**(3):685-695.

10. Keane TJ, Londono R, Turner NJ, Badylak SF: **Consequences of ineffective decellularization of biologic scaffolds on the host response**. *Biomaterials* 2012, **33**(6):1771-1781.

11. Martinez FO, Sica A, Mantovani A, Locati M: **Macrophage activation and polarization**. *Frontiers in Bioscience-Landmark* 2008, **13**:453-461.

12. Crapo PM, Gilbert TW, Badylak SF: **An overview of tissue and whole organ decellularization processes**. *Biomaterials* 2011, **32**(12):3233-3243.

13. Keane TJ, Swinehart IT, Badylak SF: **Methods of tissue decellularization used for preparation of biologic scaffolds and *in vivo* relevance**. *Methods* 2015, **84**:25-34.

14. Kasimir MT, Rieder E, Seebacher G, Silberhumer G, Wolner E, Weigel G, Simon P: **Comparison of different decellularization procedures of porcine heart valves**. *Int J Artif Organs* 2003, **26**(5):421-427.

15. Syazwani N, Azhim A, Morimoto Y, Furukawa KS, Ushida T: **Decellularization of aorta tissue using sonication treatment as potential scaffold for vascular tissue engineering**. *Journal of Medical and Biological Engineering* 2015, **35**(2):258-269.

16. Booth C, Korossis SA, Wilcox HE, Watterson KG, Kearney JN, Fisher J, Ingham E: **Tissue engineering of cardiac valve prostheses I: Development and histological characterization of an acellular porcine scaffold**. *Journal of Heart Valve Disease* 2002, **11**(4):457-462.

17. Sierad LN, Shaw EL, Bina A, Brazile B, Rierson N, Patnaik SS, Kennamer A, Odum R, Cotoi O, Terezia P *et al*: **Functional heart valve scaffolds obtained by complete decellularization of porcine aortic roots in a novel differential pressure gradient perfusion system**. *Tissue Engineering Part C-Methods* 2015, **21**(12):1284-1296.

18. Marinucci L, Lilli C, Guerra M, Belcastro S, Becchetti E, Stabellini G, Calvi EM, Locci P: **Biocompatibility of collagen membranes crosslinked with glutaraldehyde or diphenylphosphoryl azide: An *in vitro* study**. *Journal of Biomedical Materials Research Part A* 2003, **67A**(2):504-509.

19. Mestres P, Gomez LL, Lopez TN, del Rosario G, Lukas SW, Hartmann U: **The basement membrane of the isolated rat colonic mucosa. A light, electron and atomic force microscopy study**. *Annals of Anatomy-Anatomischer Anzeiger* 2014, **196**(2-3):108-118.

20. Faulk DM, Carruthers CA, Warner HJ, Kramer CR, Reing JE, Zhang L, D'Amore A, Badylak SF: **The effect of detergents on the basement membrane complex of a biologic scaffold material**. *Acta Biomaterialia* 2014, **10**(1):183-193.

21. McHugh MA, Krukonis VJ: **Supercritical Fluid Extraction: Principles and Practice**. Stoneham, Mass.: Butterworth; 1994.

22. Ferrentino G, Spilimbergo S: **High pressure carbon dioxide pasteurization of solid foods: Current knowledge and future outlooks**. *Trends in Food Science & Technology* 2011, **22**(8):427-441.

23. Ferrentino G, Belscak-Cvitanovic A, Komes D, Spilimbergo S: **Quality attributes of fresh-cut coconut after supercritical carbon dioxide pasteurization**. *Journal of Chemistry* 2013.

24. Ferrentino G, Balzan S, Spilimbergo S: **On-line color monitoring of solid foods during supercritical CO_2 pasteurization**. *Journal of Food Engineering* 2012, **110**(1):80-85.

25. Liu X, Yang DL, Liu JJ, Xu K, Wu GH: **Modeling of supercritical fluid extraction of flavonoids from *Calycopteris floribunda* leaves**. *Chem Pap* 2014, **68**(3):316-323.

26. Bagheri H, Manap MYB, Solati Z: **Response surface methodology applied to supercritical carbon dioxide extraction of Piper nigrum L. essential oil**. *LWT-Food Sci Technol* 2014, **57**(1):149-155.

27. Barry JJA, Nazhat SN, Rose F, Hainsworth AH, Scotchford CA, Howdle SM: **Supercritical carbon dioxide foaming of elastomer/heterocyclic methacrylate blends as scaffolds for tissue engineering**. *Journal of Materials Chemistry* 2005, **15**(46):4881-4888.

28. Floren M, Spilimbergo S, Motta A, Migliaresi C: **Porous poly(D,L-lactic acid) foams with tunable structure and mechanical anisotropy prepared by supercritical carbon dioxide**. *Journal of Biomedical Materials Research Part B-Applied Biomaterials* 2011, **99B**(2):338-349.

29. Tai HY, Mather ML, Howard D, Wang WX, White LJ, Crowe JA, Morgan SP, Chandra A, Williams DJ, Howdle SM *et al*: **Control of pore size and structure of tissue engineering scaffolds produced by supercritical fluid processing**. *European Cells & Materials* 2007, **14**:64-76.

30. An YH, Alvi FI, Kang Q, Laberge M, Drews MJ, Zhang J, Matthews MA, Arciola CR: **Effects of sterilization on implant mechanical property and biocompatibility**. *Int J Artif Organs* 2005, **28**(11):1126-1137.

31. Hemmer JD, Drews MJ, LaBerge M, Matthews MA: **Sterilization of bacterial spores by using supercritical carbon dioxide and hydrogen peroxide**. *Journal of Biomedical Materials Research Part B-Applied Biomaterials* 2007, **80B**(2):511-518.

32. Jimenez A, Zhang J, Matthews MA: **Evaluation Of CO_2-Based Cold Sterilization of a Model Hydrogel**. *Biotechnology and Bioengineering* 2008, **101**(6):1344-1352.

33. Tarafa PJ, Jimenez A, Zhang JA, Matthews MA: **Compressed carbon dioxide (CO_2) for decontamination of biomaterials and tissue scaffolds**. *Journal of Supercritical Fluids* 2010, **53**(1-3):192-199.

34. Zhang J, Burrows S, Gleason C, Matthews MA, Drews MJ, LaBerge M, An YHH: **Sterilizing *Bacillus pumilus* spores using supercritical carbon dioxide**. *J Microbiol Methods* 2006, **66**(3):479-485.

35. Zhang J, Dalal N, Gleason C, Matthews MA, Waller LN, Fox KF, Fox A, Drews MJ, LaBerge M, An YH: **On the mechanisms of deactivation of *Bacillus atrophaeus* spores using supercritical carbon dioxide**. *Journal of Supercritical Fluids* 2006, **38**(2):268-273.

36. Zhang J, Dalal N, Matthews MA, Waller LN, Saunders C, Fox KF, Fox A: **Supercritical carbon dioxide and hydrogen peroxide spore structures associated with high killing rate cause mild changes in of *Bacillus anthracis***. *J Microbiol Methods* 2007, **70**(3):442-451.

37. Zhang J, Davis TA, Matthews MA, Drews MJ, LaBerge M, An YHH: **Sterilization using high-pressure carbon dioxide**. *Journal of Supercritical Fluids* 2006, **38**(3):354-372.

38. Qiu QQ, Leamy P, Brittingham J, Pomerleau J, Kabaria N, Connor J: **Inactivation of bacterial spores and viruses in biological material using supercritical carbon dioxide with sterilant**. *Journal of Biomedical Materials Research Part B-Applied Biomaterials* 2009, **91B**(2):572-578.

39. Balestrini JL, Liu A, Gard AL, Huie J, Blatt KMS, Schwan J, Zhao LP, Broekelmann TJ, Mecham RP, Wilcox EC *et al*: **Sterilization of lung matrices by supercritical carbon dioxide**. *Tissue Engineering Part C-Methods* 2016, **22**(3):260-269.

40. Tsioptsias C, Paraskevopoulos MK, Christofilos D, Andrieux R, Panayiotou C: **Polymeric hydrogels and supercritical fluids: The mechanism of hydrogel foaming**. *Polymer* 2011, **52**(13):2819-2826.

41. Baldino L, Concilio S, Cardea S, De Marco I, Reverchon E: **Complete glutaraldehyde elimination during chitosan hydrogel drying by SC-CO_2 processing**. *Journal of Supercritical Fluids* 2015, **103**:70-76.

42. Bhamidipati M, Scurto AM, Detamore MS: **The Future of Carbon Dioxide for Polymer Processing in Tissue Engineering**. *Tissue Eng Part B-Rev* 2013, **19**(3):221-232.

43. Sawada K, Terada D, Yamaoka T, Kitamura S, Fujisato T: **Cell removal with supercritical carbon dioxide for acellular artificial tissue**. *Journal of Chemical Technology and Biotechnology* 2008, **83**(6):943-949.

44. Perrut M: **Sterilization and virus inactivation by supercritical fluids (a review)**. *Journal of Supercritical Fluids* 2012, **66**:359-371.

45. Duarte ARC, Mano JF, Reis RL: **Supercritical fluids in biomedical and tissue engineering applications: a review**. *International Materials Reviews* 2009, **54**(4):214-222.

46. Knez Z, Markocic E, Leitgeb M, Primozic M, Hrncic MK, Skerget M: **Industrial applications of supercritical fluids: A review**. *Energy* 2014, **77**:235-243.

47. Kim B-S, Park I-K, Hoshiba T, Jiang H-L, Choi Y-J, Akaike T, Cho C-S: **Design of artificial extracellular matrices for tissue engineering**. *Progress in Polymer Science* 2011, **36**(2):238-268.

48. Sandler SI: **Chemical, Biomedical, and Engineering Thermodynamics**, 4th edn: John Wiley & Sons; 2006.

49. King JW, Williams LL: **Utilization of critical fluids in processing semiconductors and their related materials**. *Current Opinion in Solid State and Materials Science* 2003, **7**(4–5):413-424.

50. Gupta RBS, Jae-Jin: **Solubility in Supercritical Carbon Dioxide**. Boca Raton, FL: CRC Press; 2006.

51. Ramsey E, Sun QB, Zhang ZQ, Zhang CM, Gou W: **Mini-Review: Green sustainable processes using supercritical fluid carbon dioxide**. *Journal of Environmental Sciences* 2009, **21**(6):720-726.

52. Schmidt A, Beermann K, Bach E, Schollmeyer E: **Disinfection of textile materials contaminated with *E-coli* in liquid carbon dioxide**. *Journal of Cleaner Production* 2005, **13**(9):881-885.

53. van Roosmalen MJE, Woerlee GF, Witkamp GJ: **Amino acid based surfactants for dry-cleaning with high-pressure carbon dioxide**. *Journal of Supercritical Fluids* 2004, **32**(1-3):243-254.

54. Sachlos E, Wahl DA, Triffitt JT, Czernuszka JT: **The impact of critical point drying with liquid carbon dioxide on collagen-hydroxyapatite composite scaffolds**. *Acta Biomaterialia* 2008, **4**(5):1322-1331.

55. Shah PJ, Wu Z, Sarangan AM: **Effects of CO_2 critical point drying on nanostructured SiO_2 thin films after liquid exposure**. *Thin Solid Films* 2013, **527**:344-348.

56. Wawrzyniak P, Rogacki G, Pruba J, Bartczak Z: **Diffusion of ethanol carbon dioxide in silica gel**. *Journal of Non-Crystalline Solids* 1998, **225**(1):86-90.

57. Halbritter H: **Preparing living pollen material for scanning electron microscopy using 2,2-dimethoxypropane (DMP) and critical-point drying**. *Biotech Histochem* 1998, **73**(3):137-143.

58. Williams JR, Clifford AA (eds.): **Supercritical Fluid Methods and Protocols** Humana; 2000.

59. Cormier PJ, Clarke RM, McFadden RML, Ghandi K: **Selective free radical reactions using supercritical carbon dioxide**. *Journal of the American Chemical Society* 2014, **136**(6):2200-2203.

60. You EY, Guzman-Blas R, Nicolau E, Scibioh MA, Karanikas CF, Watkins JJ, Cabrera CR: **Co-deposition of Pt and ceria anode catalyst in supercritical carbon dioxide for direct methanol fuel cell applications**. *Electrochimica Acta* 2012, **75**:191-200.

61. Wenzel J, Lee S: **Tert-butyl peroxyacetate initiated semibatch polymerization of 1,1-difluoroethylene in supercritical carbon dioxide**. *Polymer Engineering and Science* 2016, **56**(4):435-440.

62. Guibal P, Thiebaut D, Sassiat P, Vial J: **Feasability of neat carbon dioxide packed column comprehensive two dimensional supercritical fluid chromatography**. *Journal of Chromatography A* 2012, **1255**:252-258.

63. Yang JT, Sang Y, Chen F, Fei ZD, Zhong MQ: **Synthesis of silica particles grafted with poly(ionic liquid) and their nucleation effect on microcellular foaming of polystyrene using supercritical carbon dioxide**. *Journal of Supercritical Fluids* 2012, **62**:197-203.

64. Haruki M, Hasegawa Y, Fukui N, Kihara S, Takishima S: **Deposition of aromatic polyimide thin films in supercritical carbon dioxide**. *Journal of Supercritical Fluids* 2014, **94**:147-153.

65. Wang H, Li G, Shen Z, Tian S, Sun B, He Z, Lu P: **Experiment on rock breaking with supercritical carbon dioxide jet**. *Journal of Petroleum Science and Engineering* 2015, **127**:305-310.

66. van der Kraan M, Cid MVF, Woerlee GF, Veugelers WJT, Witkamp GJ: **Dyeing of natural and synthetic textiles in supercritical carbon dioxide with disperse reactive dyes**. *Journal of Supercritical Fluids* 2007, **40**(3):470-476.

67. Ma Y, Liu Z, Tian H: **A review of transcritical carbon dioxide heat pump and refrigeration cycles**. *Energy* 2013, **55**:156-172.

68. Ramalakshmi K, Raghavan B: **Caffeine in coffee: Its removal. Why and how?** *Critical Reviews in Food Science and Nutrition* 1999, **39**(5):441-456.

69. Joshi R, Babu GDK, Gulati A: **Effect of decaffeination conditions on quality parameters of Kangra orthodox black tea**. *Food Research International* 2013, **53**(2):693-703.

70. Campos-Vega R, Loarca-Piña G, Vergara-Castañeda HA, Oomah BD: **Spent coffee grounds: A review on current research and future prospects**. *Trends in Food Science & Technology* 2015, **45**(1):24-36.

71. Tai CY, You GS: **Fractionation of metal ions from water using supercritical carbon dioxide**. *Aiche Journal* 2004, **50**(7):1627-1630.

72. Wang W, Yang HJ, Hua JC, Guo CY: **Extraction of metal ions with non-fluorous bipyridine derivatives as chelating ligands in supercritical carbon dioxide**. *Journal of Supercritical Fluids* 2009, **51**(2):181-187.

73. Ferdosh S, Sarker MZI, Ab Rahman NNN, Akanda MJH, Ghafoor K, Ab Kadir MO: **Simultaneous extraction and fractionation of fish oil from tuna by-product using supercritical carbon dioxide (SC-CO_2)**. *Journal of Aquatic Food Product Technology* 2016, **25**(2):230-239.

74. Sahena F, Zaidul ISM, Jinap S, Karim AA, Abbas KA, Norulaini NAN, Omar AKM: **Application of supercritical CO_2 in lipid extraction - A review**. *Journal of Food Engineering* 2009, **95**(2):240-253.

75. Wang YF, Sun D, Chen H, Qian LS, Xu P: **Fatty acid composition and antioxidant activity of tea (*Camellia sinensis L.*) seed oil extracted by optimized supercritical carbon dioxide**. *International Journal of Molecular Sciences* 2011, **12**(11):7708-7719.

76. Machmudah S, Zakaria, Winardi S, Sasaki M, Goto M, Kusumoto N, Hayakawa K: **Lycopene extraction from tomato peel by-product containing tomato seed using supercritical carbon dioxide**. *Journal of Food Engineering* 2012, **108**(2):290-296.

77. Boutin O, Badens E: **Extraction from oleaginous seeds using supercritical CO_2: Experimental design and products quality**. *Journal of Food Engineering* 2009, **92**(4):396-402.

78. Doker O, Salgin U, Yildiz N, Aydogmus M, Calimli A: **Extraction of sesame seed oil using supercritical CO2 and mathematical modeling**. *Journal of Food Engineering* 2010, **97**(3):360-366.

79. Cunnane SC, Ganguli S, Menard C, Liede AC, Hamadeh MJ, Chen ZY, Wolever TMS, Jenkins DJA: **High alpha-linolenic acid flaxseed (*linum-usitatissimum*) -**

Some nutritional properties in humans. *British Journal of Nutrition* 1993, **69**(2):443-453.

80. Ozkal SG, Yener ME: **Supercritical carbon dioxide extraction of flaxseed oil: Effect of extraction parameters and mass transfer modeling**. *Journal of Supercritical Fluids* 2016, **112**:76-80.

81. Wang L, Wang XB, Wang P, Xiao YP, Liu QH: **Optimization of supercritical carbon dioxide extraction, physicochemical and cytotoxicity properties of *Gynostemma pentaphyllum* seed oil: A potential source of conjugated linolenic acids**. *Separation and Purification Technology* 2016, **159**:147-156.

82. Uddin MS, Sarker MZI, Ferdosh S, Akanda MJH, Easmin MS, Shamsudina SHB, Bin Yunuse K: **Phytosterols and their extraction from various plantmatrices using supercritical carbon dioxide: a review**. *Journal of the Science of Food and Agriculture* 2015, **95**(7):1385-1394.

83. Xu XA, Dong J, Mu XF, Sun LP: **Supercritical CO_2 extraction of oil, carotenoids, squalene and sterols from lotus (*Nelumbo nucifera Gaertn*) bee pollen**. *Food and Bioproducts Processing* 2011, **89**(C1):47-52.

84. Tanaka YSIO, Takeshi: **Extraction of phospholipids from salmon roe with supercritical carbon dioxide and an entrainer**. *Journal of Oleo Science* 2004, **53**(9):417-424.

85. Shah A, Akoh CC, Toledo RT, Corredig M: **Isolation of a phospholipid fraction from inedible egg**. *Journal of Supercritical Fluids* 2004, **30**(3):303-313.

86. Hanif M, Atsuta Y, Fujie K, Daimon H: **Supercritical fluid extraction of microbial phospholipid fatty acids from activated sludge**. *Journal of Chromatography A* 2010, **1217**(43):6704-6708.

87. Lee MB, Greig JD: **A review of nosocomial *Salmonella* outbreaks: Infection control interventions found effective**. *Public Health* 2013, **127**(3):199-206.

88. Weber DJ, Raasch R, Rutala WA: **Nosocomial infections in the ICU: The growing importance of antibiotic-resistant pathogens**. *Chest* 1999, **115**(3, Supplement 1):34S-41S.

89. Yuan C, Jones S, Blackburn S: **The influence of autoclave steam on polymer and organic fibre modified ceramic shells**. *Journal of the European Ceramic Society* 2005, **25**(7):1081-1087.

90. Liteplo RG, Meek ME, Bruce W: **Ethylene oxide: Hazard characterization and exposure-response analysis**. *Journal of Environmental Science and Health Part C-Environmental Carcinogenesis & Ecotoxicology Reviews* 2001, **19**(1):219-265.

91. Williams HE, Huxley J, Claybourn M, Booth J, Hobbs M, Meehan E, Clark B: **The effect of gamma-irradiation and polymer composition on the stability of PLG polymer and microspheres**. *Polymer Degradation and Stability* 2006, **91**(9):2171-2181.

92. Rideout K, Teschke K, Dimich-Ward H, Kennedy SM: **Considering risks to healthcare workers from glutaraldehyde alternatives in high-level disinfection**. *Journal of Hospital Infection* 2005, **59**(1):4-11.

93. Spilimbergo S, Mantoan D, Quaranta A, Della Mea G: **Real-time monitoring of cell membrane modification during supercritical CO_2 pasteurization**. *Journal of Supercritical Fluids* 2009, **48**(1):93-97.

94. Garcia-Gonzalez L, Geeraerd AH, Spilimbergo S, Elst K, Van Ginneken L, Debevere J, Van Impe JF, Devlieghere F: **High pressure carbon dioxide inactivation of microorganisms in foods: The past, the present and the future**. *International Journal of Food Microbiology* 2007, **117**(1):1-28.

95. Spilimbergo S, Bertucco A, Basso G, Bertoloni G: **Determination of extracellular and intracellular pH of Bacillus subtilis suspension under CO_2 treatment**. *Biotechnology and Bioengineering* 2005, **92**(4):447-451.

96. Bernhardt A, Wehrl M, Paul B, Hochmuth T, Schumacher M, Schutz K, Gelinsky M: **Improved sterilization of sensitive biomaterials with supercritical carbon dioxide at low temperature**. *Plos One* 2015, **10**(6).

97. Spilimbergo S, Dehghani F, Bertucco A, Foster NR: **Inactivation of bacteria and spores by pulse electric field and high pressure CO_2 at low temperature**. *Biotechnology and Bioengineering* 2003, **82**(1):118-125.

98. Oule KM, Dickman M, Arul J: **Properties of orange juice with supercritical carbon dioxide treatment**. *International Journal of Food Properties* 2013, **16**(8):1693-1710.

99. Fages J, Poirier B, Barbier Y, Frayssinet P, Joffret ML, Majewski W, Bonel G, Larzul D: **Viral inactivation of human bone tissue using supercritical fluid extraction**. *Asaio Journal* 1998, **44**(4):289-293.

100. Raynie DE: **Warning concerning the use of nitrous-oxide in supercritical-fluid extractions**. *Analytical Chemistry* 1993, **65**(21):3127-3128.

101. Capilla VM, M.; Moreno, M.J.; and Jimenez, R. : **Disinfection and disinfection effect of CO_2 under pressure on food matrix.** . In: *Proceedings of the 5th International Smposium on Supercritical Fluids: 2003; Versailles, France*. 2095–2100.

102. Matthews MAZ, Jian; Quick, Allan M.: **Methods and compositions for eliminating allergens and allergen-producing organisms**. In. Edited by USPTO. USA; 2006.

103. Liu JC, Han BX, Zhang HL, Li GZ, Zhang XG, Wang J, Dong BZ: **Formation of water-in-CO_2 microemulsions with non-fluorous surfactant Ls-54 and solubilization of biomacromolecules**. *Chemistry-a European Journal* 2002, **8**(6):1356-1360.

104. Tarafa PJ, Williams E, Panvelker S, Zhang JZ, Matthews MA: **Removing endotoxin from metallic biomaterials with compressed carbon dioxide-based mixtures**. *Journal of Supercritical Fluids* 2011, **55**(3):1052-1058.

105. Tarafa PJ, Matthews MA: **Phase equilibrium for surfactant Ls-54 in liquid CO_2 with water and solubility estimation using the Peng-Robinson equation of state**. *Fluid Phase Equilibria* 2010, **298**(2):212-218.

106. Keane TJ, Badylak SF: **The host response to allogeneic and xenogeneic biological scaffold materials**. *J Tissue Eng Regen Med* 2015, **9**(5):504-511.

107. Dehghani F, Annabi N: **Engineering porous scaffolds using gas-based techniques**. *Current Opinion in Biotechnology* 2011, **22**(5):661-666.

108. Garcia-Gonzalez CA, Concheiro A, Alvarez-Lorenzo C: **Processing of materials for regenerative medicine using supercritical fluid technology**. *Bioconjugate Chemistry* 2015, **26**(7):1159-1171.

109. Palocci C, Barbetta A, La Grotta A, Dentini M: **Porous biomaterials obtained using supercritical CO_2-water emulsions**. *Langmuir* 2007, **23**(15):8243-8251.

110. Bhamidipati M, Sridharan B, Scurto AM, Detamore MS: **Subcritical CO_2 sintering of microspheres of different polymeric materials to fabricate scaffolds for tissue engineering**. *Materials Science and Engineering: C* 2013, **33**(8):4892-4899.

111. Duarte ARC, Mano JF, Reis RL: **Dexamethasone-loaded scaffolds prepared by supercritical-assisted phase inversion**. *Acta Biomaterialia* 2009, **5**(6):2054-2062.

112. Li L, Jiang Z, Pan Q, Fang T: **Producing polymer fibers by electrospinning in supercritical fluids**. *Journal of Chemistry* 2013.

113. Temtem M, Barroso T, Casimiro T, Mano JF, Aguiar-Ricardo A: **Dual stimuli responsive poly(N-isopropylacrylamide) coated chitosan scaffolds for controlled release prepared from a non residue technology**. *The Journal of Supercritical Fluids* 2012, **66**:398-404.

114. Duarte ARC, Caridade SG, Mano JF, Reis RL: **Processing of novel bioactive polymeric matrixes for tissue engineering using supercritical fluid technology**. *Materials Science & Engineering C-Materials for Biological Applications* 2009, **29**(7):2110-2115.

115. Chhouk K, Quitain AT, Gaspillo PD, Maridable JB, Sasaki M, Shimoyama Y, Goto M: **Supercritical carbon dioxide-mediated hydrothermal extraction of bioactive compounds from Garcinia Mangostana pericarp**. *Journal of Supercritical Fluids* 2016, **110**:167-175.

116. Jimenez A, Thompson GL, Matthews MA, Davis TA, Crocker K, Lyons JS, Trapotsis A: **Compatibility of medical-grade polymers with dense CO_2**. *Journal of Supercritical Fluids* 2007, **42**(3):366-372.

117. Oliveira NS, Gonçalves CM, Coutinho JAP, Ferreira A, Dorgan J, Marrucho IM: **Carbon dioxide, ethylene and water vapor sorption in poly(lactic acid)**. *Fluid Phase Equilibria* 2006, **250**(1–2):116-124.

118. Hu J, Deng W: **Application of supercritical carbon dioxide for leather processing**. *Journal of Cleaner Production* 2016, **113**:931-946.

119. Yang QY, Qin SF, Chen JF, Ni W, Xu Q: **Supercritical Carbon Dioxide-Assisted Loosening Preparation of Dry Leather**. *Journal of Applied Polymer Science* 2009, **113**(6):4015-4022.

120. Baldino L, Cardea S, De Marco I, Reverchon E: **Chitosan scaffolds formation by a supercritical freeze extraction process**. *The Journal of Supercritical Fluids* 2014, **90**:27-34.

121. Dong CJ, Lv YG: **Application of collagen scaffold in tissue engineering: Recent advances and new perspectives**. *Polymers* 2016, **8**(2).

122. Gilbert TW, Sellaro TL, Badylak SF: **Decellularization of tissues and organs**. *Biomaterials* 2006, **27**(19):3675-3683.

123. Cen L, Liu W, Cui L, Zhang WJ, Cao YL: **Collagen tissue engineering: Development of novel biomaterials and applications**. *Pediatric Research* 2008, **63**(5):492-496.

124. Ramshaw JAM: **Biomedical applications of collagens**. *Journal of Biomedical Materials Research Part B-Applied Biomaterials* 2016, **104**(4):665-675.

125. Brown BN, Badylak SF: **Extracellular matrix as an inductive scaffold for functional tissue reconstruction**. *Translational Research* 2014, **163**(4):268-285.

126. Chevallay B, Herbage D: **Collagen-based biomaterials as 3D scaffold for cell cultures: applications for tissue engineering and gene therapy**. *Medical & Biological Engineering & Computing* 2000, **38**(2):211-218.

127. Li D-r, Yu X-m, Zhu B: **Extraction and characterization of human-placenta collagen**. *Shengwu Jiagong Guocheng* 2010, **8**(3):58-61.

128. Krishnan S, Sekar S, Katheem MF, Krishnakumar S, Sastry TP: **Fish scale collagen-A novel material for corneal tissue engineering**. *Artificial Organs* 2012, **36**(9):829-835.

129. An B, Kaplan DL, Brodsky B: **Engineered recombinant bacterial collagen as an alternative collagen-based biomaterial for tissue engineering**. *Frontiers in Chemistry* 2014, **2**.

130. Lowe CJ, Reucroft IM, Grota MC, Shreiber DI: **Production of highly aligned collagen scaffolds by freeze-drying of self-assembled, fibrillar collagen gels**. *Acs Biomaterials-Science & Engineering* 2016, **2**(4):643-651.

131. Sell SA, McClure MJ, Garg K, Wolfe PS, Bowlin GL: **Electrospinning of collagen/biopolymers for regenerative medicine and cardiovascular tissue engineering**. *Advanced Drug Delivery Reviews* 2009, **61**(12):1007-1019.

132. Evans HJ, Sweet JK, Price RL, Yost M, Goodwin RL: **Novel 3D culture system for study of cardiac myocyte development**. *American Journal of Physiology-Heart and Circulatory Physiology* 2003, **285**(2):H570-H578.

133. Nesbitt TL, Patel PA, Yost MJ, Goodwin RL, Potts JD: **A 3-D model of coronary vessel development**. *In Vitro Cellular & Developmental Biology-Animal* 2007, **43**(1):10-16.

134. Valarmathi MT, Yost MJ, Goodwin RL, Potts JD: **The influence of proepicardial cells on the osteogenic potential of marrow stromal cells in a three-dimensional tubular scaffold**. *Biomaterials* 2008, **29**(14):2203-2216.

135. Weadock KS, Miller EJ, Bellincampi LD, Zawadsky JP, Dunn MG: **Physical cross-linking of collagen fibers - comparison of ultraviolet-irradiation and dehydrothermal treatment**. *Journal of Biomedical Materials Research* 1995, **29**(11):1373-1379.

136. Chandran PL, Paik DC, Holmes JW: **Structural mechanism for alteration of collagen gel mechanics by glutaraldehyde crosslinking**. *Connective Tissue Research* 2012, **53**(4):285-297.

137. Speer DP, Chvapil M, Eskelson CD, Ulreich J: **Biological effects of residual glutaraldehyde in glutaraldehyde-tanned collagen biomaterials**. *Journal of Biomedical Materials Research* 1980, **14**(6):753-764.

138. Yang CR: **Enhanced physicochemical properties of collagen by using EDC/NHS-crosslinking**. *Bulletin of Materials Science* 2012, **35**(5):913-918.

139. Liu TX, Wang Z: **Collagen crosslinking of porcine sclera using genipin**. *Acta Ophthalmologica* 2013, **91**(4):E253-E257.

140. Grunert P, Borde BH, Towne SB, Moriguchi Y, Hudson KD, Bonassar LJ, Hartl R: **Riboflavin crosslinked high-density collagen gel for the repair of annular defects in intervertebral discs: An *in vivo* study**. *Acta Biomaterialia* 2015, **26**:215-224.

141. Bin Choy Y, Cheng F, Choi H, Kim K: **Monodisperse gelatin microspheres as a drug delivery vehicle: Release profile and effect of crosslinking density**. *Macromolecular Bioscience* 2008, **8**(8):758-765.

142. Balasubramanian P, Roether JA, Schubert DW, Beier JP, Boccaccini AR: **Bi-layered porous constructs of PCL-coated 45S5 bioactive glass and electrospun collagen-PCL fibers**. *Journal of Porous Materials* 2015, **22**(5):1215-1226.

143. Wei GJ, Li C, Fu Q, Xu YM, Li HB: **Preparation of PCL/silk fibroin/collagen electrospun fiber for urethral reconstruction**. *International Urology and Nephrology* 2015, **47**(1):95-99.

144. Calabrese G, Giuffrida R, Fabbi C, Figallo E, Lo Furno D, Gulino R, Colarossi C, Fullone F, Giuffrida R, Parenti R *et al*: **Collagen-Hydroxyapatite scaffolds induce human adipose derived stem cells osteogenic differentiation *in vitro***. *Plos One* 2016, **11**(3).

145. Venkatesan J, Pallela R, Kim SK: **Applications of carbon nanomaterials in bone tissue engineering**. *Journal of Biomedical Nanotechnology* 2014, **10**(10):3105-3123.

146. Chen GB, Lv YG: **Immobilization and application of electrospun nanofiber scaffold-based growth factor in bone tissue engineering**. *Current Pharmaceutical Design* 2015, **21**(15):1967-1978.

147. Allman AJ, McPherson TB, Badylak SF, Merrill LC, Kallakury B, Sheehan C, Raeder RH, Metzger DW: **Xenogeneic extracellular matrix grafts elicit a Th2-restricted immune response**. *Transplantation* 2001, **71**(11):1631-1640.

148. Ansaloni L, Cambrini P, Catena F, Di Saverio S, Gagliardi S, Gazzotti F, Hodde JP, Metzger DW, D'Alessandro L, Pinna AD: **Immune response to small intestinal submucosa (Surgisis) implant in humans: Preliminary observations**. *Journal of Investigative Surgery* 2007, **20**(4):237-241.

149. Choi JS, Kim BS, Kim JY, Kim JD, Choi YC, Yang H-J, Park K, Lee HY, Cho YW: **Decellularized extracellular matrix derived from human adipose tissue as a potential scaffold for allograft tissue engineering**. *Journal of Biomedical Materials Research Part A* 2011, **97A**(3):292-299.

150. Bolland F, Korossis S, Wilshaw SP, Ingham E, Fisher J, Kearney JN, Southgate J: **Development and characterisation of a full-thickness acellular porcine bladder matrix for tissue engineering**. *Biomaterials* 2007, **28**(6):1061-1070.

151. Fercana G, Bowser D, Portilla M, Langan EM, Carsten CG, Cull DL, Sierad LN, Simionescu DT: **Platform technologies for decellularization, tunic-specific cell seeding, and *in vitro* conditioning of extended length, small diameter vascular grafts**. *Tissue Engineering Part C-Methods* 2014, **20**(12):1016-1027.

152. Ventura RD, Padalhin AR, Min YK, Lee BT: **Bone regeneration using hydroxyapatite sponge scaffolds with *in vivo* deposited extracellular matrix**. *Tissue Engineering Part A* 2015, **21**(21-22):2649-2661.

153. DeQuach JA, Yuan SH, Goldstein LSB, Christman KL: **Decellularized porcine brain matrix for cell culture and tissue engineering scaffolds**. *Tissue Engineering Part A* 2011, **17**(21-22):2583-2592.

154. Lee W, Miyagawa Y, Long C, Cooper DKC, Hara H: **A comparison of three methods of decellularization of pig corneas to reduce immunogenicity**. *International Journal of Ophthalmology* 2014, **7**(4):587-593.

155. Ozeki M, Narita Y, Kagami H, Ohmiya N, Itoh A, Hirooka Y, Niwa Y, Ueda M, Goto H: **Evaluation of decellularized esophagus as a scaffold for cultured esophageal epithelial cells**. *Journal of Biomedical Materials Research Part A* 2006, **79A**(4):771-778.

156. Sanchez PL, Fernandez-Santos ME, Costanza S, Climent AM, Moscoso I, Gonzalez-Nicolas MA, Sanz-Ruiz R, Rodriguez H, Kren SM, Garrido G *et al*: **Acellular human heart matrix: A critical step toward whole heart grafts**. *Biomaterials* 2015, **61**:279-289.

157. Maghsoudlou P, Totonelli G, Loukogeorgakis SP, Eaton S, De Coppi P: **A decellularization methodology for the production of a natural acellular intestinal matrix**. *Jove-Journal of Visualized Experiments* 2013(80).

158. Poornejad N, Momtahan N, Salehi ASM, Scott DR, Fronk CA, Roeder BL, Reynolds PR, Bundy BC, Cook AD: **Efficient decellularization of whole porcine kidneys improves reseeded cell behavior**. *Biomedical Materials* 2016, **11**(2).

159. Baptista PM, Siddiqui MM, Lozier G, Rodriguez SR, Atala A, Soker S: **The use of whole organ decellularization for the generation of a vascularized liver organoid**. *Hepatology* 2011, **53**(2):604-617.

160. Petersen TH, Calle EA, Zhao LP, Lee EJ, Gui LQ, Raredon MB, Gavrilov K, Yi T, Zhuang ZW, Breuer C *et al*: **Tissue-engineered lungs for *in vivo* implantation**. *Science* 2010, **329**(5991):538-541.

161. Sridharan R, Reilly RB, Buckley CT: **Decellularized grafts with axially aligned channels for peripheral nerve regeneration**. *Journal of the Mechanical Behavior of Biomedical Materials* 2015, **41**:124-135.

162. Prasertsung I, Kanokpanont S, Bunaprasert T, Thanakit V, Damrongsakkul S: **Development of acellular dermis from porcine skin using periodic pressurized technique**. *Journal of Biomedical Materials Research Part B-Applied Biomaterials* 2008, **85B**(1):210-219.

163. Evaristo TC, da CruzAlves FCM, Moroz A, Mion W, Acorci-Valerio MJ, Felisbino SL, Rossi-Ferreira R, Ruiz RL, Deffune E: **Light-emitting diode effects on combined decellularization of tracheae. A novel approach to obtain biological scaffolds**. *Acta Cirurgica Brasileira* 2014, **29**(8):485-492.

164. Zvarova B, Uhl FE, Uriarte JJ, Borg ZD, Coffey AL, Bonenfant NR, Weiss DJ, Wagner DE: **Residual Detergent Detection Method for Nondestructive Cytocompatibility Evaluation of Decellularized Whole Lung Scaffolds**. *Tissue Engineering Part C-Methods* 2016, **22**(5):418-428.

165. Liao J, Joyce EM, Sacks MS: **Effects of decellularization on the mechanical and structural properties of the porcine aortic valve leaflet**. *Biomaterials* 2008, **29**(8):1065-1074.

166. Deeken CR, White AK, Bachman SL, Ramshaw BJ, Cleveland DS, Loy TS, Grant SA: **Method of preparing a decellularized porcine tendon using tributyl phosphate**. *Journal of Biomedical Materials Research Part B-Applied Biomaterials* 2011, **96B**(2):199-206.

167. Badylak SF, Taylor D, Uygun K: **Whole-organ tissue engineering: decellularization and recellularization of three-dimensional matrix scaffolds**. *Annual Review of Biomedical Engineering* 2011, **13**(1):27-53.

168. Lumpkins SB, Pierre N, McFetridge PS: **A mechanical evaluation of three decellularization methods in the design of a xenogeneic scaffold for tissue engineering the temporomandibular joint disc**. *Acta Biomaterialia* 2008, **4**(4):808-816.

169. Chen SJ, Li JX, Dong PQ: **Utilization of pulsatile flow to decellularize the human umbilical arteries to make small-caliber blood vessel scaffolds**. *Acta Cardiol Sin* 2013, **29**(5):451-456.

170. Ackbar R, Ainoedhofer H, Gugatschka M, Saxena AK: **Decellularized ovine esophageal mucosa for esophageal tissue engineering**. *Technology and Health Care* 2012, **20**(3):215-223.

171. Funamoto S, Nam K, Kimura T, Murakoshi A, Hashimoto Y, Niwaya K, Kitamura S, Fujisato T, Kishida A: **The use of high-hydrostatic pressure treatment to decellularize blood vessels**. *Biomaterials* 2010, **31**(13):3590-3595.

172. Phillips M, Maor E, Rubinsky B: **Nonthermal irreversible electroporation for tissue decellularization**. *J Biomech Eng-Trans ASME* 2010, **132**(9).

173. Sano MB, Neal RE, Garcia PA, Gerber D, Robertson J, Davalos RV: **Towards the creation of decellularized organ constructs using irreversible electroporation and active mechanical perfusion**. *Biomed Eng Online* 2010, **9**.

174. Schulte JB, Simionescu A, Simionescu DT: **The acellular myocardial flap: A novel extracellular matrix scaffold enriched with patent microvascular networks and biocompatible cell niches**. *Tissue Engineering Part C-Methods* 2013, **19**(7):518-530.

175. Lu QJ, Ganesan K, Simionescu DT, Vyavahare NR: **Novel porous aortic elastin and collagen scaffolds for tissue engineering**. *Biomaterials* 2004, **25**(22):5227-5237.

176. Moran EC, Dhal A, Vyas D, Lanas A, Soker S, Baptista PM: **Whole-organ bioengineering: Current tales of modern alchemy**. *Translational Research* 2014, **163**(4):259-267.

177. He M, Callanan A: **Comparison of Methods for Whole-Organ Decellularization in Tissue Engineering of Bioartificial Organs**. *Tissue Engineering Part B-Reviews* 2013, **19**(3):194-208.

178. Tian Z, Liu W, Li G: **The microstructure and stability of collagen hydrogel cross-linked by glutaraldehyde**. *Polymer Degradation and Stability* 2016, **130**:264-270.

179. Fullerton GD, Nes E, Amurao M, Rahal A, Krasnosselskaia L, Cameron I: **An NMR method to characterize multiple water compartments on mammalian collagen**. *Cell Biology International* 2006, **30**(1):66-73.

180. Yost MT, L.; Price, R.L.: **Collagen Processing**. In: *Encyclopedia of Biomaterials and Biomedical Engineering.* Edited by Wnek GEB, G.L., 2nd ed. edn: Taylor & Francis; 2004.

181. Panas-Perez E, Gatt CJ, Dunn MG: **Development of a silk and collagen fiber scaffold for anterior cruciate ligament reconstruction**. *Journal of Materials Science-Materials in Medicine* 2013, **24**(1):257-265.

182. Wang XN, Yan YD, Yost MJ, Fann SA, Dong S, Li XD: **Nanomechanical characterization of micro/nanofiber reinforced type I collagens**. *Journal of Biomedical Materials Research Part A* 2007, **83A**(1):130-135.

183. Usha R, Ramasami T: **Role of solvents in stability of collagen**. *Journal of Thermal Analysis and Calorimetry* 2008, **93**(2):541-545.

184. Meyer M, Prade I, Leppchen-Frohlich K, Felix A, Herdegen V, Haseneder R, Repke JU: **Sterilisation of collagen materials using hydrogen peroxide doted supercritical carbon dioxide and its effects on the materials properties**. *Journal of Supercritical Fluids* 2015, **102**:32-39.

185. Cheng HM, Wu L, Yin ZL, Chen M, Li ZQ: **The treatment of collagen fibre and cattle hide with transglutaminase in supercritical carbon dioxide**. *Journal of the Society of Leather Technologists and Chemists* 2014, **98**(5):216-221.

186. Kaltenbach M, Devenish SRA, Hollfelder F: **A simple method to evaluate the biochemical compatibility of oil/surfactant mixtures for experiments in microdroplets**. *Lab on a Chip* 2012, **12**(20):4185-4192.

187. Yan K, Kishimoto H, Develos-Bagarinao K, Yamaji K, Horita T, Yokokawa H: **Chemical compatibility of doped yttrium chromite and ceria composite materials with YSZ electrolyte**. *Solid State Ionics* 2016, **288**:88-93.

188. Shimizu A, Kawai K, Yanagino M, Wakiyama T, Machida M, Kameyama K, Naito Z: **Characteristics of type IV collagen unfolding under various pH conditions as a model of pathological disorder in tissue**. *Journal of Biochemistry* 2007, **142**(1):33-40.

189. Flory PJ, Garrett RR: **Phase transitions in collagen and gelatin systems**. *Journal of the American Chemical Society* 1958, **80**(18):4836-4845.

190. Staicu T, Circu V, Ionita G, Ghica C, Popa VT, Micutz M: **Analysis of bimodal thermally-induced denaturation of type I collagen extracted from calfskin**. *Rsc Advances* 2015, **5**(48):38391-38406.

191. Hellauer H, Winkler R: **Denaturation of collagen fibers in NaI, NaCl, and water of different pH values as studied by differential scanning calorimetric measurements**. *Connective Tissue Research* 1975, **3**(4):227-230.

192. Harrington WF: **Effect of neutral salts on the structure of collagen and gelatin**. *Nature* 1958, **181**(4614):997-998.

193. Fullerton GD, Amurao MR: **Evidence that collagen and tendon have monolayer water coverage in the native state**. *Cell Biology International* 2006, **30**(1):56-65.

194. de Moraes MC, Cunha RL: **Gelation property and water holding capacity of heat-treated collagen at different temperature and pH values**. *Food Research International* 2013, **50**(1):213-223.

195. Sanfelice D, Temussi PA: **Cold denaturation as a tool to measure protein stability**. *Biophysical Chemistry* 2016, **208**:4-8.

196. Ozcelikkale A, Han B: **Thermal destabilization of collagen matrix hierarchical structure by freeze/thaw**. *Plos One* 2016, **11**(1).

197. Ascolese E, Graziano G: **On the cold denaturation of globular proteins**. *Chemical Physics Letters* 2008, **467**(1-3):150-153.

198. Rodriguez-Rivera V, Weidner JW, Yost MJ: **Three-dimensional biomimetic technology: novel biorubber creates defined micro- and macro-scale architectures in collagen hydrogels**. *Jove-Journal of Visualized Experiments* 2016(108).

199. Greenfield NJ: **Using circular dichroism spectra to estimate protein secondary structure**. *Nature Protocols* 2006, **1**(6):2876-2890.

200. Huang GP, Shanmugasundaram S, Masih P, Pandya D, Amara S, Collins G, Arinzeh TL: **An investigation of common crosslinking agents on the stability of electrospun collagen scaffolds**. *Journal of Biomedical Materials Research Part A* 2015, **103**(2):762-771.

201. Liu YY, Ma L, Gao CY: **Facile fabrication of the glutaraldehyde cross-linked collagen/chitosan porous scaffold for skin tissue engineering**. *Materials Science & Engineering C-Materials for Biological Applications* 2012, **32**(8):2361-2366.

202. Damink L, Dijkstra PJ, Vanluyn MJA, Vanwachem PB, Nieuwenhuis P, Feijen J: **Glutaraldehyde as a cross-linking agent for collagen-based biomaterials**. *Journal of Materials Science-Materials in Medicine* 1995, **6**(8):460-472.

203. Zeiger E, Gollapudi B, Spencer P: **Genetic toxicity and carcinogenicity studies of glutaraldehyde—a review**. *Mutation Research/Reviews in Mutation Research* 2005, **589**(2):136-151.

204. Yang C, Wu XM, Zhao YH, Xu L, Wei SC: **Nanofibrous scaffold prepared by electrospinning of poly(vinyl alcohol)/gelatin aqueous Solutions**. *Journal of Applied Polymer Science* 2011, **121**(5):3047-3055.

205. Lee JW, Fukusaki E, Bamba T: **Application of supercritical fluid carbon dioxide to the extraction and analysis of lipids**. *Bioanalysis* 2012, **4**(19):2413-2422.

206. Weadock K, Olson RM, Silver FH: **Evaluation of collagen crosslinking techniques**. *Biomaterials Medical Devices and Artificial Organs* 1983, **11**(4):293-318.

207. Bigi A, Cojazzi G, Panzavolta S, Rubini K, Roveri N: **Mechanical and thermal properties of gelatin films at different degrees of glutaraldehyde crosslinking**. *Biomaterials* 2001, **22**(8):763-768.

208. Cheung DT, Nimni ME: **Mechanism of crosslinking of proteins by glutaraldehyde 2. Reaction with monomeric and polymeric collagen**. *Connective Tissue Research* 1982, **10**(2):201-216.

209. Kornyshev AA, Leikin S: **Theory of interaction between helical molecules**. *Journal of Chemical Physics* 1997, **107**(9):3656-3674.

210. Zambon A, Vetralla M, Urbani L, Pantano MF, Ferrentino G, Pozzobon M, Pugno NM, De Coppi P, Elvassore N, Spilimbergo S: **Dry acellular oesophageal matrix prepared by supercritical carbon dioxide**. *Journal of Supercritical Fluids* 2016, **115**:33-41.

211. Casali DM, Matthews MA: **Decellularization of porcine aorta using supercritical carbon dioxide**. In: *AIChE Annual Meeting: 2016; San Francisco, CA*.

212. Zhou B, Rachev A, Shazly T: **The biaxial active mechanical properties of the porcine primary renal artery**. *Journal of the Mechanical Behavior of Biomedical Materials* 2015, **48**:28-37.

213. Zhu J, Marchant RE: **Design properties of hydrogel tissue-engineering scaffolds**. *Expert Review of Medical Devices* 2011, **8**(5):607-626.

214. Sabirzyanov AN, Il'in AP, Akhunov AR, Gumerov FM: **Solubility of water in supercritical carbon dioxide**. *High Temperature* 2002, **40**(2):203-206.

215. Santana ÁL, Debien IC, Meireles MAA: **High-pressure phase equilibrium methodologies applied to food systems**. *Food and Public Health* 2015, **5**(5):184-202.

216. Lee KY, Mooney DJ: **Hydrogels for Tissue Engineering**. *Chemical Reviews* 2001, **101**(7):1869-1880.

217. Ahmed EM: **Hydrogel: Preparation, characterization, and applications: A review**. *Journal of Advanced Research* 2015, **6**(2):105-121.

218. Abramson DI (ed.): **Blood Vessels and Lymphatics**. New York: Academic Press; 1962.

219. Xu HW, Xu BS, Yang Q, Li XL, Ma XL, Xia Q, Zhang Y, Zhang CQ, Wu YH, Zhang YY: **Comparison of decellularization protocols for preparing a decellularized porcine annulus fibrosus scaffold**. *Plos One* 2014, **9**(1).

220. Twal WO, Klatt SC, Harikrishnan K, Gerges E, Cooley MA, Trusk TC, Zhou B, Gabr MG, Shazly T, Lessner SM *et al*: **Cellularized microcarriers as adhesive building blocks for fabrication of tubular tissue constructs**. *Annals of Biomedical Engineering* 2014, **42**(7):1470-1481.

221. Shazly T, Rachev A, Lessner S, Argraves WS, Ferdous J, Zhou B, Moreira AM, Sutton M: **On the uniaxial ring test of tissue engineered constructs**. *Experimental Mechanics* 2015, **55**(1):41-51.

222. Deplano V, Boufi M, Boiron O, Guivier-Curien C, Alimi Y, Bertrand E: **Biaxial tensile tests of the porcine ascending aorta**. *J Biomech* 2016, **49**(10):2031-2037.

223. de Galarreta SR, Anton R, Cazon A, Larraona GS, Finol EA: **Anisotropic abdominal aortic aneurysm replicas with biaxial material characterization**. *Medical Engineering & Physics* 2016, **38**(12):1505-1512.

224. Cebotari S, Tudorache I, Jaekel T, Hilfiker A, Dorfman S, Ternes W, Haverich A, Lichtenberg A: **Detergent decellularization of heart valves for tissue engineering: toxicological effects of residual detergents on human endothelial cells**. *Artificial Organs* 2010, **34**(3):206-210.

225. Youngstrom DW, Barrett JG, Jose RR, Kaplan DL: **Functional characterization of detergent-decellularized equine tendon extracellular matrix for tissue engineering applications**. *Plos One* 2013, **8**(5).

226. Dearth CL, Keane TJ, Carruthers CA, Reing JE, Huleihel L, Ranallo CA, Kollar EW, Badylak SF: **The effect of terminal sterilization on the material properties and in vivo remodeling of a porcine dermal biologic scaffold**. *Acta Biomaterialia* 2016, **33**:78-87.

227. Zou Y, Zhang Y: **Mechanical evaluation of decellularized porcine thoracic aorta**. *Journal of Surgical Research* 2012, **175**(2):359-368.

Appendix A: Supplemental DSC Data

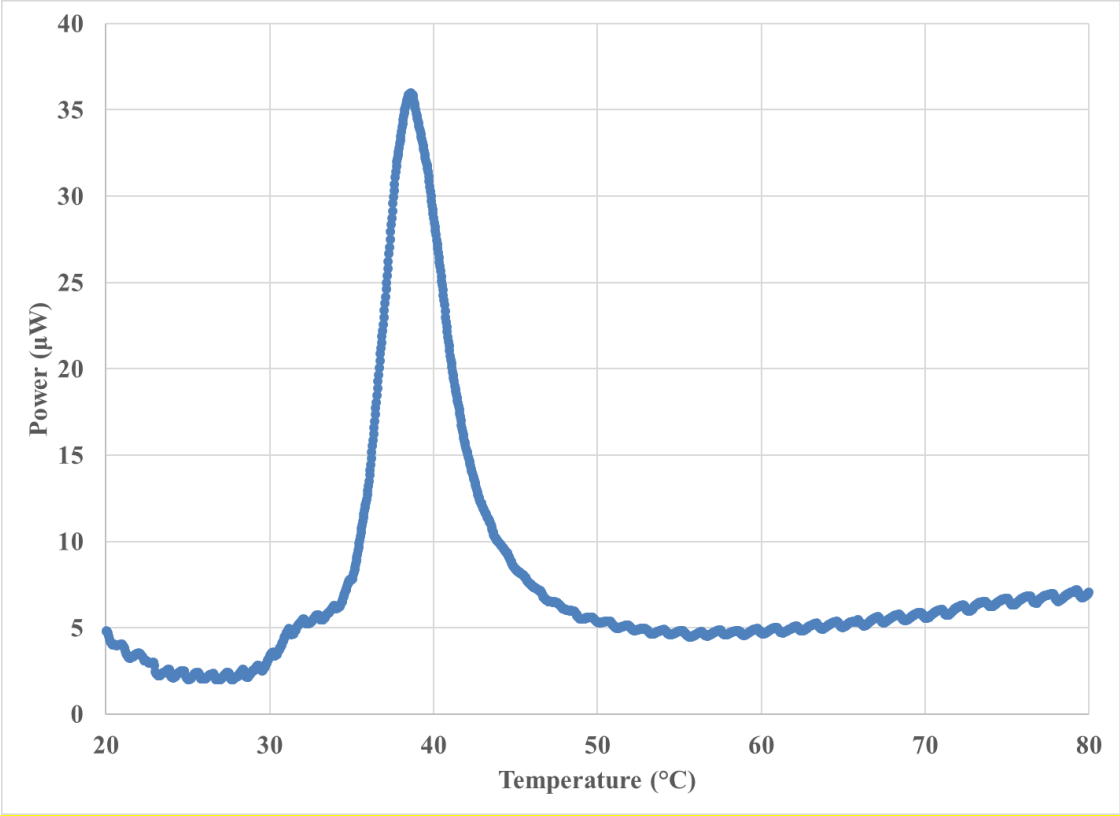

Figure A.1 – DSC Thermogram for 25°C Liquid CO_2 Treatment: This response is much more similar to collagen after scCO_2 treatment, indicating the effect of treatment temperature on collagen denaturation when treated with liquid CO_2. Noise in the thermogram resulted from the baseline scan.

Appendix B: Additional Circular Dichroism Data

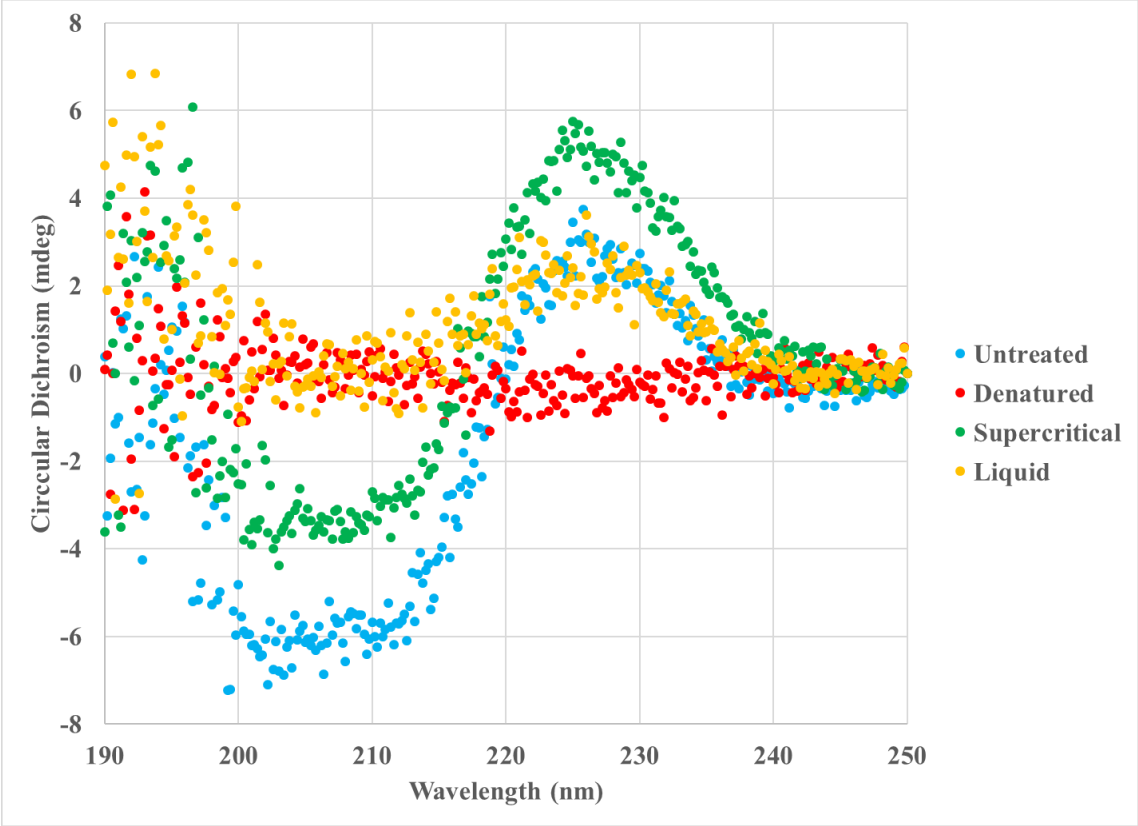

Figure B.1 – CD Spectra of Native and Treated Collagen, 10 µg/mL: Positive peak observed at 225 nm and negative peak at 205 nm. As the concentration increases, the magnitude of each peak does as well.

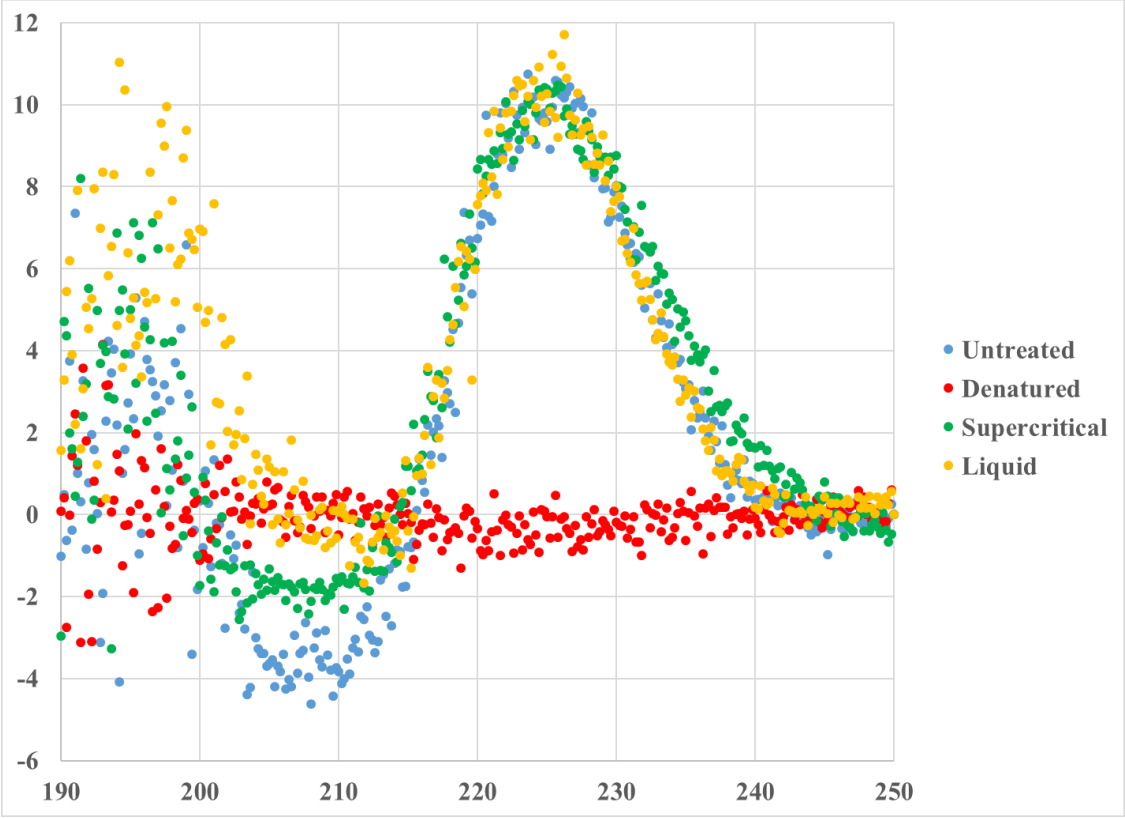

Figure B.2 – CD Spectra of Native and Treated Collagen, 20 µg/mL: No peaks are observed because the protein is completely unfolded and no longer has secondary structure.

Appendix C: Characterization of $scCO_2$ -Treated Aortas

Photographs and mass measurements were taken to analyze gross changes in appearance or weight caused by detergent and/or $scCO_2$ treatment. Photographs of aorta specimens after each treatment can be viewed in Figure C.1. One can see obvious evidence of discoloration when dry CO_2 (b) or CO_2/ethanol (d) is used, which is likely a direct result of tissue dehydration. When water presaturation is employed (c, e, and f), the color change is much less pronounced.

Changes in mass can are listed in Table C.1. These results complement the photography and histology as well, with water presaturation treatments maintaining most of the mass (88-95%) while ethanol alone and dry $scCO_2$ (to a much lesser extent) dehydrate the tissue. These findings make sense based on our past work on presaturation and tissue dehydration: one would expect water-presaturated $scCO_2$ to not disturb water in the tissues, dry $scCO_2$ to extract to some water based on the solubility of water in $scCO_2$, and an ethanol-$scCO_2$ mixture to extract the most water because of the increased polarity compared to dry $scCO_2$.

Scanning electron microscopy (SEM) was performed to determine if $scCO_2$ treatment disrupted the endothelium or three-dimensional ECM ultrastructure. SEM was performed for untreated aorta and for treatments A and C. Micrographs of the endothelial surface can be viewed in Figure C.2. It is clear that treatment C, with ethanol alone as the additive, is more disruptive to the aorta surface, and that adding water prevents some of the damage.

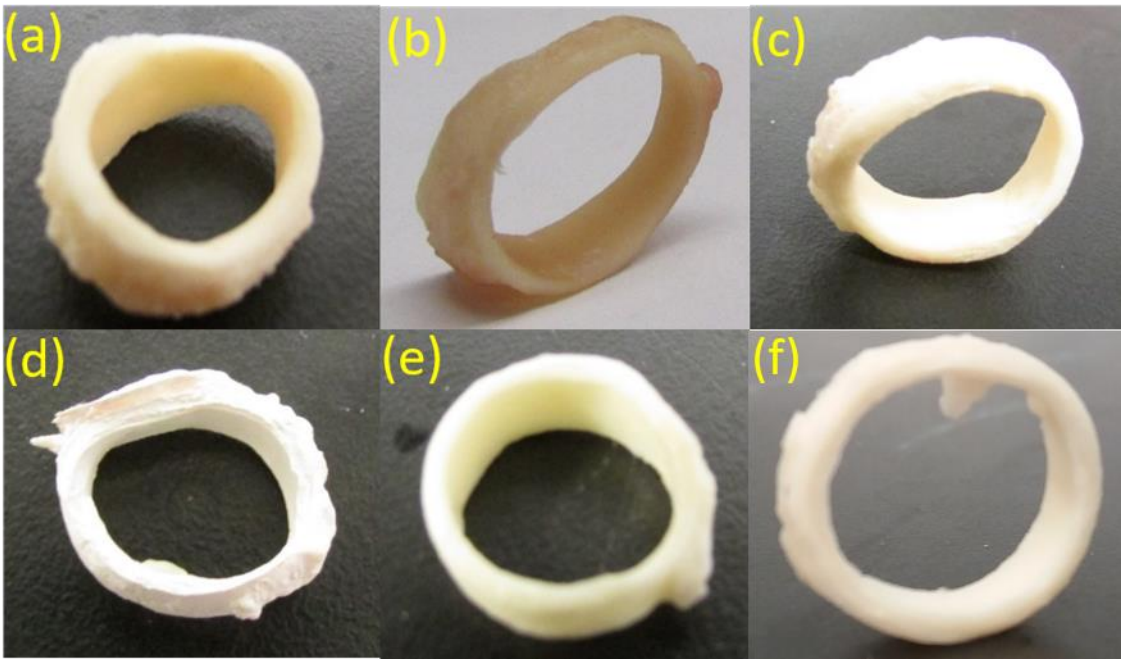

Figure C.1 – Visual Appearance of Aorta Samples: (a) Untreated, (b) Dry CO_2 treatment, (c) Water/scCO_2 treatment, (d) Ethanol/scCO_2 treatment, (e) Water/Ethanol/scCO_2 treatment, (f) Water/Ls-54/scCO_2 treatment

Table C.1 – Changes in Tissue Mass During $scCO_2$ Decellularization

Treatment	Starting Mass (mg)	Final Mass (mg)	% Mass Retained
Dry CO_2	372.4	271.0	72.8
A (CO_2 + Water)	250.1	238.7	95.4
B (CO_2/H_2O/Ls-54)	284.6	245.1	86.1
C (CO_2 + EtOH)	273.7	84.4	30.9
D (CO_2/H_2O/EtOH)	245.6	216.7	88.2

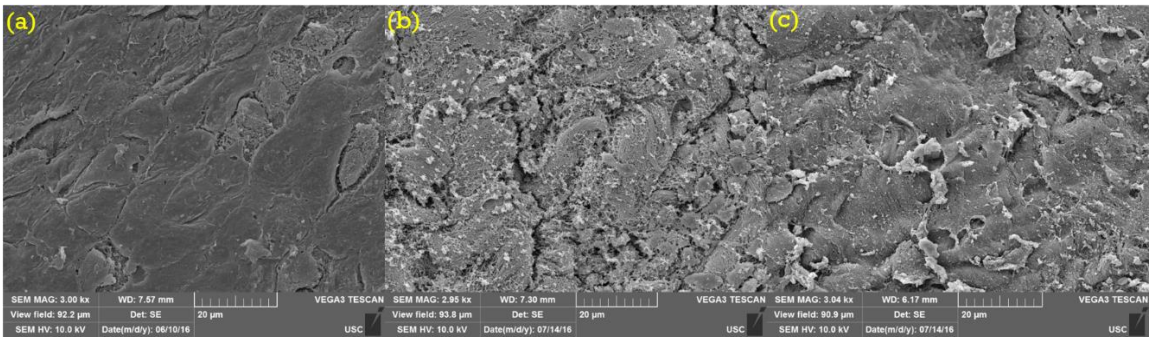

Figure C.2 – Endothelium SEM: SEM micrographs of the endothelium for (a) untreated aorta, (b) CO_2/ethanol-treated aorta, and (c) CO_2/ethanol/water-treated aorta.

A look at the cross-sections of ethanol-treated and water/ethanol-treated aorta is shown in Figure C.3. Here, it is clear that ethanol treatment disrupts the elastic fibers much more than when water is employed as an additive; Figure C.3a shows a tangled mass of different size fibers, while Figure C.3b shows a much more uniform fiber structure, both in terms of size and alignment; the latter is much more like the cross-section of the native aorta [227]. This confirms histological observations (Figures 6.3 and 6.5) that preventing dehydration by using water as an additive also helps preserve matrix ultrastructure.

It is should also be noted that it is inappropriate to look for cells in this circumstance because of the much larger magnification used in electron microscopy compared to light microscopy. SEM is primarily concerned with surface structure and physical properties. Additionally, the value of SEM is limited in this study because biological samples must be dehydrated before viewing for the method to work properly.

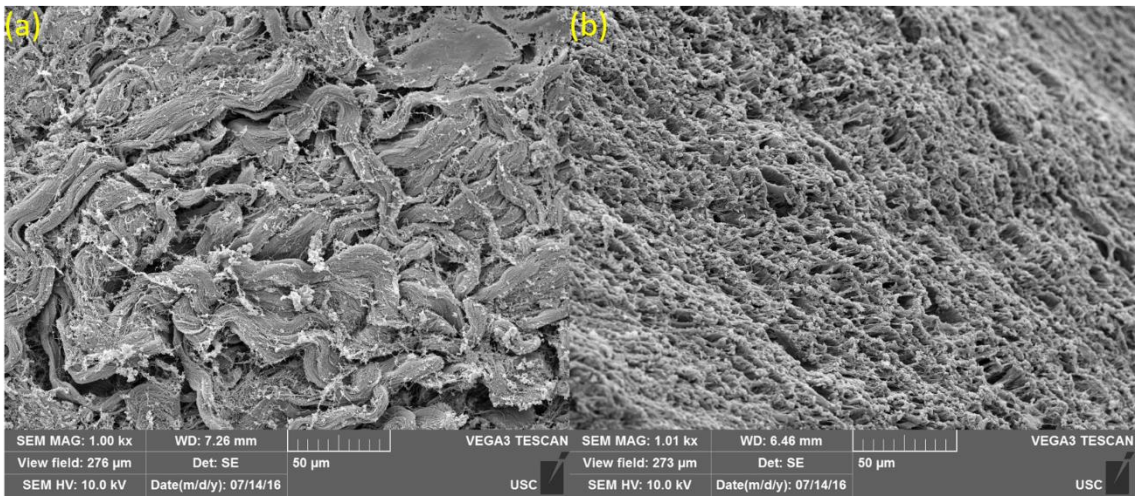

Figure C.3 – Cross-sectional SEM: SEM micrographs of the endothelium for (a) CO_2/ethanol-treated aorta, and b CO_2/ethanol/water-treated aorta.